NUMO-TR-12-05

TOPAZ Project

Long-term Tectonic Hazard to Geological Repositories

an extension of the ITM probabilistic hazard assessment methodology to 1 Myr

Neil Chapman[1], Mick Apted[2], Willy Aspinall[3], Kelvin Berryman[4], Mark Cloos[5], Charles Connor[6], Laura Connor[6], Olivier Jaquet[7], Koji Kiyosugi[6], Ellie Scourse[1], Steve Sparks[3], Mark Stirling[4], Laura Wallace[4], Junichi Goto[8]

[1] MCM Consulting, Switzerland
[2] INTERA, USA
[3] University of Bristol, UK
[4] GNS Sciences, New Zealand
[5] University of Texas, USA
[6] University of South Florida, USA
[7] In2Earth Modelling Ltd, Switzerland
[8] NUMO, Japan

October 2012

Nuclear Waste Management Organization of Japan (NUMO)

2012 年 10 月　初版発行

〒108-0014　東京都港区芝 4 丁目 1 番地 23 号　三田 NN ビル 2 階
原子力発電環境整備機構　技術部
電話 03-6371-4004（技術部）　FAX 03-6371-4102

Inquiries about copyright and reproduction should be addressed to:
Science and Technology Department
Nuclear Waste Management Organization of Japan
Mita NN Bldg. 1-23, Shiba 4-chome, Minato-ku, Tokyo 108-0014 Japan

NUMO-TR-12-05

TOPAZ Project

Long-term Tectonic Hazard to Geological Repositories

an extension of the ITM probabilistic hazard assessment methodology to 1 Myr

Neil Chapman[1], Mick Apted[2], Willy Aspinall[3], Kelvin Berryman[4], Mark Cloos[5], Charles Connor[6], Laura Connor[6], Olivier Jaquet[7], Koji Kiyosugi[6], Ellie Scourse[1], Steve Sparks[3], Mark Stirling[4], Laura Wallace[4], Junichi Goto[8]

[1] MCM Consulting, Switzerland
[2] INTERA, USA
[3] University of Bristol, UK
[4] GNS Sciences, New Zealand
[5] University of Texas, USA
[6] University of South Florida, USA
[7] In2Earth Modelling Ltd, Switzerland
[8] NUMO, Japan

October 2012

Nuclear Waste Management Organization of Japan (NUMO)

各章の和文要約

1　序論

NUMOは，地震・断層活動や火山・火成活動などの自然現象の地層処分システムに対する影響を評価する手法の一つとして，ITM[1]の海外専門家とともに，確率論的な評価手法（ITM手法）の構築を進めてきた。ITM手法は，将来 10 万年程度の期間と広域的な領域の評価を対象とし，これまで東北地方や九州地方のケーススタディを通じて日本の地質環境に対する基本的な適用性を確認してきた（Chapman, et al., 2009 など）。地層処分における安全評価では，数 10 万～100 万年といった超長期の自然現象の影響評価が求められる可能性がある。このため，将来 10 万年を超える期間と処分場規模の数km四方の領域における自然現象の影響の確率論的評価手法を構築するために，TOPAZ[2]プロジェクトを設立した。本手法（TOPAZ手法）では，まず将来の時間枠毎に，プレート運動の変遷に伴い生じうる広域およびサイトスケールの現象を記述する広域変遷シナリオ（RES[3]）とサイト変遷シナリオ（SES[4]）を設定する。次に，それらの現象の地層処分システムに対する影響を記述する影響シナリオ（IS[5]）を設定する。それらをロジックツリーに統合し，専門家の意見集約（EE[6]）やITM手法に基づき，各シナリオの確信度（起こりやすさ）を設定し，確率論的な評価を行う。以上の方法論に基づき，ITM手法による検討実績のある東北地方を対象にケーススタディを実施した。

2　広域変遷シナリオ（RES）とサイト変遷シナリオ（SES）の設定

日本列島周辺の過去数千万年前からの情報を分析し，現在～１万年後，１万年後～10 万年後，10 万年後～100 万年後の三つの時間枠に対して，四つの RES（RES1~4）を設定した。RES1 は現在から将来 100 万年にかけてプレート収束速度が現在のまま継続する，RES2 はプレート収束速度が 2 倍になる，RES3 はプレートの運動方向が変化する，RES4 は太平洋プレートの沈み込み角度が急傾斜になるというシナリオである。次に，地質条件の異なる四つの仮想サイト（A, B, C, D）を設定し，上記四つの RES のもとに各サイトにおいて生じうる自然現象を概念的に記述した SES を作成した。

3　ロジックツリーの構築

上記のシナリオを統合し，ロジックツリーを構築する方法について検討した。地震・断層活動については，四つの RES の後に岩盤の変形速度の変化に対する三つの SES を設定した（変形速度が現在と同様，2 倍に増大，1/2 に減少）。さらに，それぞれの SES について，それらの発生確率を求めるための ITM 手法の三つのモデル（GPS，地震，

---

[1] ITM：International Tectonics Meeting の略。わが国のようなテクトニクス活動が盛んな環境での地層処分事業におけるサイト選定のための調査・評価技術の妥当性について，国内外のテクトニクスの専門家の合意形成・情報発信の場として NUMO が主催した会議体。
[2] TOPAZ：Tectonics Of Preliminary Assessment Zones の略。
[3] RES：Regional Evolution Scenario の略。
[4] SES：Site Evolution Scenario の略。
[5] IS：Impact Scenario の略。
[6] EE：Expert Elicitation の略。

地表変位に基づく歪速度モデル）の選択肢を示す分岐を設定した。火成活動については，四つの RES の後に，まず火山の活動頻度の変化に関する SES の分岐を設定し，さらに火山の発生確率を求めるための ITM 手法（カーネル法，コックスプロセス法）の選択肢を示す分岐を設定した。

4　専門家の意見集約（EE）によるシナリオの確信度の設定

ロジックツリーの各分岐の確信度（起こりやすさ）は，透明性・正当性・中立性・公平性を確保しながら専門家の意見を集約する科学的な手法（Cooke, 1991）を用いて設定する。この手法では，専門家に対して事前に課題に関連する専門分野のテストを行い，正しい値を答える確からしさと回答の振れ幅（不確実性）の与え方の傾向を示す二つの指標を得て，専門家ごとに重み付け係数を設定する。続いて専門家の議論において各専門家の意見（回答）に係数を適用した上で集約し，専門家の意見の総意となる回答と不確実性（回答の取りうる範囲）を得る。今回，国内の専門家の協力を得て，一部のロジックツリーのシナリオについて確信度を設定する演習を行い，基本的な手順を確認した。

5　影響シナリオ（IS）における事象の発生確率の設定

地層処分システムへの影響評価では，対象とする事象を定義し，発生確率を設定する必要がある。ここでは，M6.5~7.5 の地震とM5 の火山噴火 [7]を例に，発生確率の設定方法を提示した。地震については，ITM手法の三つのモデル（GPS，地震，地表変位）による歪速度を地震モーメントに変換し，さらにグーテンベルクーリヒター分布からM6.5~7.5 の地震の発生頻度（確率）を求めた。火山噴火については，ITM手法の二つの手法（カーネル法，コックスプロセス法）を用いて発生確率を求めた。

6　影響シナリオ（IS）の設定

まず既存情報に基づき，影響シナリオの前提となる廃棄体や人工バリアの状態の時間的な変遷について整理した。続いて，地震・断層活動，火山・火成活動，隆起・侵食に起因する様々な事象の影響のシナリオを設定するための考え方を提示した。さらに，断層変位と地表接近の有無，そしてマグマの直撃と間接的影響の有無のパターンの組合せ表を作成し，多数のシナリオを統合して効率的に評価を行う方法を考案した。

7　結論

規制機関を含む様々なステークホルダーと自然現象の影響や放射性物質による健康被害について議論する際には，それらの発生可能性や不確実性を決定論的あるいは確率論的に明確に示す必要がある。TOPAZ 手法は，安全性の評価に向けて幅広い地球科学的な情報や専門家の意見を集約するための有効なツールとなりうる。これまで，ケーススタディの限られた範囲の中で方法論の適用性を検討してきた。今後は，実際への適用に向けて，手法のさらなる検証・改良を進める必要がある。

---

[7] M5 の火山噴火：ここでの M（マグニチュード）は，噴出物の体積や噴煙の高さに基づき噴火の強さを表すための指標(M0~M8)。M5 は噴出量 1km^3，噴煙高 25km 程度。

Contents

1 Introduction and Context

NUMO (the Nuclear Waste Management Organisation of Japan) is responsible for the siting, development and operation of a deep geological repository for high-level waste (HLW) and TRU in Japan. The process is expected to take at least 15 years to reach the point of repository construction. During the period before this, NUMO will need to evaluate sites that emerge from the 'volunteer process' (whereby local communities have been invited to volunteer to be considered as potential hosts for the repository) and select a preferred site. This evaluation will involve initially surface-based and then underground site-characterisation work. Underground characterisation work will only take place at the preferred site.

Prior to the surface-based investigations, volunteer sites will have first had to pass a test of general suitability (NUMO, 2004) and NUMO will then have carried out a detailed, literature-based preliminary evaluation of suitability, prior to accepting them as 'Preliminary Investigation Areas' (PIAs). Because Japan lies in such a tectonically active region of the world on the Pacific rim (the so called 'ring of fire'), a key aspect of all these steps is consideration of the susceptibility of a site to future tectonic activity and tectonically driven processes and events. For repository safety evaluation, the focus is predominantly on long-term (thousands of years) post-closure tectonic processes leading to progressive perturbations of the repository environment. These may possibly lead to the initiation of disruptive tectonic events at repository depth, although potential impacts of other tectonic events during the multi-decade, operational period also have to be taken into account in many locations. The importance of this requirement was dramatically reinforced by the impacts of the March 2011 Tohoku post-earthquake tsunami on the coastal Fukushima nuclear power plant and the 'permanent' co-seismic tectonic deformation and crustal changes in the region. .

The present study is concerned with repository susceptibility to post-closure tectonic impacts over many thousands of years. In this respect, the potential for long-term volcanic and rock deformation impacts on a repository site needs to be considered in particular, at each stage of NUMO's siting programme. Whilst the nationwide evaluation factors for qualification (EFQs) for PIA acceptance are designed to remove clearly unsuitable sites from consideration, they cannot guarantee that, over the next tens of thousands of years, the risks of tectonic hazard for a chosen PIA will be acceptable. This is because large parts of Japan that are potentially geologically suitable for siting are directly affected to varying extents by rock deformation, the peripheral impacts of volcanic activity or the possibility of new magma intrusion or volcanic activity. The EFQs were only intended as preliminary screening guidelines to prevent obviously unsuitable candidates entering the siting process.

1.1 The ITM Methodology: probability – the likelihood of future tectonic impacts on a repository

NUMO recognised that an integration of additional and more refined techniques would be required to evaluate sites that pass the EFQ test, so that they could have a clear, quantitative indication of the likelihood and potential impacts of tectonic events and processes at each PIA. NUMO's ITM project (2005 – 2009) developed such a methodology (the 'ITM Methodology'), based upon state-of-the-art approaches used internationally, developed and extended for the specific purposes of NUMO and the specific conditions of Japan.

The ITM methodology is essentially probabilistic in nature. A probabilistic approach was seen by the ITM expert group (Chapman et al., 2008) as the only realistic means of addressing the uncertainties in predicting possible hazards when there is marked variability in the spatial distribution, the timing, the intensity and style of the volcanic and deformational events, and processes being evaluated (for convenience, in this report, we frequently group these together within the general term 'tectonic events and processes'). The consequences of ignoring very low probability events with significant impacts were highlighted by the Fukushima disaster.

During the course of the ITM project, both NUMO and the Japanese regulatory agencies were considering how best to handle the evaluation of low probability, disruptive events (e.g. volcanic intrusion, fault rupture) and deformation processes that are discontinuous in time and magnitude in response to continuous regional strain, when carrying out safety assessments

of geological repositories for radioactive wastes. Essentially, two approaches have been adopted internationally to address this situation:

- To calculate the health risk[1] to people in the future by combining the probability of a disruptive event occurring with its radiological consequences in terms of releases from a repository: simply, risk = probability x consequence. With this approach, regulatory standards or targets can be defined in terms of risk to an individual.
- To consider the impacts of a disruptive event and calculate the radiological doses[2] to people in the future and then, separately, to discuss the likelihood that this might happen (the so-called 'disaggregated' approach). With this approach, separate regulatory targets for radiation doses might be set for events (or scenarios) with different degrees of likelihood (often expressed qualitatively; e.g. 'likely', 'less likely', 'highly unlikely').

In either approach, an evaluation of probability is essential: in the first 'risk approach' a sound quantitative estimate will provide more confident estimation of risk; in the second, some form of quantification of 'likelihood' is needed to decide which category to place an event or scenario into.

The probabilistic approach developed by ITM is based upon and strongly supported by deterministic models of the underlying tectonic processes that lead to magma intrusion, volcanism and rock deformation.

The ITM methodology will be used at three important stages of NUMO's repository siting programme:

- SITING STAGE 1: during the literature survey (LS) stage when potential PIAs are being assessed. The ITM methodology will use currently available information to allow comparison of sites in terms of confidence that they are likely to prove acceptable with respect to tectonic impacts.
- SITING STAGE 2: during the planning of the PIA site investigations, to identify geoscientific information requirements that will be needed to refine the Stage 1 analysis.
- SITING STAGE 3: at the point where PIAs are being evaluated and compared in order to select a preferred site (or sites) for detailed investigation (as DIAs).

The ITM project was mainly concerned with Stages 1 and 2 and focussed on evaluating comparative hazards of small (25 km^2) areas within a regional or sub-regional context of 100,000 to 10,000 km^2. This is partly because the project originally developed to compare several possible alternative volunteer sites that might arise within a region. However, it is clear that regional to sub-regional scale assessment of tectonic hazard will also be required even for single sites.

Application of the methodology in Siting Stage 3 is several years into the future and it is expected that it will be most efficient to carry out any necessary updates/refinements on a region-specific basis during the PIA investigations, when NUMO has narrowed down to a group of sites. The overall structure of the ITM methodology is described in Chapman et al. (2008) and consists of:

- assembling nationally available data and alternative models of the nature, causes and locations of tectonic processes and events;
- using probabilistic techniques to evaluate the likelihood and scale of future tectonic processes and events, shown as a function of their type and geographical distribution;

[1] Health risk is normally defined as the risk of death or serious genetic effects.

[2] Of course, a radiological dose can also be expressed in terms of health risk, by applying accepted dose-to-risk conversion factors.

- feeding information on these potential likelihoods and impacts to NUMO's performance assessment team so that feedback can be provided on repository performance under tectonic stress;

- providing clearly justified and traceable input to decision-making on consequent site suitability.

For convenience, the methodology for rock deformation and volcanic hazards assessment has been applied as two parallel tasks. This recognises the fact that, although the concept of each approach as shown above is similar, in some parts of the methodology they differ significantly in detail. Consequently, it was found that two teams with different specialities (structural, geophysics and tectonics specialists; volcanologists) worked efficiently in parallel. At the time of the ITM Methodology development it was noted that the two 'discipline' teams would need to integrate their work efficiently, as there are clear overlaps in the processes being evaluated (e.g. magma intrusion has an impact on rock stress regimes and vice versa). NUMO recognised it is important that such integration be carried out effectively when the methodology is applied to 'real' sites.

The methodology was first tested during its development by means of a Case Study of the Tohoku region of northern Honshu (Chapman et al., 2008) and then further developed and tested by application to a second Case Study region covering the whole of Kyushu (Chapman et al, 2009). The complete methodology is described in the latter report and is not presented again here in detail. The Tohoku Case Study looked into the varied strain response of the crustal plate to subduction of the Pacific Ocean plate (the key current tectonic driver for much of Japan) and the mechanisms that underlie the apparent clustering of Quaternary volcanoes in much of Honshu. The Kyushu Case Study region is among the more dynamic and rapidly changing plate boundaries in the world, with the tectonic situation being intrinsically more complex than in Tohoku. The observed modes of strain accommodation in Kyushu are varied but not yet fully understood, and the style of volcanism and geochemistry of the magmas varies considerably across Kyushu, compared to the reasonably simple arc volcanism in Tohoku. Forecasting future volcanism and faulting in Kyushu is less certain because the geological setting is evolving more rapidly. The fundamental assumption in Tohoku, that the plate boundary configurations and plate motions influencing rock deformation and volcanism are relatively stable over periods up to a million years, are less appropriate in Kyushu. Consequently, these two Case Studies allowed development and testing of the ITM Methodology under significantly different tectonic conditions that span a significant part of the range of tectonic environments across the Japanese archipelago.

1.2 Timescales and tectonic impacts on a geological repository

The impact of tectonic events and processes on the long-term safety of a geological repository is highly dependent on the time at which they might occur. Figure 1.1 shows the declining hazard of HLW (and spent fuel) as a function of time after production. Hazard is represented here as the ingestion radiotoxicity of all the radionuclides in the waste relative to the radiotoxicity of the amount of uranium ore required to manufacture the fuel from which the HLW was produced. It can be seen that the hazard declines rapidly over the first hundreds of years and, after about 3000 to 4000 years, reaches the same level as the uranium ore. At this time after disposal, a HLW repository would have a similar hazard potential (in terms of mobilisation and migration of radionuclides in groundwater to cause exposure to people and the environment) as a rich uranium ore body buried at a similar depth. It can be argued that the isolation and containment function of the geological repository for HLW has been largely fulfilled within the first ten thousand years.

Nevertheless, quantitative safety evaluations of repositories for HLW are required in most countries out to times of at least 100,000 years – the period addressed in the ITM project. In several countries, even those dealing with disposal of spent fuel, which can be seen from Figure 1.1 not to reach the natural cross-over point with uranium ore until about 100,000 years after disposal, only qualitative statements of safety are required after 100,000 years. Such statements are expected to discuss the longevity of safety functions into the distant future, to compare hazard to natural radiotoxic hazards and to discuss the long-term fate of

the wastes as the repository degrades. The engineered barriers and the waste itself are expected to be substantially degraded in the period 100,000 to 1 million years and beyond.

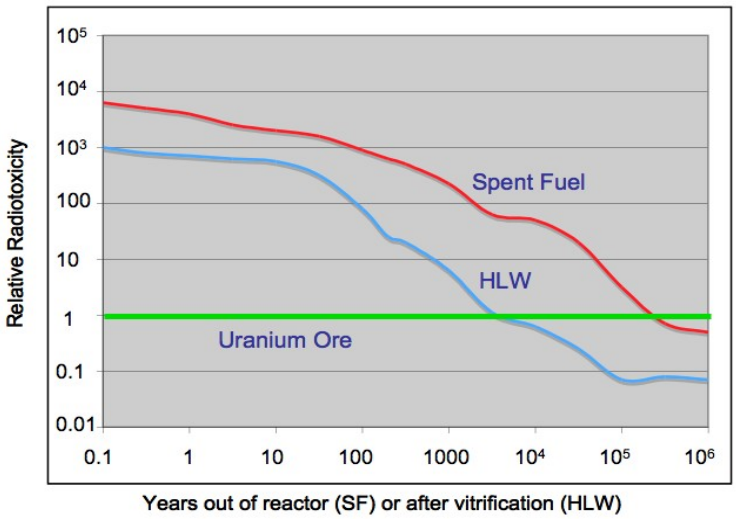

Figure 1.1: Declining radiotoxicity of HLW and spent fuel as a function of time after production: see text for description (after NUMO, 2004 and Chapman & Hooper, 2012).

One of the main reasons that only qualitative descriptions are expected in many countries is that many uncertainties associated with making quantitative estimates of actual radiological health impacts increase significantly and such forecasts loose credibility as actual indicators of safety. The other main reason is that, as can be seen, the hazard potential of the waste by mobilisation into the deep groundwater system will, over these protracted timescales, eventually start to approach levels similar to naturally occurring sources of radioactivity in the environment. The concepts discussed above are shown schematically in Figure 1.2.

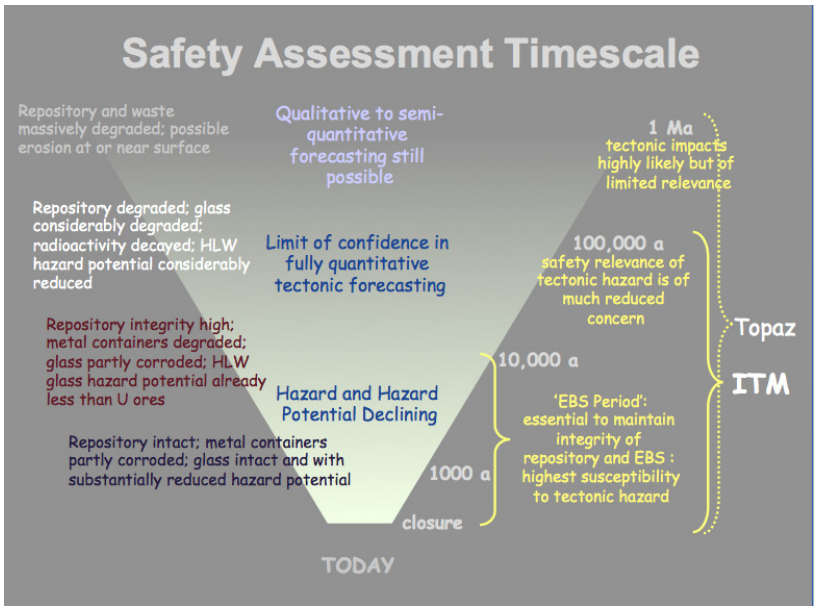

Figure 1.2: Schematic representation of the progressive degradation of a geological repository with time, the diminishing ability to make quantitative forecasts as uncertainty increases, and the decreasing importance of tectonic impacts to safety as the hazard potential also decreases. The ITM and TOPAZ project timescales are shown on the right hand side of the diagram.

Returning to tectonic impacts, it can be seen that events and processes that might disrupt a repository over the first 10,000 years are critical and need to be avoided, so far as possible, by correct siting in regions of low tectonic susceptibility. Thus, the probability of occurrence of

events and processes is an extremely important factor. The ITM project develops the tools to assess such probabilities out to 100,000 years – not only the period for which quantitative evaluations of doses or risk are typically required, but also the limit of confident forecasting of the tectonic framework of the Japanese islands, before major restructuring might be expected.

However, as the regulatory framework for geological disposal is still under development in Japan, NUMO wished to prepare a measure for providing information out to longer periods – up to 1 million years – again in the form of probabilities (or 'likelihoods') that could be used to express degrees of belief to alternative forecasts of the evolution and fate of a repository.

1.3 Going Beyond 100,000 years: the TOPAZ project

Consequently, following the completion of the ITM project, NUMO proposed that the expert team involved look at the possibilities and constraints of making forecasts of the likelihood and nature of tectonic impacts for longer periods into the future, from 100,000 years out to one million years.

The 'TOPAZ' project (**T**ectonics **O**f **P**otential **A**ssessment **Z**ones) was developed to see how the ITM methodology could be extended for this purpose. The approach developed is an extension of the concepts developed in the preceding ITM project. *Although intended for looking at very long times into the future, it is important to recognise that the approach is not limited to this period and can be deployed for the whole period over which hazard assessment is required.* The main steps of the TOPAZ methodology (see Figure 1.3) involve the development of alternative conceptual models characterising how the tectonic situation in a region might develop in the future and attaching expert degrees of belief to these alternative 'Regional Evolution Scenarios' (RES), using a formal expert elicitation methodology. These, in turn, are used to develop 'Site Evolution Scenarios' (SES), which describe how an RES might 'play out' at a specific location within the region being evaluated.

The ITM Kyushu Case Study (KCS) illustrated the importance of considering alternative framework models of evolution, especially in complex regions. In the KCS, the time period being assessed was 100,000 years but, owing to the complexity of the tectonic regime (compared to Tohoku, for example), regional evolution scenarios were considered, even for this timeframe. Thus, the KCS initiated thinking on the RES approach for TOPAZ and also led the expert team to consider that the TOPAZ methodology could be especially useful for regions with complex tectonics when considering **any** period of time into the future.

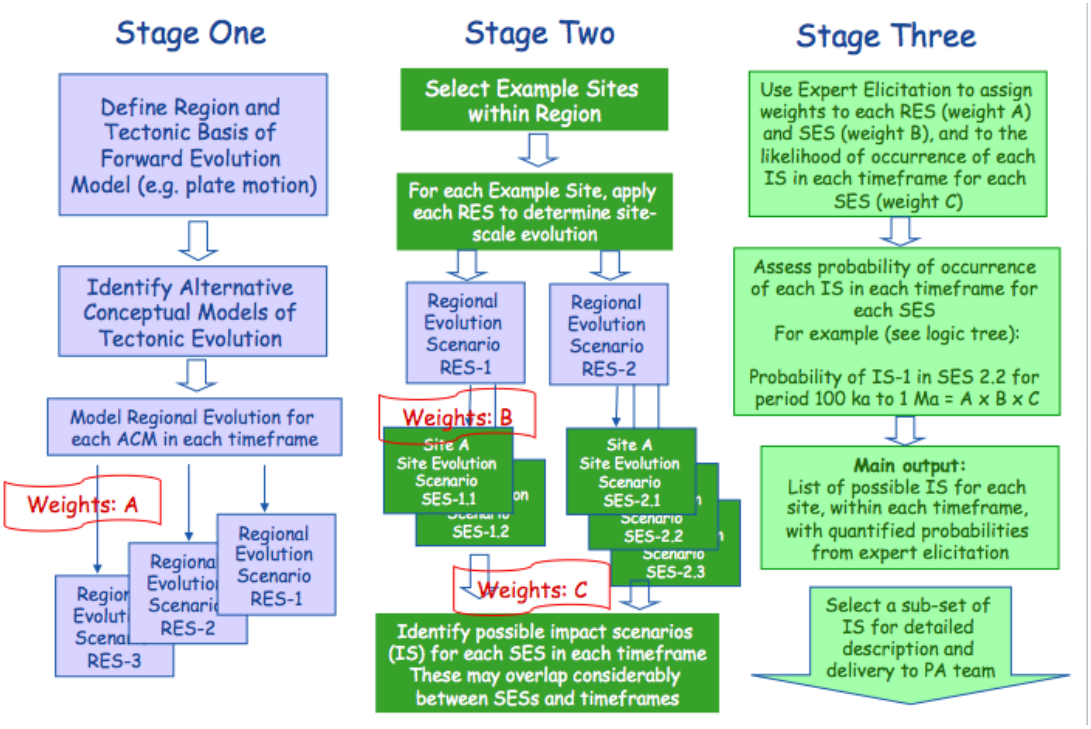

Figure 1.3: The main steps of the TOPAZ methodology

Stage 1 of the TOPAZ methodology thus involves the identification of credible alternative tectonic evolution scenarios at a regional level that incorporate different views on how major plate driving forces or geometries may change over a period of 1 million to a few million years, or on how crustal and upper mantle units may respond to such changes. These RES are developed at a scale typically of the order of 100,000 km^2 (the same area as the ITM Case Study regions). The procedure is as follows:

1. Identify region to be evaluated (typically of the order of 100 x 100 km around a potential repository siting area) – for the purposes of developing and demonstrating the TOPAZ methodology, the ITM Tohoku Case Study area was used as an example;
2. A set of RESs is proposed by one or more experts, for review and analysis by a wider group. The set should encompass know alternative views on tectonic evolution, including any 'outlier' opinions;
3. A group of experts reviews the set and adds any alternative RESs that it considers might be plausible, based upon current scientific knowledge;
4. The group is asked to provide relative weights to each RES, such "weights" being quantitative expressions of their belief that any particular RES is the most likely, or the relative likelihoods of alternative RESs for the next 1 to a few million years: this is done by a formal process of expert elicitation.

The development of a set of RESs for the Case Study area used in the TOPAZ project is described in **Section 2**.

A key feature of TOPAZ methodology is to incorporate the range of opinions of a wide group of experts in an objective manner to derive quantitative estimates of relative probabilities ('weights') of each RES (and, subsequently in Stages 2 and 3, of other key scenarios). This is done by a formal process of Expert Elicitation. *This is a critical step as it allows NUMO to solicit expert opinion from across the Japanese and international geoscience communities, as well as to ensure that the full range of opinion is incorporated into its site-suitability decision-making procedures.* The establishment and testing of the expert elicitation approach and its applications to the set of RESs for the Case Study area used in the TOPAZ project is described in **Section 4**.

Stage 2 of the TOPAZ Methodology looks at the evolution of a specific site of interest (potential repository site) in response to the RESs. As shown in Figures 1.3 and 1.4, in the TOPAZ project, an example site was chosen from the set used in the ITM-TCS.

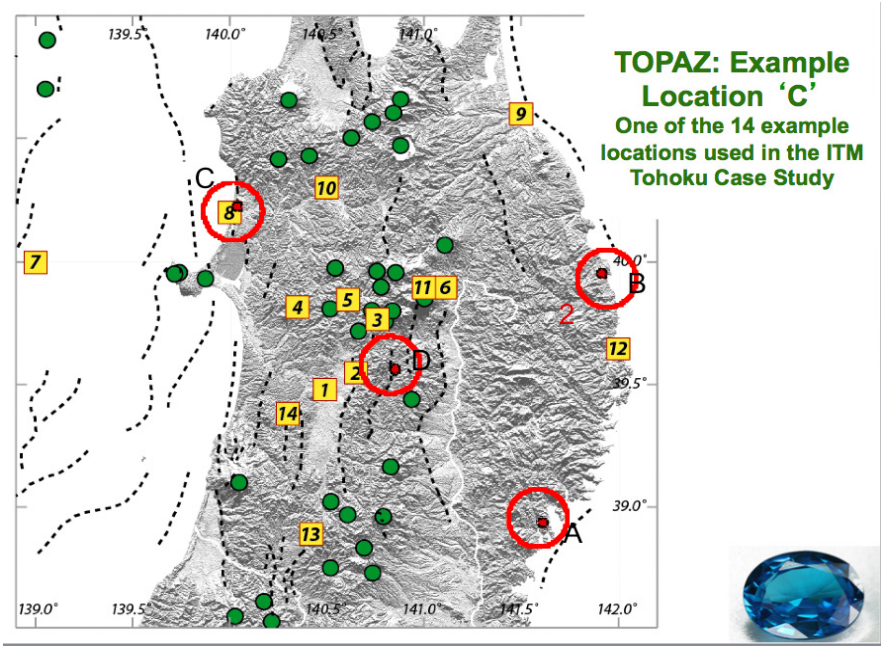

Figure 1.4: The example location used in TOPAZ to demonstrate the methodology: location 'C' from the ITM Tohoku Case Study.

As with ITM, sites are defined as being 5 km x 5 km in size, which allows the hazard mapping developed in ITM for this Case Study to be used for TOPAZ. As discussed below, however, it may also be necessary to consider applying the ITM-style hazard analyses at a greater scale to account for peripheral impacts on the repository. The procedure for Stage 2 is similar to that for Stage 1 and is as follows:

1. Apply each of the most highly weighted RESs to the site and develop a descriptive Site Evolution Scenario (SES) that postulates how the site will respond to the conditions imposed by the RES – this description will be in terms of whether specific tectonic events and processes become more or less likely or dominant in the evolution of the site. Each RES might generate one or more SESs;
2. Define Impact Scenarios (ISs) for each SES, identifying how specific impacts of relevance to the safety case might evolve or occur in response to each SES. This is facilitated if the safety assessment analysts are able to specify events that may be of concern or interest for them to analyse (i.e. omitting those of little significance to the performance of the repository). For instance, an IS might be development of a new volcano at the site, leading to occurrence of a volcanic event greater than a certain magnitude, or evolution of a fracture system to an active fault generating displacement greater than a certain magnitude.
3. Use the expert elicitation approach described for Stage 1 to assign quantitative degrees of belief (weights) to each SES and IS.

Stage 3 of the methodology integrates RES, SES and IS weights from Stage 2 with the ITM-derived probabilities of events (from the regional hazard maps developed using the ITM methodology) to produce an overall probability for each IS. The approach can be represented by a series of branches in a logic tree, as shown in Figure 1.5 below:

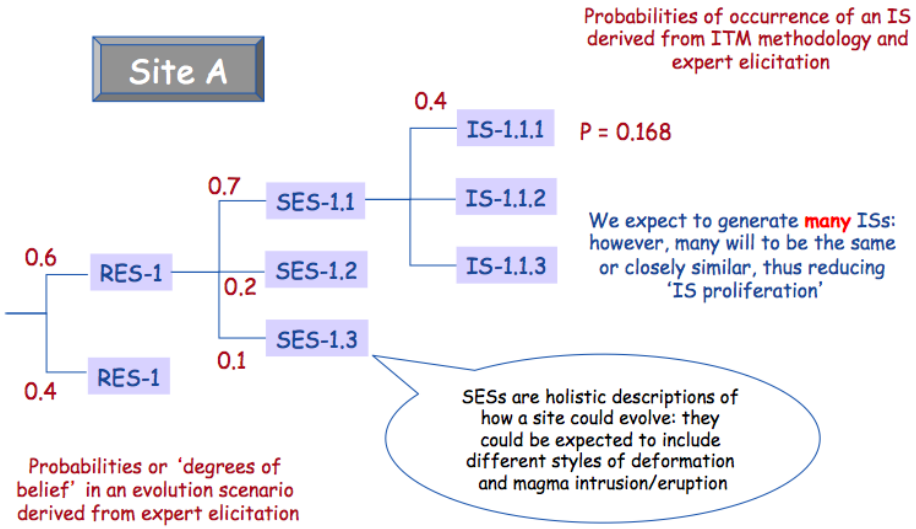

Figure 1.5: Estimating the probability of an Impact Scenario for a specific site ('Site A') by means of weighted degrees of belief in alternative scenarios on a logic tree.

In a comprehensive analysis, such as shown in Figure 1.5, a wide range of ISs might be developed, although with numerous redundancies of ISs expected along the many RES-SES branches. As many ISs will be very similar, or their consequences for the repository will be broadly equivalent, they can be amalgamated into 'bins' in a complete assessment (with individual probabilities of common ISs being added together).

For the purposes of developing and demonstrating the TOPAZ methodology, not all ISs were identified for the expert elicitation process, and a reduced set of three was identified for

consideration (one each for volcanic intrusion, fault displacement and uplift/exhumation), with only two of these being propagated through to a full probabilistic analysis for the Case Study Example Location. For the three ISs, four scenario logic trees were developed (see **Section 3**), as follows:

- **Logic Tree 1:** volcanic activity of any type and magnitude occurring within a 5 km x 5 km area at the site;
- **Logic Tree 1:** an explosive volcanic event > VOGRIPA M5 occurring within a 5 km x 5 km area at the site;
- **Logic Tree 2:** rock deformation occurring that leads to a Mw 6.5-7.5 earthquake at <10 km depth within the 5 km x 5 km area of the site;
- **Logic Tree 3:** rock deformation or tectonic uplift occurring that leads to point estimates of partial exhumation of the repository exceeding 200 m.

The two that were selected for propagation through the full TOPAZ methodology concerned new volcanic intrusion and fault displacement, and are defined in more detail as:

- New volcano formation occurring within a 5 km x 5 km area at the site:
    - from this, using the VOGRIPA frequency v. magnitude database, the probability of an explosive volcanic event > VOGRIPA M5 occurring within a 5 x 5 km area at the site is estimated.
- A shallow (<5 km) M 6.5-7.5 earthquake occurring on a concealed, undetected fault within the 5 km x 5 km area of the site that could be expected to propagate into the repository rock volume (approx. equivalent to a 0.3 m displacement).

The rationale for the selection of an M 6.5-7.5 earthquake on an undetected fault was discussed at a TOPAZ workshop on concealed active faults, held in Christchurch, New Zealand in January 2012, a note of which is included as **Appendix** to this report.

The rock deformation hazard component estimates the likelihood of an earthquake Mw 6.5 *or larger* (up to a prescribed Mmax value, which varies from region to region) impacting the repository. If an extremely large (M9 or similar) earthquake is deemed plausible within a given region, this possibility can be easily accounted for by raising the Mmax value to 9 or larger. However, current understanding is that M9 earthquakes are probably restricted to subduction interface faults, which have the extremely large surface area required for such a giant event. Most, if not all, onshore crustal faults probably do not have enough surface area to support the occurrence of such a huge earthquake.

Effectively, the demonstration work in TOPAZ has identified ISs in advance, rather than generating all potentially relevant ISs via the expert elicitation process, as is shown in Figure 1.5. This identification has been done from first principles, informed by known sensitivities in geological repository safety cases. It is emphasised that, at a 'real site', the more comprehensive approach involving Japanese geoscientists would be required. The 'demonstration approach' for a specified IS in Stage 3 is illustrated in Figure 1.6, which shows the important interplay between the team developing the scenario and impact probabilities and the team carrying out safety assessment.

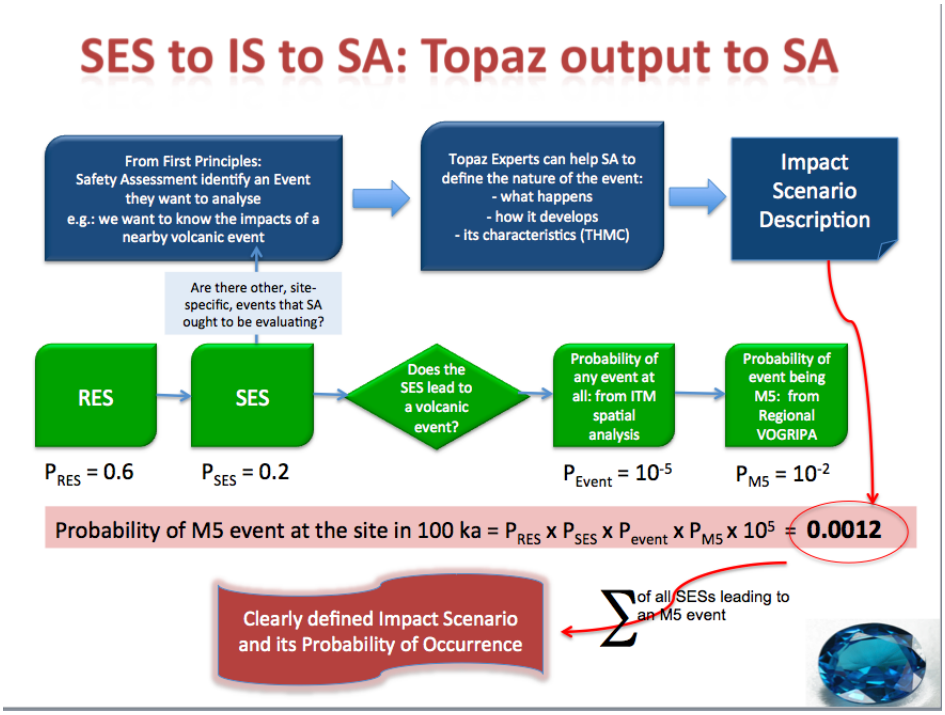

Figure 1.6: How an impact scenario probability (here, defined as the probability of occurrence of a specified magnitude of event) is derived by combing RES and SES weights with ITM-derived probabilities.

As noted above, the ITM hazard maps are based on estimated probability values in each 5 km x 5 km square. This roughly represents the possible size or 'footprint' of the geological repository. For some tectonic events, safety assessors will be interested in a 'near miss' event on the repository – that is, the probability that an event could occur close enough to the 5 km x 5 km repository footprint to impact its performance. Figure 1.7 shows an example of the formation of a new volcanic vent close enough (15 km in this example: equivalent to NUMO's EFQ exclusion factor for proximity to an existing volcano) to the repository that it could affect its performance. As discussed in NUMO (2004), it is generally considered that peripheral thermal, hydrogeological, gas and minor intrusion impacts of a new vent that could occur outside this radius would not be significant enough to consider in the first stage of repository siting – hence the value has been used as an initial Nationwide Evaluation Factor. It can be seen that, to avoid the 15 km exclusion zone use din this example, performance assessors would need to know the probability of a new vent being formed with an area about 50 times larger than the repository footprint. This can be defined as an interest in probability values that are 1.5 orders of magnitude (50 times) lower than the probability estimated for a single 5 km x 5 km area.

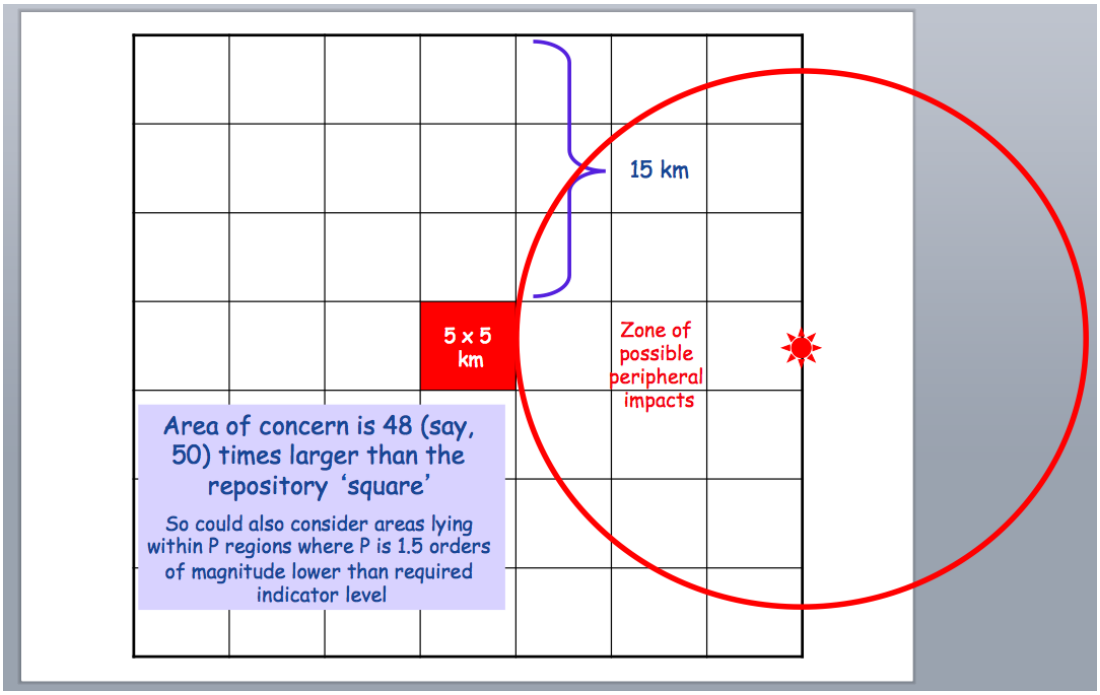

Figure 1.7: The increased area of interest for probability estimation (white square) that would be required to account for the peripheral impacts of a new volcanic vent formation (see text for further description).

1.4 This report

This report presents a demonstration of the methodology described in Section 1.3. It is emphasised that this is a partial demonstration, as it was not possible to explore all aspects of the approach. For example, only a sub-set of safety-relevant ISs was addressed and expert elicitation exercises were not carried out on all steps in the methodology. This was also the first time that a structured expert elicitation methodology had been used by the Japanese radioactive waste community, so this approach was novel in its own right. Also, it should be noted that the team did not have any of the site-specific stratigraphic, lithographic or structural information that would be obtained during an initial literature survey site investigation phase.

The output of a complete ITM-TOPAZ analysis of a site will be an essential underpinning component of any NUMO safety assessment and will comprise the following main elements:

- a complete description of the tectonic situation of a site;
- alternative conceptual models of how that situation might evolve over the period of interest to the safety assessment;
- a comprehensive list of impact scenarios for transfer to repository consequence analysis;
- the relative probabilities of each IS affecting the repository, which can be incorporated into a risk-based safety assessment and used to generate either radiological risks (to compare with regulatory standards) or probabilities of occurrence of scenarios to present along with dose consequences in a disaggregated dose-likelihood approach to regulatory standards.

Regardless of the direction that regulatory standard development takes in Japan, this information will be a central part of NUMO's safety case.

1.5 TOPAZ International Project Team Members

The Project involved the close interaction of Japanese and international experts to gain the necessary understanding to carry out the methodology development and testing. The international project team members all worked on the ITM project.

The international experts came from the following organisations (the acronyms used in this report are indicated):

MCM MCM Consulting, Switzerland
UBR University of Bristol, UK
USF University of South Florida, USA
UTX University of Texas, USA
GNS GNS Science, New Zealand
INT INTERA, USA
I2E In2Earth Modelling Ltd, Switzerland

TOPAZ International Project Team Members		
Rock Deformation	Dr Kelvin Berryman Dr Mark Stirling Dr Laura Wallace	GNS Science, New Zealand
	Professor Mark Cloos	University of Texas, USA
Volcanism	Professor Charles Connor Laura Connor Koji Kiyosugi	University of South Florida, USA
	Professor Steve Sparks	University of Bristol, UK
	Dr Olivier Jaquet	In2Earth Modelling, Switzerland
Interface with PA	Dr Mick Apted	INTERA, USA
Project Co-ordination	Professor Neil Chapman Ellie Scourse	MCM Consulting, Switzerland

2 Regional and Site Evolution Scenarios

As described in Section 1, the TOPAZ methodology first establishes a range of plausible Regional Evolution Scenarios (RES) considered to capture the range of evidence-based expert views on the principal evolution trends for the region of interest and then applies these at the site scale to develop an equivalent set of Site Evolution Scenarios (SES) in response to the different RESs. The RESs developed here are intended as examples to demonstrate the RES approach. We base the example RESs on plausible future scenarios for Tohoku tectonics, based on our understanding of how tectonics have evolved in Tohoku in the past. When the RES approach is eventually applied to a specific site, more exhaustive RESs should be developed by a panel of experts, who would also ensure the provision of more extensive and robust supporting data for the scenario development. This Section describes that process for the Tohoku region and the four example sites selected for demonstration purposes.

2.1 Tectonic Setting of Tohoku

Since the advent of plate tectonic theory, the Tohoku region, in northern Japan, from 35°N to 43°N, has been widely recognised as the type example of an active subduction zone. The northern Japan subduction zone, like nearly all others, can be subdivided into the trench axis, trench slope, forearc, volcanic arc, and back-arc regions. The tectonic activity associated with subduction comes in the form of faulting, magmatic intrusions and extrusions and vertical movements that range from folding to tilting of fault blocks to regional warping.

The Tohoku region forms most of northern Honshu. This region is an area of land primarily because of the interaction between the Pacific, North American, and Eurasian plates (Takeuchi et al., 1970; Taira, 2001). Tohoku and Hokkaido Island are on a prong of the North American plate that projects southward from the Bering Sea region. Geologic studies long indicated and geodetic studies recently confirmed (Wei and Seno, 1998; Heki et al., 1999) that the prong of the North American plate is moving slightly differently (generally a few mm/a differential motion) than the main part of the plate. These small differential movements result in the recognition of this plate segment as the Okhotsk subplate. Similarly, the segment of the Eurasian plate containing the crust of the Sea of Japan has a small differential movement, resulting in the recognition of the Amur subplate. From east to west, the Pacific plate subducts beneath the Okhotsk subplate, which in turn converges with the Amur subplate. A mountainous belt, including several large volcano clusters runs roughly along the centerline of Tohoku and is commonly referred to as the Ou Backbone Range.

The present phase of westward dipping subduction began at about 130 Myr (Sugimura and Uyeda, 1973; Engebretson et al., 1985). Cretaceous and Cenozoic intrusives and volcanics of the northern Honshu island were emplaced into and on top of several different basement terranes. Early Cretaceous plutonics are most abundant near the eastern coastline and occur offshore (Finn, 1994). Late Cretaceous arc magmatism appears to have been concentrated near the west coast of Honshu. These magmatic rocks were down-dropped during the rifting associated with the opening of the Sea of Japan and mostly buried by sediments (Finn et al., 1994). The volcanic arc appears to have maintained its present position since about 20 Myr. Crustal thickness beneath most of northern Honshu is between 30 to 35 km.

2.1.1 Basement of Tohoku

The basement of Japan is largely composed of Paleozoic and Mesozoic rock terranes created during westwards subduction along the eastern edge of Asia (Taira, 2001). The northernmost part of Honshu is underlain by the Oshima Belt, a Jurassic accretionary prism. Central Honshu is underlain by the Ashio Belt, largely composed of Triassic to Jurassic rocks that are variably deformed and little metamorphosed accretionary prism materials and the Abukuma Belt which is thoroughly metamorphosed under high-temperature / low-pressure conditions. Between these two Mesozoic terranes is the Kitakami Belt, a varied mixture of sedimentary, igneous and metamorphic rocks of Paleozoic age. This juxtaposition makes it appear that the early Mesozoic history of subduction and accretionary prism growth was followed by an episode of transform faulting (Taira, 2001). Strike-slip faulting shuffled the

accretionary prism - forearc basin terranes (Abakuma-Ashio and Oshima belts) with the arc-basement terrane (Kitakami Belt) that had formed along the edge of the Asian continent.

2.1.2 Forearc Region

The subducting Pacific plate directly underlies the forearc region. The geology of the forearc region of northeast Japan records a long history of subsidence and volcanogenic sediment accumulation. Because the upward flow of heat from the descending plate and through the forearc block is slower than the speed of subduction, geothermal gradients are very low across the forearc region (Honda, 1985). High-pressure/low-temperature blueschist metamorphic conditions are present at depth and the crystalline basement underlying the forearc region is cold and relatively strong. This forearc region has a rather smooth and continuous slope down to the Japan Trench and the forearc basin sediments as old as Cretaceous is little deformed.

One of the major discoveries, only possible because of the DSDP/ODP coring program, is that the forearc region of Northeast Japan is largely one of non-accretion during the Cenozoic with slow subsidence resulting from subduction erosion of the base of the hanging wall block above the descending Pacific plate (von Huene and Lallemand, 1990; Heki, 2004).

2.1.3 Volcanic Arc Region

The area around active volcanic arcs is a region of high heat flow because heat is advected to shallow levels in the subduction-generated magmas. Recent seismic tomography studies indicate most of the active volcanoes in northeast Japan are centred above areas with slow seismic velocities in the upper mantle and crust (Tamura et al., 2002). The current volcanic arc position was established at about 20 Myr (Kondo et al., 2004). The lifespan of typical large arc-type composite volcanoes appears to be about 1 to 2 million years (Davidson and De Silva, 2000) and numerous volcanic edifices have formed and decayed since the middle Miocene. Volcanic arcs are noted for giant composite volcanoes, but surrounding clusters of satellite cones and flows are typical. Along the northeast Japan arc, ten volcanic clusters about 50 km wide are separated by gaps between 30 to 75 km wide (Tamura et al., 2002).

Volcanic arc regions are areas of relatively thin, weak lithosphere. Many are areas with little non-volcanic tectonism, but some are areas with episodes of shortening or extension. Northern Honshu has a mountainous spine, the Backbone Range, that is largely a product of convergent deformation since the early Pliocene, but perhaps somewhat earlier (Nakajima et al., 2006).

2.1.4 Backarc Region

The geology of the backarc and arc region of northern Japan records a history of a recent profound change. Until mid-Cenozoic time, the crust forming the bulk of the basement of Japan was the edge of the Asia continent. The Japan Sea formed by continental rifting which evolved into seafloor spreading with ocean crust formation between 23 to 14 Myr (Jolivet et al., 1994). This rifting event occurred along the line of late Cretaceous volcanism, which paralleled the western edge of Honshu.

Additionally, backarc areas commonly have a few volcanoes that are tens of kilometres behind the line of the arc. The backarc area of Tohoku contains several active volcanic clusters. They are volumetrically minor, but others probably existed since the current phase of arc stability began in the Miocene.

Volcanic arcs that became a region of divergence that evolved into seafloor spreading have occurred at several sites along the western margin of the Pacific basin. Major episodes of backarc spreading have occurred along Izu-Bonin-Mariana and Tonga-Kermadec subduction zones. In the backarc regions of these oceanic subduction zones, lines of extinct volcanoes parallel the current volcanic arc with a region of new ocean crust in between.

It is evident that rifting is localised to the part of the lithosphere that was sufficiently weakened by the ascent of magmas that a change in the force balance near the subduction zone led to lithospheric divergence that was centred on the arc. Backarc spreading is a subordinate process to subduction. During the time seafloor spreading created a 200 km width of new

ocean crust beneath the Japan Sea, an approximately 2000 km width of Pacific plate was consumed by subduction at the Japan Trench.

In contrast to the low heat flow of the Tohoku forearc region, the backarc region is an area of high heat flow because of magmatism and the rifting that thinned the lithosphere. The Miocene phase of rifting that led to the phase of seafloor spreading that formed the Sea of Japan created many normal faults in the basement. Some of these high-angle faults have been reactivated since the latest Pliocene as reverse faults generating large folds in the overlying Miocene and younger strata. A long period of slow subsidence and sediment accumulation has become a recent period of uplift and erosion.

2.1.5 Active Tectonics

Most of the active tectonic movements in the region are directly a response to subduction along the plate interface zone that surfaces at the Japan Trench. This movement, at a speed of 9 cm/yr, causes the frequent earthquakes that form the inclined Wadati-Benioff seismic zone beneath northeast Japan and the belt of arc volcanism along the Backbone Range. The disastrous March 11, 2011, M9.0 earthquake is the most recent manifestation of subduction along the Japan Trench and is probably the largest seismic event in the area since 869AD (Minoura et al., 2001). As slip at the focus of the earthquake was on the order of 30 to perhaps 50 m, this event accounts for about 300 to 500 years of plate convergence (Simons et al., 2011). Whether several centuries of plate motion must occur before mechanical asperities lock a subduction zone and begin to build up large elastic strains that can lead to the next large 'megaslip' event is a matter of much interest.

A significant secondary interaction that has affected the Tohoku region results from convergent deformation that has been distributed between the eastern margins of the Sea of Japan and the Backbone Range. This ~200 km wide region accommodates significant folding with reverse faulting at several areas near the west coast of northern Honshu and a broad region of uplift and high-angle faulting forming the Backbone Range along the line of the volcanic arc. Across this region, convergence is occurring at speeds of at least 10 mm/a to perhaps 15 mm/a (Tamaki and Honza, 1985; Okamura et al., 1995; Sagiya et al., 2000; Miura et al. 2002). Folded and faulted strata indicate the current phase of crustal shortening began at ~4 Myr and that the zone of deformation appears to have widened from west to east. The westward limit of shortening in the Sea of Japan is well defined as a deformation front.

Most earthquakes in the region of the volcanic arc and backarc occur at depths less than 15 km (Zhao et al., 2000). Seismicity is sparse and shallow in areas of high heat flow and nearly lacking beneath volcanoes. A distinct belt of seismicity and surface faulting extends along the western coast of northeast Japan north and south of Niigata. Scattered reverse-slip earthquakes as large as M7.8 nucleate at depths of 10 to 20 km (Okubo and Matsunaga, 1994). Faulting and folding in the belt is a result of > 1 cm/yr convergence between Amur and Okhotsk subplates. This area of active folding, reverse faulting, uplift and erosion was an area of subsidence during the Miocene phase of rifting.

Normal faults created during Miocene rifting were buried by volcanogenic sediment shed westward into the widening depression. The convergent deformation in the Niigata region began in the late Pliocene, at about 3 Myr (Okamura et al., 1995). The crystalline basement in this region primarily deforms by reversing the movement on normal faults created during the rifting phase – "inversion tectonics." The overlying sediments respond to the deformation primarily by drape folding over the rising fault blocks. Geometrical complexities and new breakouts occur in many areas because the old fault system does not everywhere have optimal orientations for the imposed movements.

Some convergence is occurring within the region of the volcanic arc. These movements have created the Backbone Range, a topographic divide that has profoundly affected regional drainage and sedimentation patterns (Sato, 1994). Between volcanic clusters, some of the shortening occurs by episodic earthquake-generating stick-slip movement along reverse faults (Zhao et al., 2000). Directly beneath most volcanic clusters, the temperatures are high, making much of the crust ductile, hence, there is little seismicity. Especially rapid uplift of the Backbone Range began at about 2 Myr (Sato and Amano, 1991).

In summary, the tectonic environment of northern Japan is dominated by subduction at the Japan Trench causing arc magmatism with second-order convergent motions that are

concentrated in the backarc region, but extend into the area of the arc. The current mode of tectonism in northern Honshu began at about 4 Myr and has been well established since 2 Myr (Taira, 2001). The initiation of this tectonic regime is probably a manifestation of the creation and movement of the Amur and Okhotsk subplates. Why these convergent movements began, which are secondary compared to fast, long-term subduction at the Japan Trench, is not known. They may be a result of a modest reorientation of plate motions about the Pacific basin that occurred between 5 to 3 Myr (Cox and Engebretson, 1986; Pollitz, 1986).

2.2 Overview of Regional Evolution Scenarios for Tohoku

For the purposes of demonstrating the RES approach, we assess Regional Evolution Scenarios for three time periods of interest: 0-10 kyr, 10-100 kyr, 100 kyr – 1 Myr. Other alternative Regional Evolution Scenarios could also be developed for the Tohoku region, although we suggest that the four presented here are a representative range of plausible scenarios for the future tectonic evolution of Tohoku.

2.2.1 RES 1: Tectonic boundary conditions are the same from the present to 1 Myr

In this scenario, we assume that the overall tectonic boundary conditions in the Tohoku region remain the same as they are today for the next 1 Myr (Fig. 2.1). As part of this scenario, we assume that the rate of permanent plate boundary deformation occurring within the upper plate (>15 mm/a) remains similar to what it is today, and that the subducting Pacific slab maintains its current configuration (configuration defined by Hasegawa et al., 1994) with respect to the upper plate. We also assume that the crust underlying the Sea of Japan continues underthrusting beneath Honshu at its current rate of ~15 mm/a, eventually evolving into a subduction margin (cf. Tamaki and Honza, 1985). The results of this RES for the various timeframes are shown schematically in Figure 2.2.

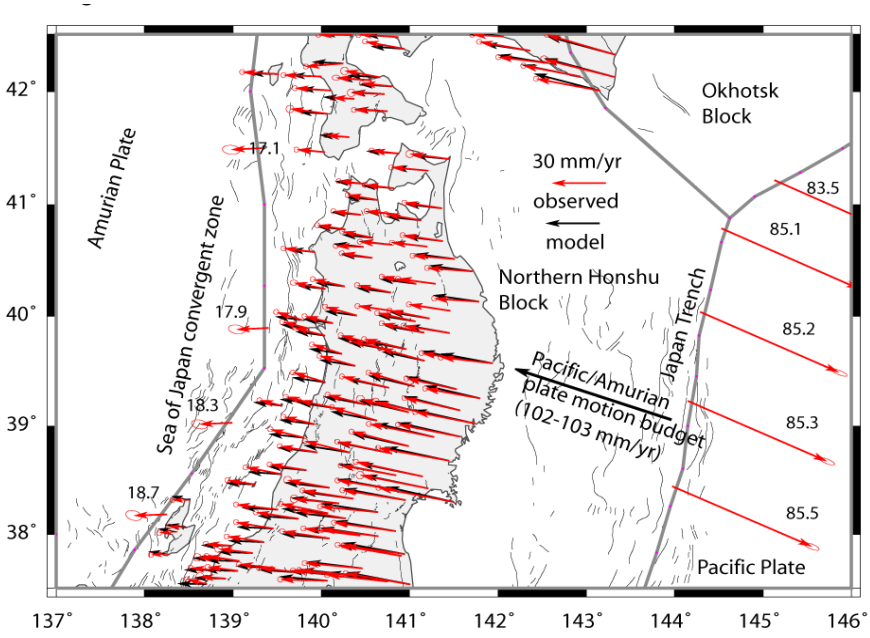

Figure 2.1: Tectonic setting and GPS velocity field in Northern Honshu (shown relative to a fixed Eurasian plate). Thinner grey lines are active fault traces. Ellipses show uncertainty at 65% confidence level. Velocities are derived from daily solutions provided by Geographical Survey Institute of Japan. Block boundaries (heavy grey lines) used in the elastic block modelling to interpret GPS velocity field in terms of long-term block motion (Pacific, Amurian, and northern Honshu Block) and fits to the GPS velocities (red arrows) from the best-fitting model (black arrows) (from Wallace et al., 2009). Arrows on the boundaries with numbers beside them (mm/a) show the motion of the Northern Honshu block relative to the Amurian and Pacific Plates. Interpretation of the GPS velocities also suggest that 3-4 mm/a of contraction occurs in the Backbone Range of northern Honshu (Miura et al., 2004; Wallace et al., 2009).

Although this scenario assumes relatively constant tectonic boundary conditions, it could lead to some degree of temporal and spatial change in the distribution of faulting and volcanism with time. For example, as the convergent margin and associated fold and thrust belt evolves near the west coast of Tohoku, more localization of deformation could be expected onto individual structures, and/or spatial changes in distribution of active deformation could occur as a result of the natural evolution of the fold and thrust belt there. This could lead to substantial changes in rock deformation strain and uplift rates at particular locations out to longer time periods. It is also likely that optimally oriented bedrock faults (i.e., approximately north-south striking) could become reactivated. Although we expect the location of volcanism in the arc to be relatively stable, it is possible that volcanism could move into the "gap" region between volcanoes, possibly driven by temporal and spatial changes in magmatic supply and mantle wedge flow regimes over longer timeframes (although we consider a stable location for the magma supply and subsequent volcanism more likely).

- ***Present day – 10 kyr scenario.*** We do not expect this scenario to be significantly different from what is observed today, particularly in terms of the location of deformation, uplift, and active volcanism.
- ***10 – 100 kyr scenario.*** We do not expect this scenario to be significantly different from the present day to 10 kyr scenario, although it is possible that some spatial changes in the rates and location of volcanism, deformation, and uplift could begin to occur during this longer time period, as fault and volcanic systems evolve. We anticipate that most of the contractional deformation accommodated in the upper plate during this period will continue to occur within the Backbone Range contractional domain (Hasegawa et al., 2000) and along the evolving convergent margin adjacent to the Sea of Japan. Volcanism is unlikely to migrate significantly outside of the current location of active volcanism due to the stability of magma supply systems.
- ***100 kyr – 1 Myr scenario.*** Over longer time periods it is possible that some spatial and temporal changes in the distribution of volcanism and rock deformation could occur, but we anticipate that rock deformation will still remain focused within the Backbone Range and the western part of Honshu. It is possible that migration of arc volcanism into the gaps between the currently active volcanoes will occur start during this period, but it is unlikely that active volcanism will have migrated significantly within or across the margin (for example, into the forearc domain). If the Sea of Japan convergent zone deformation becomes progressively localised and evolves towards an incipient subduction margin, it is possible that larger portions of the convergent component of plate motion will be shifted into the Sea of Japan region, possibly localizing on structures just offshore. The future localization of slip in the Sea of Japan region will depend on the details of evolution of the associated fold and thrust belt, and the distribution of optimally oriented bedrock structures. If the Sea of Japan is evolving into a subduction margin (e.g., Tamaki and Honza, 1985), we expect that 1 Myr into the future the leading edge of the underthrusting Sea of Japan crust will have migrated eastward by ~15 km, and will have reached ~37 km depth, compared to ~30 km depth that we assume for its current depth (note that the location of the leading edge of the underthrusting Sea of Japan crust is highly uncertain).

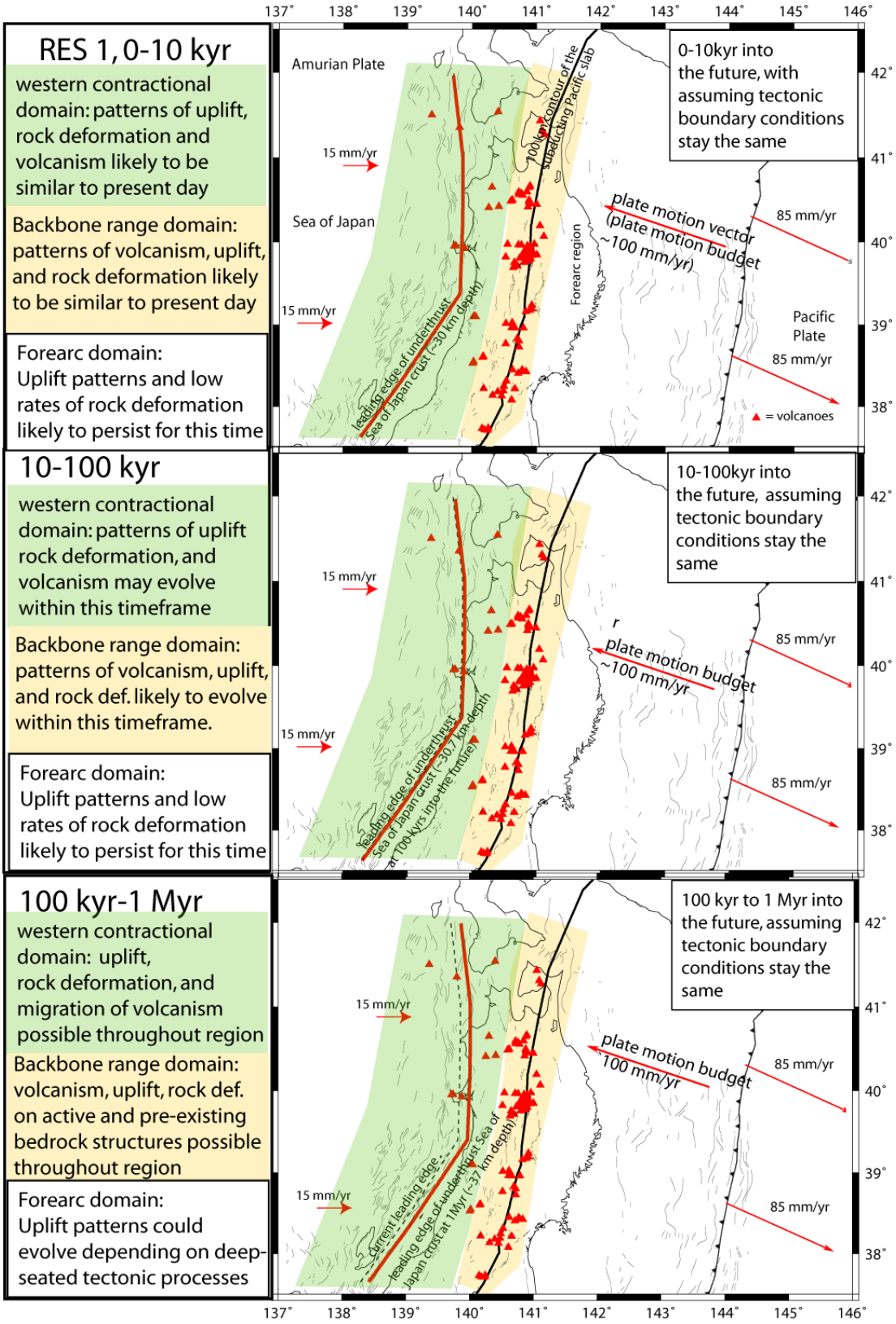

Figure 2.2: Schematic of major tectonic domains and likely evolution of faulting and volcanism into the future for all 3 stages of RES 1. The light green highlighted region indicates the evolving contractional domain associated with underthrusting of the Sea of Japan, while the light orange highlighted area shows the currently active arc and the Backbone Range contractional domain. The dashed black line represents schematically the current likely leading edge of the underthrusting Sea of Japan crust, while the red line shows the likely position of the leading edge at the end of each timeframe. Red triangles are Quaternary volcanoes and black lines are active faults.

2.2.2 RES 2: The amount of relative plate convergence accommodated in the upper plate doubles from present to 1 Myr in the future

In this scenario we assume that the amount of permanent horizontal convergence accommodated within the upper plate doubles from its current value (~15 mm/a) in a linear fashion to ~30 mm/a at 1 Myr into the future. This is similar to the increase in upper plate deformation that occurred in northern Honshu around 2.4 Myr (Sato and Amano, 1991). There are a number of potential triggers for this scenario, including: (1) an increase in the convergent component of Pacific/Eurasian plate motion in the Tohoku region (this could occur by an anti-clockwise shift in Pacific-Eurasia relative motion vector, or by acceleration of the motion between the two plates); (2) the subducting Pacific slab flattens its subduction angle (similar to what currently occurs along parts of the Andean margin), causing transmission of a larger component of plate boundary strain into the upper plate; (3) the Sea of Japan convergent zone evolves into a self-sustaining subduction plate boundary with a negatively buoyant slab, allowing a progressively larger amount of the plate motion budget to be accommodated in the Sea of Japan region. In this RES (see summary in Fig. 2.3) we expect that most of the rock deformation will still be accommodated in the Backbone Range and within western Honshu, but it is very likely that any optimally oriented bedrock structures (approximately north-south striking) anywhere in Tohoku could be reactivated to accommodate these changes in plate tectonic boundary conditions. In this scenario, it is plausible that rock deformation rates and uplift rates could double in the regions of current active deformation. Increased uplift and erosion in the areas of most intense shortening could lead to decompression melting of the crust and triggering of ignimbrite and caldera formation. For the most part there is unlikely to be a major change in the position of the volcanic arc in this RES during the time period of interest. However, if an onset of flat slab subduction occurs, the volcanic arc could migrate westward of its current position (Fig. 2.3). Perturbation of the flow regime in the mantle wedge is also likely to occur in the flat slab scenario, as well as the scenario where the Sea of Japan evolves into an early stage subduction margin. This should be considered in the context of the volcanic evolution of the region. This RES could open up the possibility of future volcanism anywhere in the Backbone Range and western northern Honshu during the longer timeframes of interest.

- ***0-10 kyr timeframe:*** We do not expect this scenario to be significantly different from what is observed today, particularly in terms of the location of deformation, uplift, and active volcanism.
- ***10-100 kyr timeframe:*** We do not expect this scenario to be significantly different from the present day to 10 kyr scenario, although it is possible that some spatial changes in the rates and location of volcanism, deformation, and uplift could begin occurring during this longer time period, as fault and volcanic systems evolve. We anticipate that most of the contractional deformation accommodated in the upper plate during this period will continue to occur within the Backbone Range contractional domain and along the evolving convergent margin adjacent to the Sea of Japan. The steady increase in horizontal convergent rates accommodated within the upper plate during this period (from 15-17 mm/a) could cause rates of faulting on known active faults to increase correspondingly, or for optimally oriented bedrock structures to be reactivated to accommodate this. Volcanism is unlikely to migrate significantly outside of the current arc.

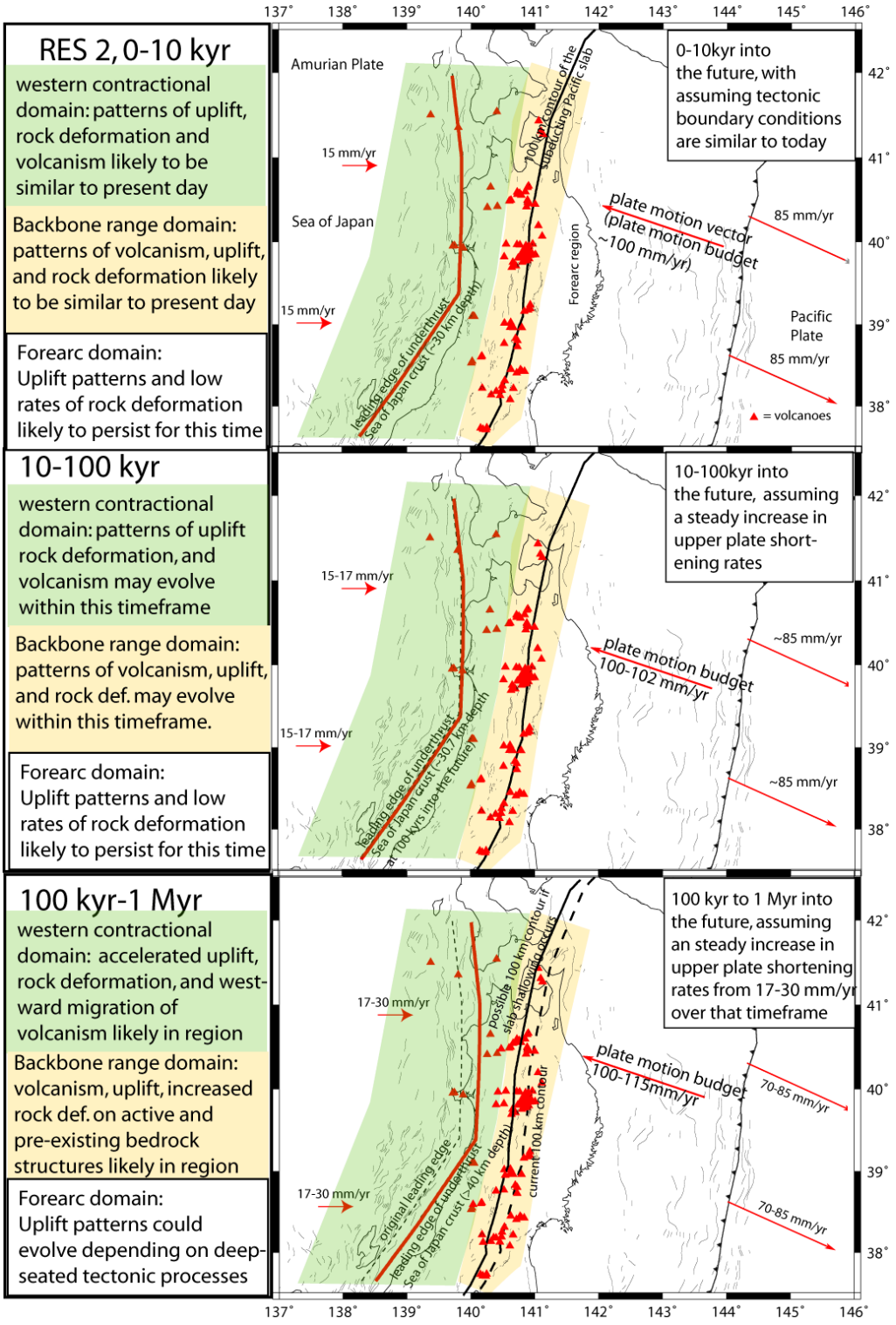

Figure 2.3: Schematic of major tectonic domains and likely evolution of faulting and volcanism into the future for all 3 stages of RES 2. The light green highlighted region indicates the evolving contractional domain associated with underthrusting of the Sea of Japan, while the light orange highlighted area shows the currently active arc and the Backbone Range contractional domain. The dashed black line represents schematically the current likely leading edge of the underthrusting Sea of Japan crust, while the red line shows the likely position of the leading edge at the end of each timeframe. The heavy dashed black contour shows the current position of the 100 km contour to the surface of the subducting Pacific slab, while the heavy line shows the possible position of this at 1 Myr in the future if the increase in upper plate shortening is related to a westward advance of the subducting slab.

- ***100 kyr – 1 Myr timeframe:*** During this period the convergent component of plate motion accommodated in the upper plate increases from 17-30 mm/a. During this time we anticipate that rock deformation will still remain focused within the Backbone Range and the western part of Honshu, with some reactivation of optimally oriented bedrock structures across the Tohoku region. It is possible that migration of arc volcanism into the gaps between the currently active volcanoes will occur during this period. If a period of subducted Pacific slab flattening occurs, then the location of active arc volcanism could be expected to migrate westward from its current position (probably by no more than 20-40 km during this period). If the Sea of Japan convergent zone deformation becomes progressively localised and evolves into an incipient subduction zone, it is possible that larger portions of the convergent component of plate motion being accommodated within the upper plate could shift into the Sea of Japan region during this time, possibly localizing on structures just offshore. The future localization of slip in the Sea of Japan region will depend on the details of evolution of the associated fold and thrust belt, and the distribution of optimally oriented bedrock structures. If the Sea of Japan is evolving into a subduction margin, we expect that 1 Myr into the future the leading edge of the underthrusting Sea of Japan crust will have migrated eastward by ~23 km, and will have reached >40 km depth, compared to ~30 km depth that we assume for the its current depth (note: this is not well-constrained). The incipient Sea of Japan subduction zone scenario would significantly perturb the flow regimes and magma supply within the mantle wedge, and we expect that this scenario could lead to a shut down of active volcanism near the west coast of northern Honshu as the underthrusting Sea of Japan encroaches on and perturbs the magma supply to those regions.

2.2.3 RES 3: Pacific-Eurasia relative plate motion becomes more oblique from present to 1 Myr in the future.

Pacific Plate absolute motion has undergone a number of changes throughout the Cenozoic (Wessel and Kroenke, 2007, and references therein). In particular, at ~6 Myr Pacific absolute plate motion (APM) underwent shift in direction of motion, leading to more rapid northerly absolute motion of the Pacific Plate, although in northern Japan the result was to shift Pacific Plate APM to a more southerly direction (by ~15 degrees) (Wessel and Kroenke, 2000). It is suggested that this change occurred due to a change in plate boundary forces related to Ontong Java Plateau collision with the Pacific/Australia Plate boundary in the western Pacific and ongoing subduction at the northern and western boundaries of the Plate (Wessel and Kroenke, 2000, 2007). This change was not likely to be abrupt, and we expect that it occurred more gradually over a period of ~1 Myr.

In this RES, we assess the possibility that Pacific Plate motion could take a similar shift in the opposite direction over the next 1 Myr period, leading to more oblique relative motion with more northerly-directed Pacific Plate motion in the northern Japan region. In RES 3, we assume that the relative motion vector between the Pacific and Eurasian Plates undergoes a 15 degree anti-clockwise shift from present to 1 Myr in the future; the effect of this shift is to have a larger northward component for the motion of the Pacific Plate relative to Eurasia. This would shift the angle between relative plate motion and the direction perpendicular to the trench (e.g., obliquity angle) from 10º (currently) to 25º at 1 Myr. At subduction plate boundaries such as Sumatra, partitioning of the margin-parallel component of relative plate motion onto strike-slip faults within the upper plate begins to occur when the obliquity angle exceeds some critical angle (dependent on the strength of the upper plate, and the shear stresses acting on the plate boundary; McCaffrey, 1991). In Sumatra and the Philippines, this critical angle is ~20-25º, while it is as high as 25-45º in Alaska (McCaffrey, 1991; McCaffrey et al., 2000). One of the major outcomes of an increase in plate motion obliquity suggested in this RES is the potential for reactivation of bedrock structures in the Tohoku region such as the Tanakura Fault and the Hizume-Kesennuma Fault (Fig. 2.4). These currently inactive bedrock structures strike NNW, and are in an ideal orientation to accommodate a more northerly component of Pacific-Eurasia relative plate motion. The results of this RES for the timeframes are summarised schematically in Figure 2.5.

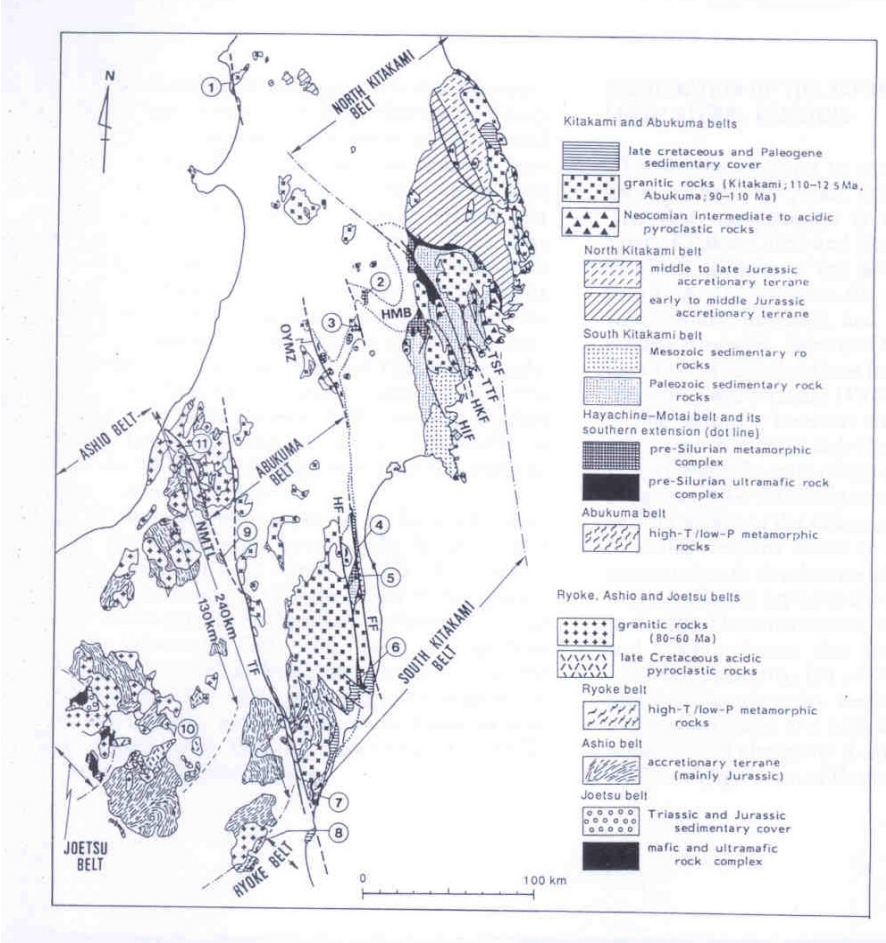

Figure 2.4: Bedrock and fault map from Otsuki (1992). This figure illustrates much of the pre-existing bedrock faulting, including extensive NNW striking faults in the forearc region. It is possible that such faults could become reactivated if there is a change in orientation of relative plate motion.

- ***0-10 kyr timeframe:*** We do not expect this scenario to be significantly different from what is observed today, particularly in terms of the location of deformation, uplift, and active volcanism.
- ***10-100 kyr timeframe:*** We do not expect this scenario to be significantly different from the present day to 10 kyr scenario, although it is possible that some spatial changes in the rates and location of volcanism, deformation, and uplift could begin occurring during this longer time period, as fault and volcanic systems evolve. We anticipate that most of the contractional deformation accommodated in the upper plate during this period will continue to occur within the Backbone Range contractional domain (Hasegawa et al., 2000) and along the evolving convergent margin adjacent to the Sea of Japan. Volcanism is unlikely to migrate significantly outside of the current volcanic arc.

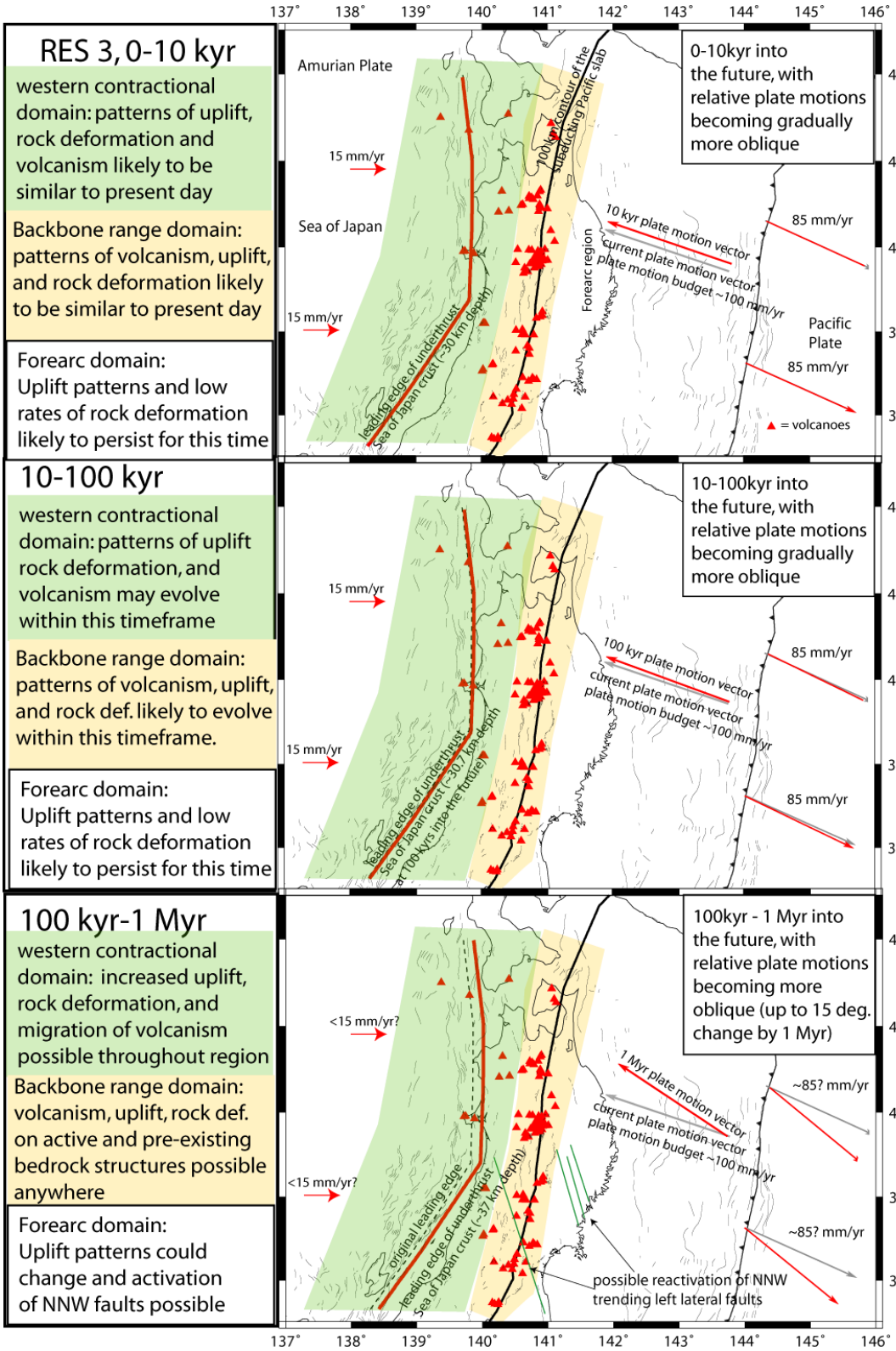

Figure 2.5: Schematic of major tectonic domains and setting between 100 kyr – 1 Myr into the future for RES 3. The light green highlighted region indicates the evolving contractional domain associated with underthrusting of the Sea of Japan, while the light orange highlighted area shows the currently active arc and the Backbone Range contractional domain. The dashed black line represents schematically the likely leading edge of the underthrusting Sea of Japan crust at present, while the red line shows the likely position of the leading edge at the end of each timestep. The dark green lines in the forearc schematically show the location of some of the NNW trending bedrock structures, such as the Tanakura fault.

- ***100 kyr – 1 Myr timeframe:*** As relative plate motion becomes more oblique to the plate boundary through this time period (the obliquity will increase from just above 10º to 25º by 1 Myr), the potential for reactivating NNW trending bedrock faults in the Tohoku region (Figs. 2.4 and 2.5) such as the Tanakura fault increases. We expect that this will particularly come into play during the latter half of this time period (>500 kyr into the future). The point at which slip partitioning in the upper plate begins will depend on the details of the strength of the upper plate and the shear stresses acting on the plate boundary interface and other major faults in the system. Over longer time periods it is possible that some spatial and temporal changes in the distribution of volcanism and rock deformation could occur, but we anticipate that most rock deformation will remain focused within the Backbone Range and the western part of Honshu, and along optimally oriented NNW trending bedrock faults such as the Tanakura fault. It is possible that migration of arc volcanism into the gaps between the currently active volcanoes will occur during this period, but it is unlikely that active volcanism will migrate substantially relative to its current position, or migrate across the margin (for example, into the forearc domain). If deformation in the Sea of Japan convergent zone becomes progressively localised and evolves towards an incipient subduction margin, it is possible that larger portions of the convergent component of plate motion being accommodated within the upper plate could shift into the Sea of Japan region, possibly localizing on structures just offshore. The future localization of slip in the Sea of Japan region will depend on the details of evolution of the associated fold and thrust belt, and the distribution of optimally oriented bedrock structures. If the Sea of Japan is evolving into a subduction margin, we expect that 1 Myr into the future the leading edge of the underthrusting Sea of Japan crust will have migrated eastward by ~15 km, and will have reached ~37 km depth, compared to ~30 km depth that we assume for the its current depth.

2.2.4 RES 4: The amount of plate convergence accommodated within the upper plate decreases linearly to a neutral state at 1 Myr

Tectonics in northern Honshu throughout the Cenozoic have been dominated by alternating periods of extension and contraction (Sato and Amano, 1991, among others). From 22-13 Myr, northern Japan tectonics was strongly influenced by back-arc rifting in the Sea of Japan, while 13-2.4 Myr was a period of transition from upper plate rifting to upper plate contraction. 2.4 Myr to present has seen a shortening dominated regime in Tohoku upper plate tectonics. Extension in the upper plate of the Sea of Japan region and northern Honshu was most likely driven by the initiation of a phase of rollback of the subducting Pacific slab, as suggested for other plate boundaries worldwide (cf. Schellart and Lister, 2004, and references therein). Oceanic crust subducting at the Japan Trench is Cretaceous in age, and is among the oldest oceanic crust on earth. It is certainly plausible that the slab could founder and that an episode of slab rollback could occur again sometime in the next few million years. RES 4 (see Fig. 2.6) considers the possibility that a phase of slab rollback and a shift to upper plate extension could occur in the near future, and that over the next 1 Myr we could see a transition from the current upper plate shortening regime to a more or less neutral state of stress in the upper plate in the lead up to a phase of back-arc extension.

- ***0-10 kyr timeframe:*** We do not expect this scenario to be significantly different from what is observed today, particularly in terms of the location of deformation, uplift, and active volcanism in Tohoku.
- ***10-100 kyr timeframe:*** We do not expect this scenario to be significantly different from the present day to 10 kyr scenario, although it is possible that some spatial changes in the rates and location of volcanism, deformation, and uplift could begin occurring during this longer time period, as fault and volcanic systems evolve and the plate tectonic boundary conditions begin to change. We anticipate that most of the permanent contractional deformation accommodated in the upper plate during this period will continue to occur within the Backbone Range contractional domain and along the evolving convergent margin adjacent to the Sea of Japan. Volcanism is unlikely to migrate significantly outside of the current volcanic arc.

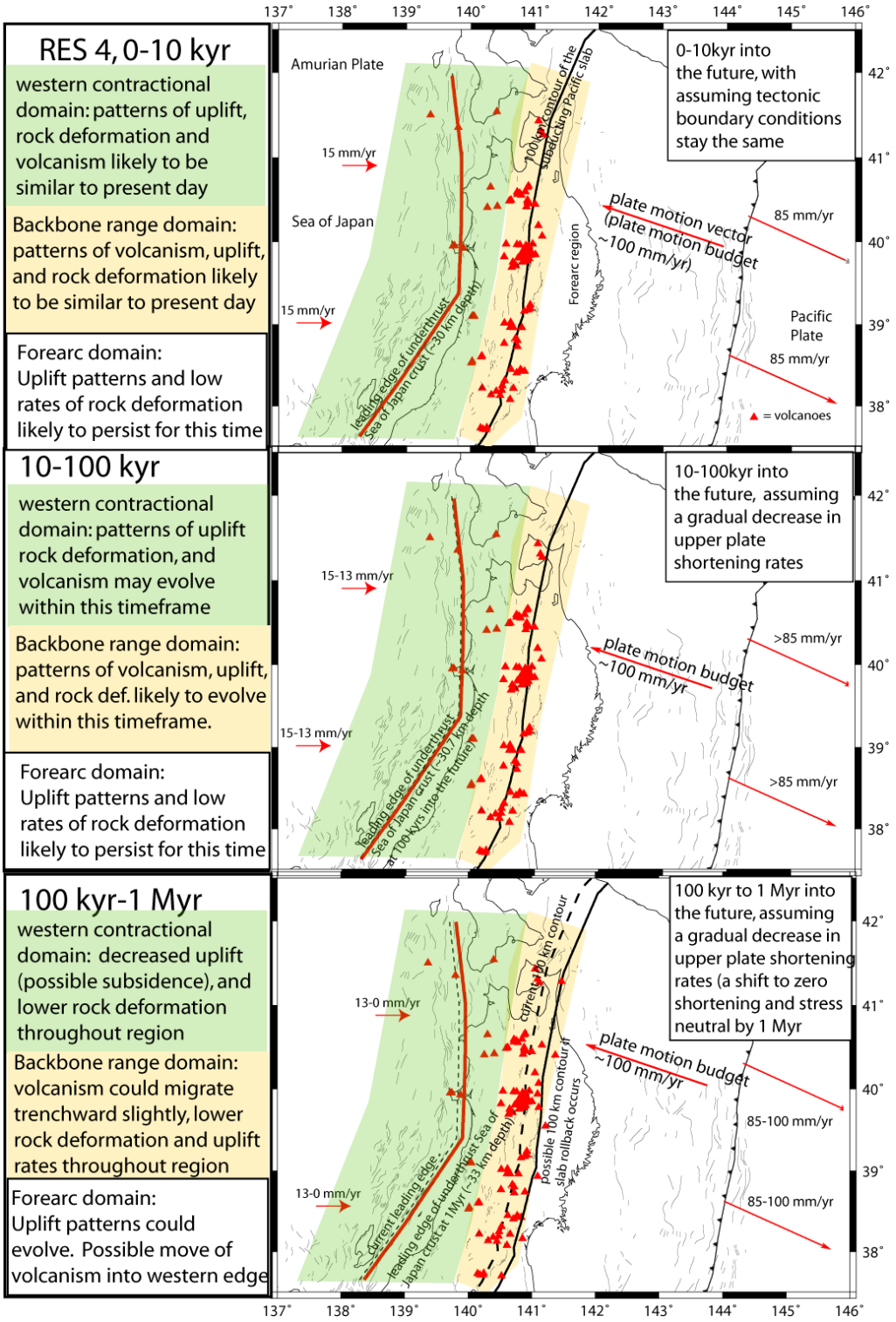

Figure 2.6: Schematic of major tectonic domains and likely evolution of faulting and volcanism into the future for all 3 stages of RES 4. The light green highlighted region indicates the current contractional domain associated with underthrusting of the Sea of Japan, while the light orange highlighted area shows the currently active arc and the Backbone Range contractional domain. The dashed black line represents schematically the current likely leading edge of the underthrusting Sea of Japan crust, while the red line shows the likely position of the leading edge at the end of each timeframe. The heavy dashed black contour shows the current position of the 100 km contour to the surface of the subducting Pacific slab, while the heavy line shows the possible position of this at 1 Myr in the future if the decrease in upper plate shortening and shift to a stress neutral state is related rollback of the subducting Pacific slab.

- ***100 kyr – 1 Myr timeframe:*** During this time, a substantial decrease in the component of plate motion accommodated as permanent deformation in the upper plate will occur, going from ~15 mm/a to ~0 mm/a from 100 kyr to 1 Myr. This will lead to a gradual decrease in the magnitude of contractional deformation in the upper plate. During the latter half of this timeframe (500 kyr to 1 Myr) the rates of rock deformation and uplift will decrease compared to the present day. With the shift to an extensional upper plate environment, volcanism could become more voluminous than is currently observed. It is also likely that the gradual onset of a phase of slab rollback would perturb the flow regime within the mantle wedge substantially, and this could cause some migration of the arc and the current location of volcanism in Tohoku. One possibility is that a small trenchward migration of the volcanic arc (resulting from slab rollback) could occur. The amount of trenchward migration will depend on the rate of slab rollback. Perturbation of the mantle wedge by the onset of slab rollback would also disrupt the "hot fingers" (Tamura et al, 2002) in the mantle wedge that are feeding the currently active volcanoes, and could lead to volcanism within the gap areas between the active arc volcanoes.

2.2.5 Examples of additional aspects of tectonic evolution that could be integrated into the RES.

The well-developed volcanic arc in central northern Honshu (coinciding with the Backbone Range) has remained roughly in its current location since at least 10 Myr (e.g., Finn et al., 1994). Conceptual models have been developed to explain the distribution of arc volcanism in northern Honshu, such as the "hot finger" model (Tamura et al., 2002). The hot finger model helps to explain the clustering of volcanic centres along the arc (with non-volcanic gaps in between) as well as some volcanism in the back-arc region of western northern Honshu. An important consideration for Tohoku RES is how models such as the "hot finger model" might be expected to evolve into the future, and how this will influence the locations of future magmatism and rock deformation.

It is also important to consider the impact that deep-seated processes could have on rates of tectonic uplift in Tohoku. For example, processes such as deep underplating of subducted sediment can lead to rapid uplift at subduction margins (e.g., Walcott, 1987). In contrast, deep basal subduction erosion can lead to subsidence of the margin, as has been suggested for the east coast of northern Honshu by Heki (2004) in order to explain observed subsidence at continuously running GPS sites. Assessment of the potential influence of these and other deeply seated subduction zone processes on the future vertical tectonic motion in the Tohoku region can be incorporated into alternative RES and/or as options within the suggested RES presented here.

2.3 Site Evolution Scenarios

We develop potential Site Evolution Scenarios for each of the 4 RESs (discussed in section 2.1) at four example sites (Figure 2.7). The Site Evolution Scenarios are shown as storyboards in Figures 2.9 to 2.12 for example locations A-D. The site evolution scenarios are intended to demonstrate visually how each of the RESs might manifest itself as a variety of site evolution scenarios, which may impact the repository footprint during the time periods of interest. These are largely intended to demonstrate the use of storyboards to develop these scenarios, and are not to be considered as complete or detailed descriptions of the impact of the various RES at any of the example sites. Undoubtedly, there is a larger variety of SESs that could be considered at these sites than are shown in this demonstration. Note that location C is the only example that is used in the Expert Elicitation demonstration.

The SESs for this region are based upon geological studies that indicate the convergent differential motion between the Eurasian/Amur plate/subplate and North American/Okhotsk plate/subplate are at least 10 mm/a and may be 15 mm/a (Figure 2.8). Over a 10 kyr timescale, this corresponds to differential horizontal movements across the region totalling 100 to 150 m. The resultant folding and faulting will cause surface uplift, perhaps highly localised. As subplates are fragments of larger plates that are moving in ways that differ at speeds measured in mm/a from the parent plate, it is probable that they can speed up or slow down over timespans that are much less than 1 Myr.

2.3.1 Description of sites used in the SES demonstration

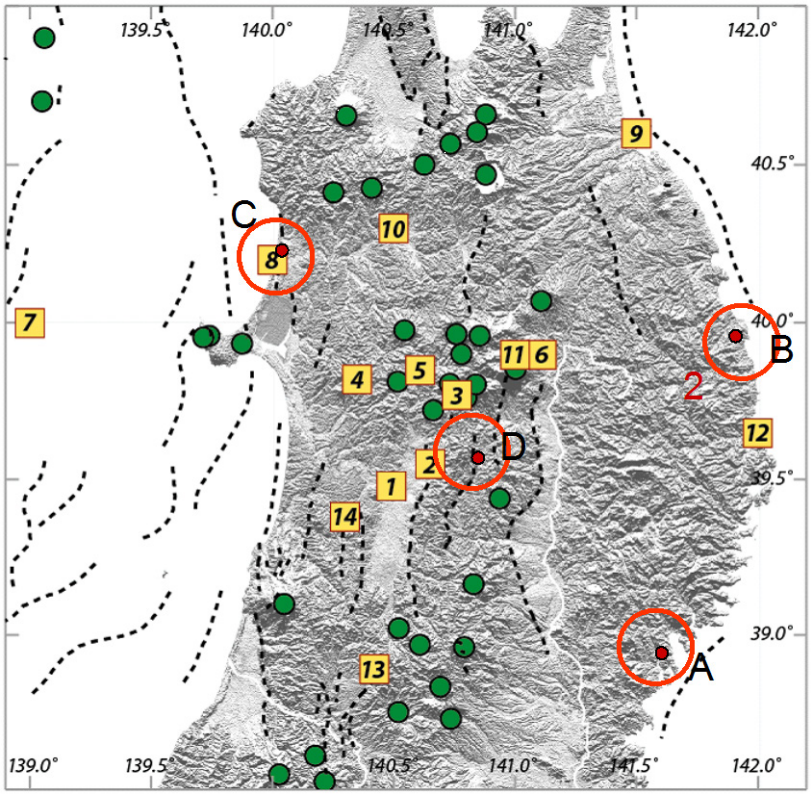

Figure 2.7: Example site locations in northern Honshu that are developed in the storyboard exercise. The green dots show recent volcanic edifices, and the dashed lines are known active faults. The numbers in the yellow boxes are the sites used in the ITM Tohoku Case study.

Location A: Site is in the forearc region of Tohoku, within early Cretaceous mafic volcanic rocks and volcanogenic sedimentary material. Site A is within a relatively stable region of slow uplift that has produced marine platforms cut into the previously deformed and fractured/faulted rocks. Coastal uplift suggests the possibility of an active fault offshore. Pre-existing NNW trending inactive bedrock structures cut through the 5 x 5 km footprint. There is no nearby volcanism.

Location B: This example location is within the northern part of the stable forearc block, where the bedrock is composed of early Cretaceous, shale and sandstone, with thin layers of chert. The site is within a relatively stable region of slow uplift that has produced marine platforms cut into the previously deformed and fractured/faulted rocks. Coastal uplift suggests the possibility of an active fault offshore.

Location C (used for the remainder of this methodology demonstration): Example location C is located within the crest of a growing anticline, on the Sea of Japan Coast, within the fold and thrust belt comprising the Sea of Japan contractional zone. The area is marked by high historical seismicity rates. The location is north-west of the Sengan Cluster, in the low-lying inter-cluster region, and the nearest volcano (Kampu Volcano) is 32 km distant. The bedrock in this region is Mid-Miocene hard mudstone, with sandstone and acid tuff.

The strata exposed in the folds are mostly hard, Mid-Miocene mudstone, with beds of sandstone and felsic tuff. The crystalline basement is probably variably deformed (both folding and faulting) and metamorphosed Mesozoic accretionary prism materials. The Miocene rift fill near location C was as much as 6 km. The major folds extend for several tens of kilometres. Okamura et al. (2007) have shown that the folds in the Niigata area to the south are forming above steep reverse faults that are mostly reactivated normal faults formed during Miocene rifting. A close association of deep-seated fault slip with near surface folding is probable near location C. The region near location C has high seismicity. The nearest

mapped active fault is located about 3 km north of the site. The style of faulting and folding in the region indicates that blind thrusts are associated with flexural slip faulting.

Location D: is situated within the Backbone Range, within a volcanic 'gap' region and near to an active fault. Bedrock faults also exist within a few hundred metres of the location. The site is within an actively deepening tectonic basin. It is situated within bedrock comprising Upper Miocene tuff and sandstone.

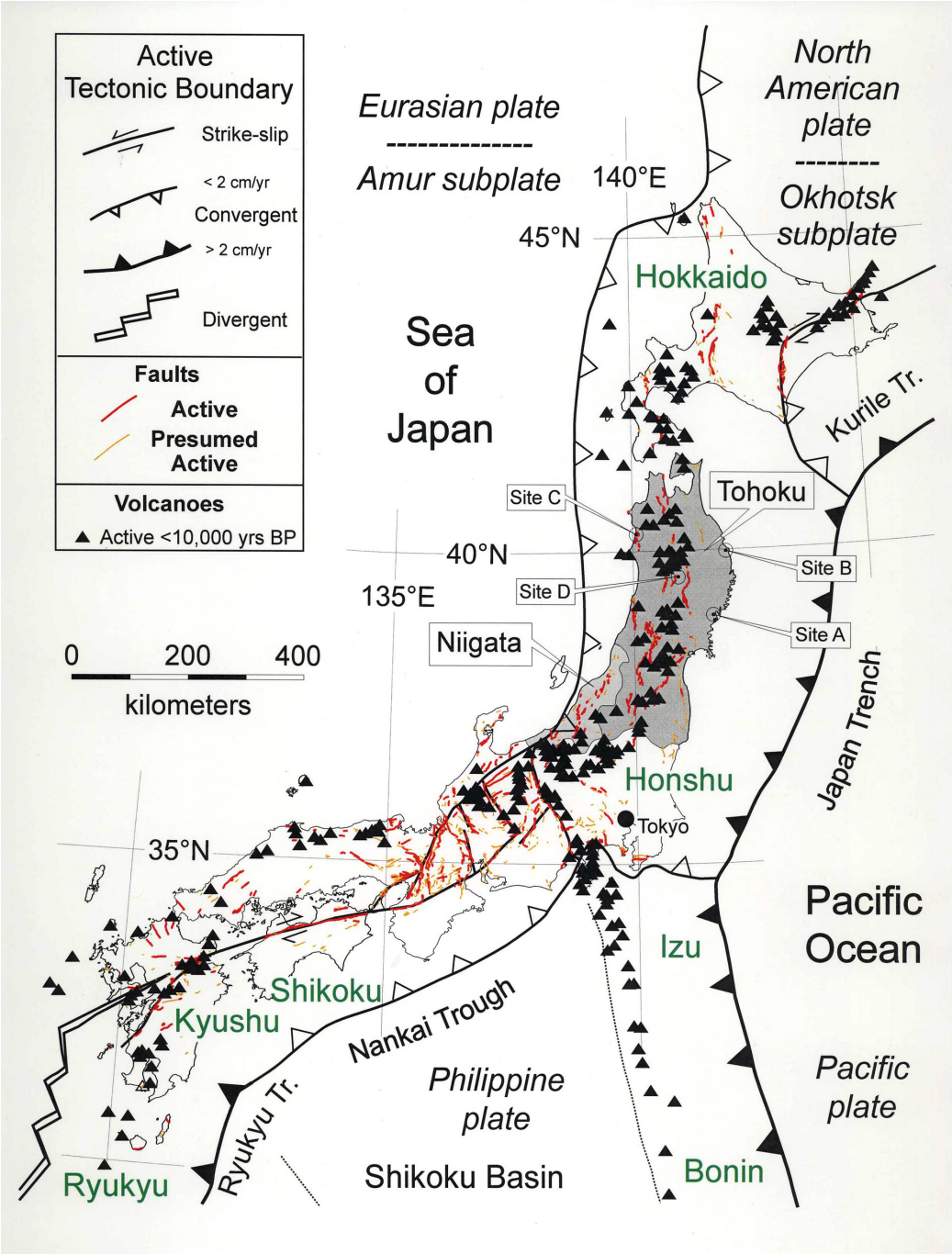

Figure 2.8: Regional tectonic setting of the four example locations, with respect to major plate boundaries.

Figure 2.9: Storyboard for the SES for example location A.

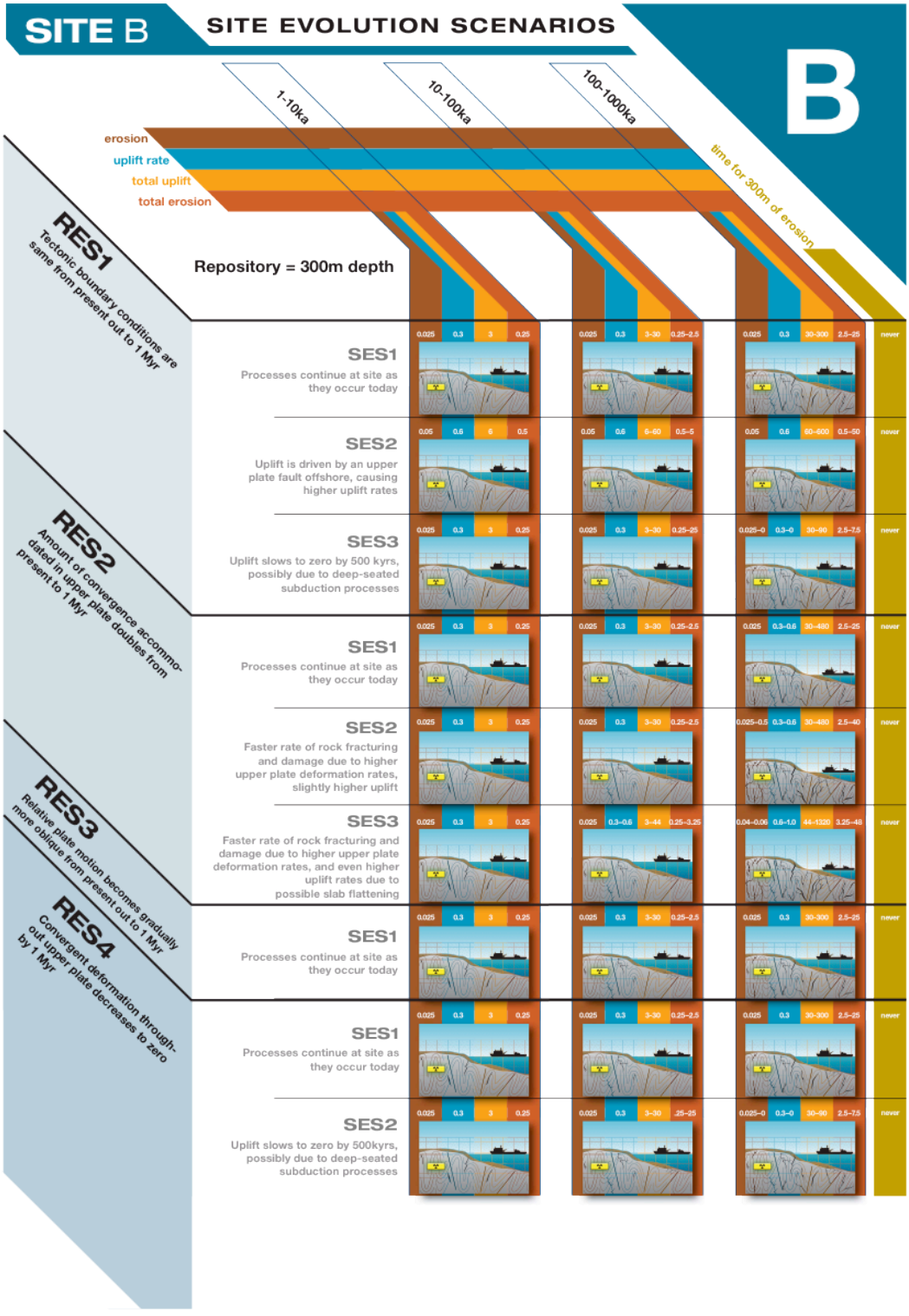

Figure 2.10: Storyboard for the SES for example location B.

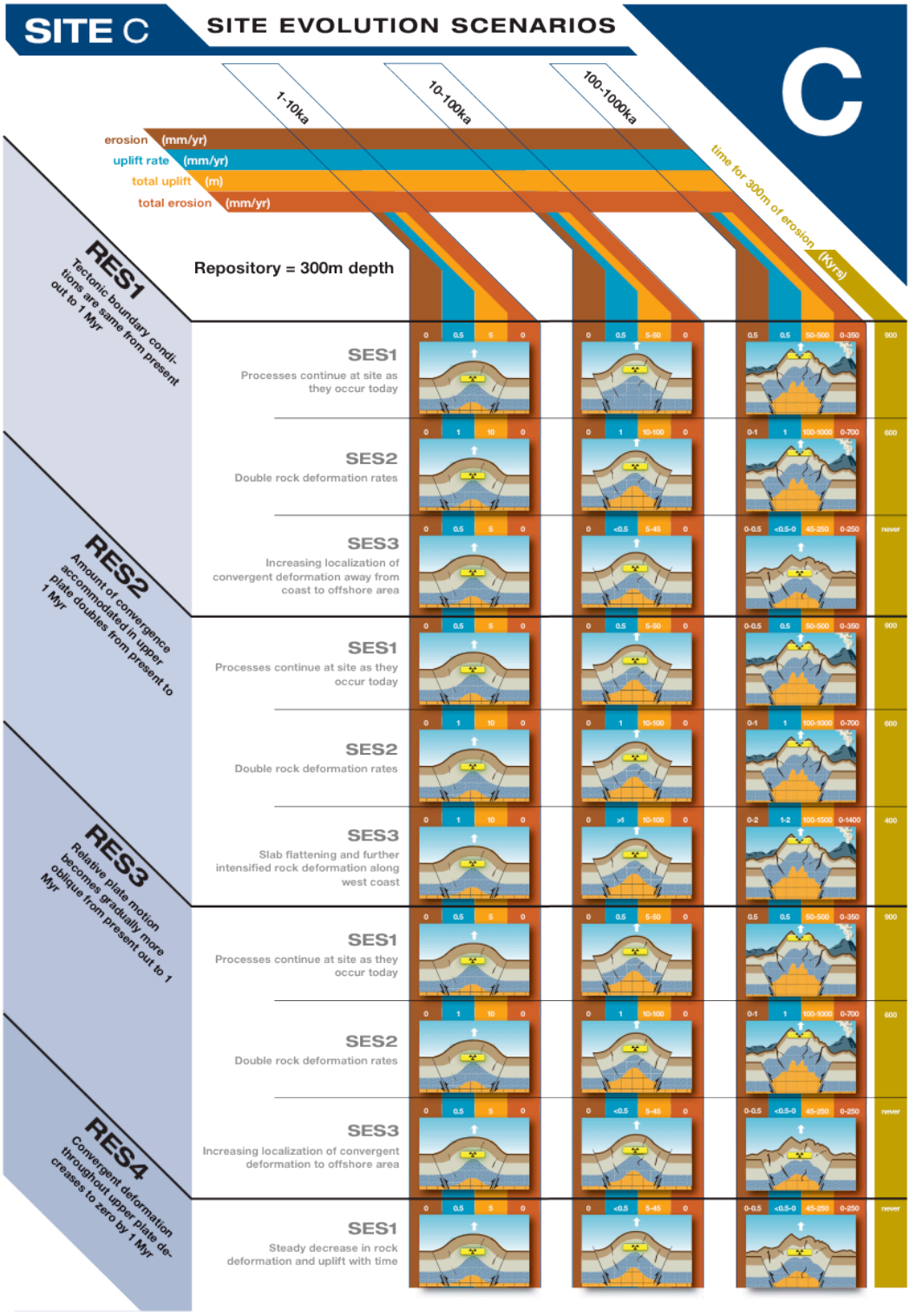

Figure 2.11: Storyboard for the SES for example location C.

Figure 2.12: Storyboard for the SES for example location D.

2.3.2 Site Evolution Scenarios for Site A

See storyboard at Figure 2.9.

RES1

- *SES1:* Over the 1 Myr time period the platform continues to be gradually uplifted and eroded, achieving 30-300 m of uplift, and 2.5-25 m of erosion (assuming erosion rates of 0.025 mm/a). Possible fracturing related to regional earthquakes, and chemical weathering promote degradation of the repository host rock over longer time periods.
- *SES2:* As for SES1, except with more rapid rates of uplift and consequent erosion.
- *SES3:* Platform uplift and consequent erosion decreases to nil by 500 kyr, with only 30-90 m of uplift and less than 10 m erosion achieved by 1 Myr.

RES2

- *SES1:* As for RES1/SES1.
- *SES2:* As for RES1/SES1, except greater uplift of marine platform achieved by 1 Myr.
- *SES3:* As for SES 2 above, except for even more rapid rates of uplift and erosion at later stages, due to higher upper plate deformation rates and possible slab flattening. If maximum uplift and exhumation rates are reached, the repository could be exhumed.

RES3

- *SES1:* As for RES1/SES1.
- *SES2:* As for RES1/SES1, except that bedrock faults are reactivated in the 100 kyr -1 Myr timeframe to accommodate increasing plate motion obliquity. The repository is potentially displaced by motion on these faults later in this time frame.

RES4

- *SES1:* As for RES1/SES1.
- *SES2:* As for RES1/SES3.

2.3.3 Site Evolution Scenarios for Site B

See storyboard at Figure 2.10.

RES1

- *SES1:* The repository lies within early Cretaceous bedrock and beneath a stable marine platform on the east coast. The area continues its low and uniform rates of uplift and erosion over the next 1 Myr. The main potential impacts on repository integrity over time are bedrock fracturing due to shaking from regional earthquakes, and chemical weathering in the near-surface bedrock, particularly along fractures.
- *SES2:* As for SES1, except an upper plate fault offshore drives higher uplift and higher consequent erosion rates.
- *SES3:* Uplift and consequent erosion progressively slows to nil by 500 kyr. Regional earthquakes and chemical weathering gradually weaken the bedrock surrounding/ above the repository.

RES2

- *SES1:* As for RES1/SES1, except slightly higher uplift rate and total uplift of the platform by 1 Myr.
- *SES2:* As for RES1/SES1, except greater uplift of marine platform achieved by 1 Myr.

- *SES3:* As for SES 2 above, except for even more rapid rates of uplift and erosion at later stages, due to higher upper plate deformation rates and possible slab flattening. If maximum uplift and exhumation rates are reached, the repository could be exhumed.

RES3

- *SES1:* As for RES1/SES1.

RES4

- *SES1:* As for RES1/SES1.
- *SES2:* As for RES1/SES3.

2.3.4 Site Evolution Scenarios for Site C

See storyboard at Figure 2.11.

RES1

- *SES1:* The repository lies within a growing anticline in mid Miocene sedimentary rocks. Over the 1 Myr timeframe the anticline becomes tighter, and fault displacement accumulates at the margins, as well as secondary faulting, and possible flexural slip faulting within the repository footprint. Up to 350 m of vertical erosion results in exhumation of the repository within the 100 kyr - 1 Myr timeframe. Volcanism could also initiate nearby within that same timeframe.
- *SES2:* As for SES1 except more rapid uplift and erosion rates result in more rapid rock deformation and repository exhumation.
- *SES3:* Anticline development and associated uplift decreases over time as convergent deformation becomes increasingly localised offshore. Vertical erosion over the 100 kyr - 1 Myr time period reduces the anticline by up to 250 m.

RES2

- *SES1:* As for RES1/SES1.
- *SES2:* As for RES1/SES2.
- *SES3:* As for SES2 above, but slab flattening in the vicinity of the west coast results in even more intense rock deformation in the repository area. Uplift of 100-1500 m, and vertical erosion of up to 1400 m results in repository exhumation in the 100 kyr - 1 Myr timeframe. Possible initiation of volcanism nearby.

RES3

- *SES1:* As for RES1/SES1
- *SES2:* As for RES1/SES2
- SES3: As for RES1/SES3

RES4

- *SES1:* As for RES1/SES3

2.3.5 Site Evolution Scenarios for Site D

See storyboard at Figure 2.12.

RES1

- *SES1:* The repository lies within Miocene sedimentary rocks, and beneath the centre of an actively developing basin. Over the million-year timeframe the basin slowly deepens as a result of progressive fault displacement at the basin margins. Basin margin volcanism could also initiate in the 100 kyr - 1 Myr timeframe, if the arc

volcanism migrates into the volcanic gap region. Negligible erosion rates do not alter repository depth throughout the 1 Myr time frame of basin development.

- *SES2:* As for SES1, except that accelerating rock deformation rate over time produces secondary fault displacement within the basin and potentially through the repository. Vertical erosion of between 100 and 200 m occurs above the repository in the 100 kyr - 1 Myr time period.
- *SES3:* As for SES1 except that volcanism develops more rapidly and intensely due to lateral migration of volcanism into this 'gap area'.

RES2

SES1: As for RES1/SES1

SES2: As for RES1/SES2

SES3: As for above SES2 except that deformation rates, including secondary faulting within the basin, become even more intense. Also, vertical erosion of between 100 and 200m occurs above the repository in the 100-1000 kyr time period, and lateral migration of volcanism could occur earlier due to possible large-scale tectonic perturbations on the system.

RES3

- *SES1:* As for RES1/SES1.
- *SES2:* As for RES1/SES2.
- *SES3:* As for RES1/SES3.

RES4

- *SES1:* As for RES1/SES1.
- *SES2:* Rate of development of the basin decreases over time, with cessation of all rock deformation by 1 Myr. Vertical erosion of between 100 and 200 m occurs in the 100 kyr - 1 Myr time period.

3 Estimating Scenario Probabilities Using Scenario Logic Trees

The concept of using logic trees to incorporate scenario probabilities in the form of expert degrees of belief was introduced in Section 1.3.

Logic, or scenario, trees are increasingly applied in volcanology, both for long-term and short-term eruption forecasts and for mitigation of volcanic hazards (e.g., Newhall and Hoblitt, 2002; Marzocchi et al., 2004; Aspinall et al., 2003). Logic and scenario trees provide a mechanism for organizing the approach to the complex problem of assessment of the potential for different forms and intensities of volcanic activity and the potential consequences (impacts) of such events. In volcanology generally, a probabilistic approach is used because any volcanic action is a complex process, characterised by many unknowns. Except in a few cases, this complexity means that future evolution of specific areas is intrinsically variable. The evolution of volcanic hazards at specific sites and over the long term cannot be forecast within a deterministic framework and, therefore, deterministic models for characterising future volcanic activity are inadequate. More generally, the key drawback to deterministic approaches is that there is no way to achieve uniformity or comparability across different hazards or risks, and hence no way to rank or prioritise them without some expression of their probabilities. Therefore, the volcanological community has developed logic and scenario trees as a means of estimating probabilities of different forms of future volcanic activity. Such an approach is required for quantification of the uncertainty related to imperfect knowledge of non-linear volcanic processes, to space-time variability of distribution and intensity of volcanic events, as well as to a limited amount of information. For example, the International Atomic Energy Agency recommends a probabilistic approach to volcanic hazard assessment for nuclear facilities of all types. For assessment of hazards at HLW facilities, volcanic hazard assessments have also been conducted using probabilistic approaches and logic trees specifically (Coppersmith et al., 2009).

For the TOPAZ methodology development, three scenario logic trees were developed (uplift and exhumation, rock deformation and volcanic intrusion), although only the latter two were analysed for demonstration. All three are described in the following sections.

3.1 The Rock Deformation and Uplift/Exhumation Logic Trees

The logic trees in Figure 3.1 were developed to incorporate the impact of various RES for (a) the rock deformation hazard and (b) hazard due to uplift and exhumation of the repository. Probability weightings for many of the branches (see elicited branches in red) on the rock deformation logic tree were elicited during the October 2011 expert elicitation workshop. However, we did not address the uplift and exhumation tree during the workshop (it was not feasible to consider all of the SESs in the time available), and only show it here as an example of what could be developed for the uplift/exhumation problem.

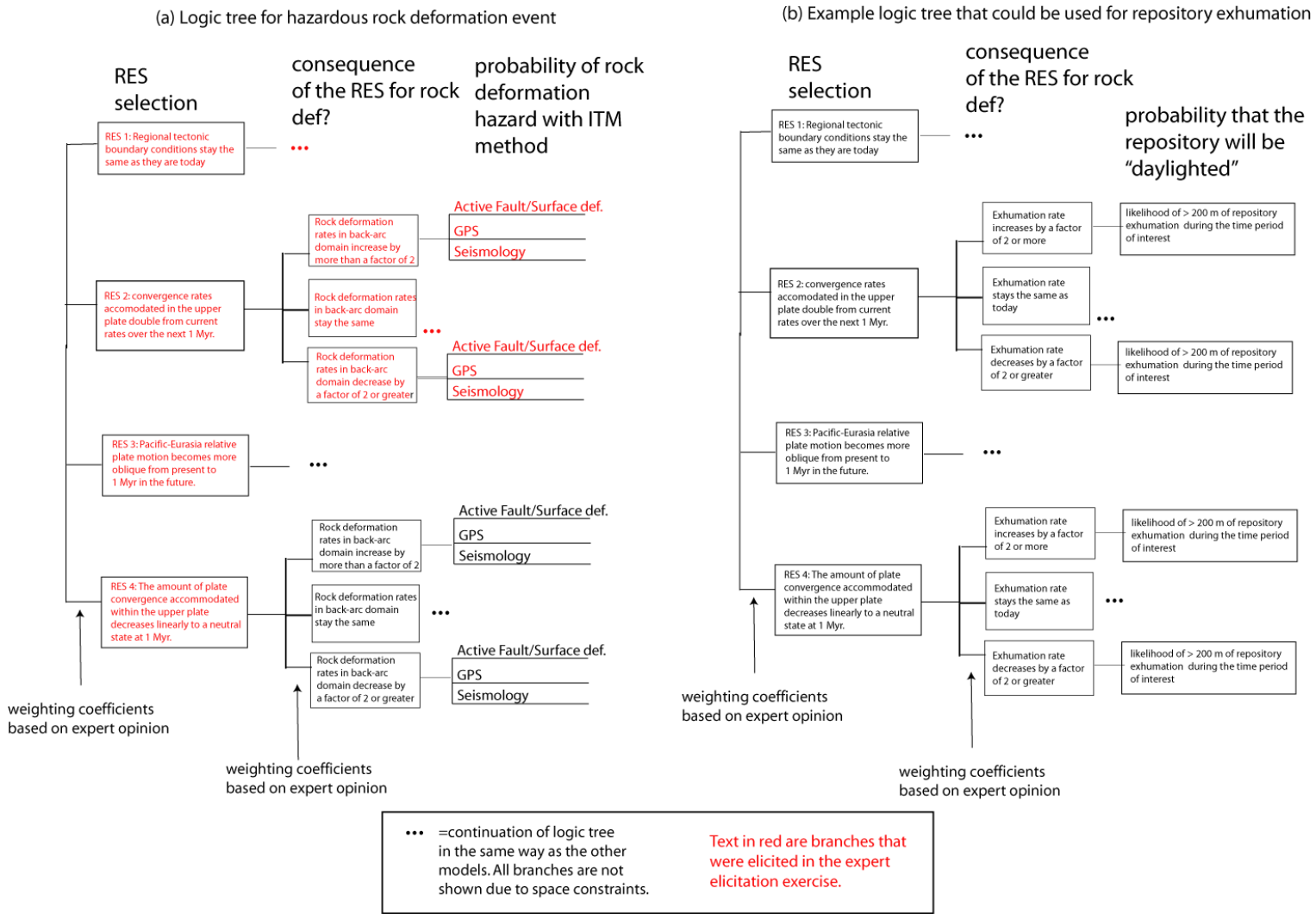

Figure 3.1: Scenario logic trees for rock deformation (left) and uplift/repository exhumation (right).

On both logic trees, the left-most branches on both trees involve weighting each of the four different Regional Evolution Scenarios (see Section 2.1), while the second row of branches addresses the consequences at the candidate site for each RES.

In the rock deformation tree, the final set of branches includes the three alternative deformation datasets (e.g., GPS, active fault/surface deformation, and seismicity). During the expert elicitation workshop, weightings were assigned for RES 1-4, on the first set of branches. However, given the limited time available for the workshop, weightings for subsequent branches were only assigned for RES 1 and 2 – additional time would have been needed to give proper, detailed consideration to further scenarios.

3.2 The Volcanism Logic Tree

In application to volcanic hazard assessment for HLW facilities, a scenario tree is a branching graph representation of possible events. Individual branches represent alternative progressive steps from one event, or condition, to the next. For example, an early node on the tree may represent the state of volcanic unrest, in which geophysical evidence suggests that magma intrusion has occurred. Later nodes may represent the state of eruption, or alternatively the state of no eruption, two states that generally follow from the state of volcanic unrest. As this example illustrates, in scenario trees these events are often ordered in sequence, such that time progresses from early events to later events as the scenario tree branches. Eventually, these branches terminate at final outcomes that represent specific hazardous events, such as the probability of dyke injection into a HLW repository. In practice, the branches between states are weighted with probabilities. Often these probabilities are determined using data, models, and expert judgment. Such scenario trees are now commonly used in volcanology to estimate the probability of specific events at active volcanoes, especially in light of monitoring data (Marzocchi et al., 2006).

Here, we differentiate between logic trees and scenario trees. Whereas scenario trees are constructed around events, logic trees are constructed around models. A set of logic tree branches represents exclusive and exhaustive alternatives (with probabilities summing to unity), whereas event trees can have incomplete branch sets, with weights or probabilities that may not sum to unity (e.g. if two or more events can happen in one event). In logic trees, nodes consist of specific geoscientific models that are used to estimate the probability of specific events, rather than consisting of the events themselves. For example, ITM and TOPAZ work has produced a number of different models of the spatial density of volcanism. These models include the Cox process model, the kernel density model, empirical models and homogeneous spatial density models. These models, or their aggregates, represent nodes on the volcanism logic tree. On the logic tree, the transition probabilities represent the weights that experts assign to specific models. As in scenario trees, logic trees are hierarchical, leading to increasing detail required to estimate hazard. The models themselves rely on data and calculations to produce a probability of the specific volcanic event.

There are several advantages to using logic trees in the assessment of volcanic hazards. First, a complex sequence of events or models is described explicitly using a logic tree. This lends transparency to the entire analysis, which is essential in both internal and external review of the volcanic hazard assessment. Second, experts estimating the weights to give to each model node need not be directly concerned with the probability calculation, but only with the geological relevance of the individual models. Third, it is possible to frequently assess impacts of new data on estimated probabilities as these data become available. In long-term site investigations, it is inevitable that new data will emerge and will be discussed in terms of impacts on all types of hazard models, including volcanic hazards. Fourth, logic trees can provide an efficient means of assessing both epistemic (model) uncertainty and aleatoric (data) uncertainty on the estimated probability of specific volcanic hazards. Just as new data may emerge during prolonged site investigations, new data, models and interpretations (e.g. RES and SES models, and data constraining these models) may emerge as well. These models are readily incorporated into the logic tree and their impact (or not) on probability estimates can be assessed. Again, this has proven to be essential in siting of HLW facilities because new models invariably emerge (Coppersmith et al., 2009).

In the following, the specific logic tree used in the assessment of models in TOPAZ is described in detail (Figure 3.2). *N1* is the current state of the volcano-tectonic system. Our

goal is to consider all credible models of how this system will evolve during the performance period of the site, out to 1 Myr and to assign weights, based on expert judgment, to these alternative scenarios. We create a logic tree to perform this evaluation. The logic tree contains states, represented by nodes on the tree. These states represent alternative models for the system that are required in order to estimate the probability of a credible site evolution scenario. Transition probabilities on the logic tree represent the weights assigned to alternative models of igneous activity. The first part of the tree represents our understanding of the regional tectonic setting of volcanism and the evolution of this tectonic setting during the next 1 Myr. This ends with weighting of alternative RESs. The second part of the tree represents the site-specific processes that may give rise to igneous activity at the site. By following a single branch through the logic tree, a single site evolution scenario (SES) is specified. Each SES branch gives rise to a probability of igneous activity affecting the site. The weights assigned to each branch are multiplied to estimate the probability that a given SES will occur. The aggregate probability of igneous activity affecting the site is determined by summing the weighted SES probabilities for the entire logic tree.

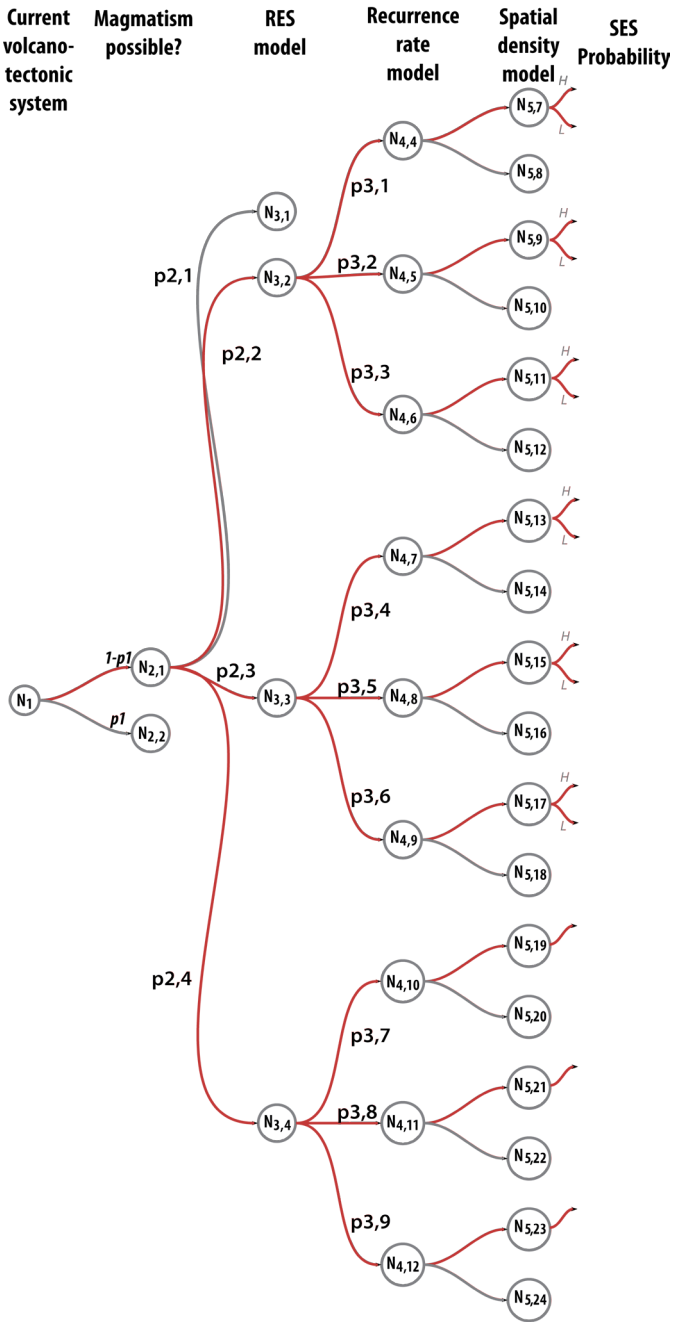

Figure 3.2: The volcanism logic tree.

For a proposed HLW facility, the main issue is estimation of the probability and consequences of volcanic activity during the performance period of the facility (e.g., up to the next 1 Myr). Therefore, impact scenarios scenarios must be developed for non-zero branches of the logic tree (SES probability > 0). The impact scenarios consider alternative models of impact (e.g., direct disruption of the repository barrier system by igneous dyke injection or indirect thermal, hydrological, chemical, and mechanical effects).

For volcanism, states *N2,1* and *N2,2* represent alternative models for the credibility of magmatism occurring at any time within the next 1 Myr in the site region, where the site region is taken to be a circle 100 km in radius centred on the site. This radius is considered to be sufficiently large to provide a clear picture of the tectonic setting of the site and also large enough to encompass any nearby changes in the tectonic setting, for example a transition from forearc to arc tectonic environment, which might indicate that change in the tectonic setting is possible during the 1 Myr performance period of the site (e.g., maximum rate of

change on order 1 mm/a). The transition probability, *p1* indicates the weight assigned the model that no credible scenario can give rise to magmatism in this region during the next 1 Myr. The transition probability *1-p1* indicates the weight assigned to the model that magmatism is credible in the site region within the next 1 Myr. If *p1* can be demonstrated to equal one, then no further analysis for the site is required. If *p1* < 1 then alternative conceptual models for volcanism need to be developed in the RES and SES stages.

For the volcanism scenario tree, this node is essential because there are numerous sites where there is no credible potential for future volcanic activity, even in a 1 Myr timeframe. Therefore, there are some locations, (e.g., example location A) for which no reasonable RES can give rise to volcanic activity in the next 1 Myr. It is not efficient to debate alternative RESs for such sites. For example, locations in the Shikoku region may have a complete analysis for volcanism simply by demonstrating that *p1*=1 (location A, in the forearc of Tohoku, is considered to be in this category).

If *p1* < 1 then alternative conceptual models for the evolution of the site region need to be considered. The RESs summarise the range of conceptual models of the tectonic evolution of the site, represented by the states *N3,1 – N3,4* on the logic tree. Weights are assigned to the alternative RESs using *p2,1 – p2,4*. These weights must sum to unity. These weights were developed using an informal process in the March 2011 Topaz workshop.

For volcanism, the site evolution scenario process involves considering the regional recurrence rate of volcanism and the spatial density of volcanism, based on each RES. For methodology development, a range of alternative models is considered. States *N4,1– N4,12* (not all shown on the logic tree) represent recurrence rate models, based on the RESs. Three basic recurrence rate models are shown. For example, RES1 (tectonic conditions persist as they are today) is assigned to *N3,3. N4,7* represents a state of increasing recurrence rate of igneous activity, *N4,8* represents a state in which recurrence rate persists as it is currently, and *N4,9* represents a decrease in recurrence rate of igneous activity. For the TOPAZ methodology, we should consider a probability distribution of recurrence rates for each of these states. For example, for *N4,8* (recurrence rate remains as today), the model should specify a mean recurrence rate and standard deviation in recurrence rate, based on TOPAZ and VOGRIPA data. Similar distributions should be developed for *N4,7 and N4,9*. Then, these same distributions should be used for alternative RESs. Individual experts may choose to weight the recurrence rate models differently on different branches, but would not choose the range of recurrence rates represented by the nodes.

Given an RES and recurrence rate of volcanism, nodes *N5,1 – N5,24* (not all shown) represent alternative spatial density models. These are the cluster models, represented by spatial distributions based on the Cox or kernel methods, and the empirical model (based on distance from existing volcanoes and a threshold cut off value). In addition, models can be developed that are completely spatially random, such as homogeneous Poisson models. In such models, a zone is defined, perhaps based on some geological criteria, and the distribution of volcanism within this zone is considered to be completely spatially random. In this case, the estimate of the recurrence rate of activity within this zone using this model is simply the average density of volcanoes within the zone. Weights are assigned to the different spatial density models by the experts. It follows that, for expert assessment, individual experts were asked a simple question: Should a tight cluster (Cox) model or smooth (Kernel) model or homogeneous Poisson model be used to estimate spatial density and, by elicitation, what weight should be assigned to each type?

The results comprise an aggregate probability, the sum of the weighted SES probabilities. Each SES probability may be a range, e.g., based on a range of recurrence rate and spatial density models, represented by high (H) and low (L) values, or as a distribution. This brings us to the conclusion of the SES stage and sets the scene for Impact Scenarios (ISs), where the tree is further developed to consider alternative site impacts, if necessary.

4 Using Expert Elicitation to Derive Scenario Probabilities

The concept of incorporating differing expert views and alternative interpretations and models using a formal expert elicitation approach has not been used before in the Japanese radioactive waste programme. Consequently, as well as using the technique as part of the TOPAZ methodology, it was being introduced generically for the first time to Japanese tectonics and radioactive waste experts as well. This was done by means of a single workshop, where selected RES and SES probabilities were elicited from a group of experts, after first calibrating experts in terms of their ability to provide informative judgements for establishing probabilities and ranges of probabilities in the face of uncertainties.

The workshop demonstration of a structured expert judgment (SEJ) elicitation was held on 25th - 26th October 2011 in Tokyo. About thirty people attended the elicitation workshop, with twenty-one experts and specialists participated actively in the elicitation exercise. Because of time constraints on processing data, the responses of a subset of twelve experts were selected at random to exemplify the process, comprising eight Japanese experts and four international experts. The workshop is reported in detail in Aspinall, 2011, and only a brief outline is provided in the current report.

The elicitations were conducted using a structured questionnaire and analysed with the Cooke Classical Model and the EXCALIBUR software package. Before the Workshop took place, a set of draft Target Item questions were prepared by members of the TOPAZ group, and a set of Seed Items devised.

Overall, the exercise was judged successful, and achieved its main goal of providing a demonstration of a rational and defensible structured expert judgment basis for ascribing initial uncertainty distributions to parameters, models and variables in relation to long-term future volcanic and tectonic hazards and risks at proposed geological repository sites for radioactive wastes in Japan.

For many of the factors addressed by the expert panel, the scientific uncertainties associated with these risk factors are large, and their quantification is a crucial element for supporting decision making related to hazards, repository siting and risk management. The elicitation showed how, using expert judgment in a formalised manner, objective quantitative estimates for certain hazard and risk factors could be derived - crucial for supporting policy decision-making under conditions of severe scientific uncertainty. In addition, the exercise also illustrated how the structured elicitation framework can help identify major knowledge gaps, topics where definitions and terms may need clarification, and critical areas where additional research and investigation may be worthwhile.

4.1 Background to Expert Elicitation

When expert advice is needed as support to critical, science-based decision-making, a structured way of eliciting a variety of opinions is helpful. In this context, seeking a “rational consensus” refers to a group decision process in which a formalised approach is followed, based on performance-based scoring rule optimization. The group of experts involved needs to agree on a method according to which representations of parameter uncertainty will be generated for the purposes for which the panel was convened, without knowing a priori the outcomes of this method. However, it is not required that each individual member adopts the results as his personal degree of belief.

To be rational, this method must comply with necessary generic conditions devolving from the scientific method. Cooke (1991) formulates the necessary conditions or principles, which any method warranting the designation “scientific” should satisfy, as:

- Scrutability/accountability: All data, including experts' names and assessments, and all processing tools are available for peer review and results must be open and reproducible by competent reviewers.
- Empirical control: Quantitative expert assessments are subjected to empirical quality controls.

- Neutrality: The method for combining/evaluating expert opinion should encourage experts to state their true opinions, and must not bias results.
- Fairness: Experts' competencies are not pre-judged, prior to processing the results of their assessments.

Thus, a method is desired which satisfies these conditions and to which the parties commit, beforehand. The principles outlined above have been implemented for expert elicitation in the so-called "Classical Model", a performance-based linear pooling or weighted averaging model (Cooke 1991). The weights are derived from experts' calibration and information scores, as measured on seed variables. Seed variables serve a threefold purpose:

- to quantify experts' performance as subjective probability assessors,
- to enable performance-optimised combinations of expert distributions, and
- to evaluate and hopefully validate the combination of expert judgments.

The name "Classical Model" derives from an analogy between expert calibration measurement and classical statistical hypothesis testing. In the Classical Model, performance-based weights use two quantitative measures of skill with respect to the statement of uncertainty: calibration and information. Loosely, calibration measures the statistical likelihood that a set of measurable or experimental results correspond, in a statistical sense, with the expert's assessments. Relative information measures the degree to which an expert's uncertainty distribution is concentrated around the true answers to a set of seed questions – this latter evaluation is sometimes referred to, in the context of expert elicitations, as the expert's "informativeness".

However, it is essential to stress here that the connotation of "expert informativeness" and the use of the adjective "informative" can be different in this respect from their vernacular meaning in the "real world". In some societies, "informative experts" - in any situation other than a formal elicitation - are those who are recognised by their peers or judged by others to be authoritative in what they say. In the context of a structured elicitation, informative experts are taken to be those who demonstrate an ability to express an appropriate range of uncertainties over a combination of variables, and thus assist decision-making.

The EXCALIBUR procedure implements a method for combining experts' subjective probabilities based on mathematical and statistical theory, and is therefore more rigorous than other, less formalised, approaches. The aim is to find some way of combining several distributions, given by different experts, into one distribution, representative of the spectrum of their opinions. What is frequently used is a linear opinion pool, which is just a weighted arithmetic mean of the distributions provided by the experts. This pooling can use either simple equal weights or it can use a performance-based weighting scheme. The aim of the latter is to create a basis for achieving rational consensus. Since each individual has his/her own subjective probability, it is necessary to find a way of achieving this convergence. In EXCALIBUR, weights are determined from the participating experts' performances on 'calibration' questions, questions whose answers are known to the analyst but not to the experts.

Suppose the experts are asked for their uncertainty ranges over a number of calibration variables. In a typical application, each expert gives quantile information for his or her uncertainty distributions, such that for each calibration variable there are four intervals:

- 0 to 5%; 5% to 50%; 50% to 95%; 95% to 100%

The quality of calibration of an expert is measured by looking at how far the empirical distribution given by the calibration variables differs from that given by the expert. The analyst wants to identify those experts for whom the corresponding statistical hypothesis is well supported by the data obtained from the calibration variables. The calibration score is the probability that the divergence between the expert's probabilities and the observed values of the calibration variables might have arisen by chance. An illustrative example of how calibration via seed questions works is shown in Figure 3.3.

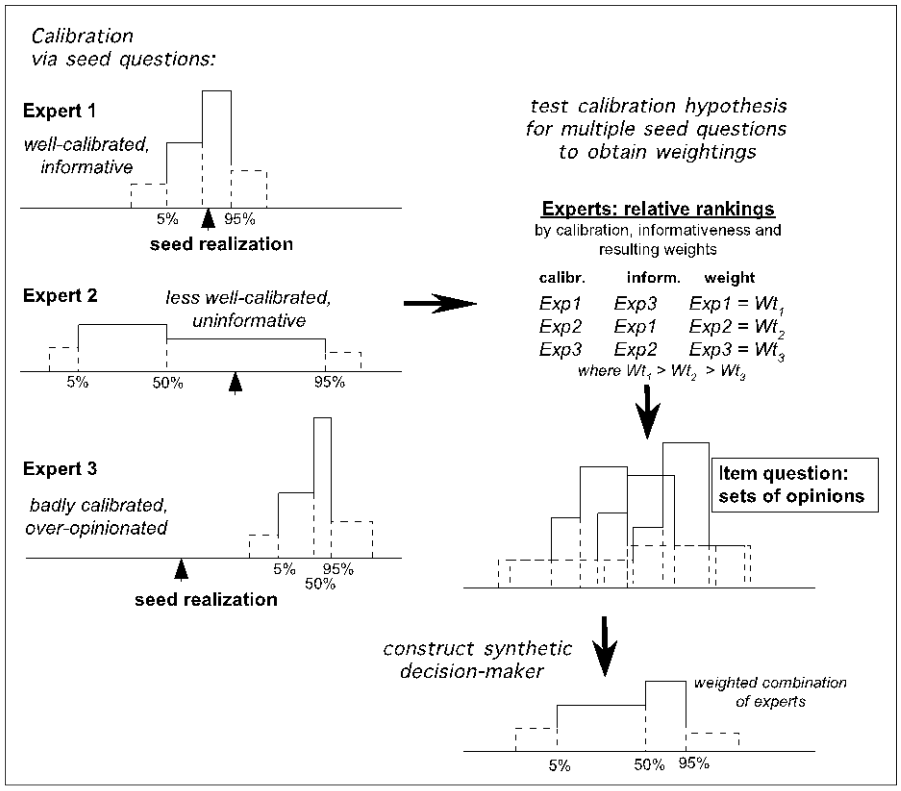

Figure 3.3: Schematic chart showing how experts' responses are calibrated against (multiple) seed questions at given quantiles to produce performance-based weights, which are then used to pool the experts' opinions for the corresponding quantiles of target items.

Calibration is not the only way to measure the quality of an expert opinion. Another criterion is relative information (as noted earlier, sometimes referred to as "informativeness" in the context of expert elicitation). Relative information represents the degree to which an expert's distribution is concentrated, relative to some user-selected background measure. The relative information is calculated for each expert at each query variable and then averaged over all the query variables to get the overall information score of expert *e*. The information score is a positive number, with increasing values indicating greater information relative to the background measure.

Experts with distributions closest to the realization values are given higher calibration scores, and experts with smaller uncertainty bands are given higher information scores. The "ideal" expert would have predicted close to the true value with little uncertainty – thus, "good expertise" corresponds to high statistical likelihood and high information.

In order to determine the performance-based weight that an individual expert gets, their information and calibration scores are combined together as a product. In this situation, the calibration scores are the more important: calibration dominates over relative information (or informativeness), while the relative information score serves to adjust between equally calibrated experts.

The seed question used and the results of the calibration exercise are described in the FY2011 report for NUMO and are not presented here.

4.2 Questions Posed in the Expert Elicitation

The experts were asked to provide their best estimate and confidence bounds to the following questions (note: these are much abbreviated: the full details of the questions are not provided here but were outlined in an internal briefing note and thus provide weights for each option:

- which of the four RESs was considered most appropriate (or whether another model might apply)

- given each RES, would strain rates at Location 'C' increase, decrease or stay the same over the next 1 Myr;
- which strain dataset (as used in the ITM methodology) is most reliable for indicating strain rates;
- given each RES, would the long-term average rate of formation of new volcanoes in the Tohoku region increase, decrease or stay the same over the next 1 Myr;
- which spatial density model (as used in the ITM methodology) is most reliable for estimating volcanic hazard at Location 'C';
- which spatial density model is most appropriate for the situation that the long-term average rate of formation of new volcanoes increases.

The following sections show only the full results of the expert elicitation for the first question, as an example of the type of output derived from expert elicitation, with a summary table of the results of the other questions.

4.3 Evaluation of RESs

The results of the RES questions are presented in full below. Each diagram shows the responses of the experts, plus a group-averaged solution and a performance-based weighted solution where, in the latter, responses of the experts are weighted according to their statistical calibration and informativeness and then pooled, as described above. The label "Perf" is used for a performance-based weighted solution of opinions, with individual weights determined from the analyst's choice of model constraints. "Equal" is used to denote an equal weights solution. As noted above, the questions are given in shortened format here.

Experts were asked to provide three values: a median (50%ile) value and their view on the 90% credible interval values about their central value (i.e. their judgment of the 5%ile value and the 95%ile value). The spread of each expert and the median value are indicated on the diagrams for the four RESs and an 'any other RES' alternative in Figures 4.1 to 4.5. Also shown is the facilitator's commentary on each result.

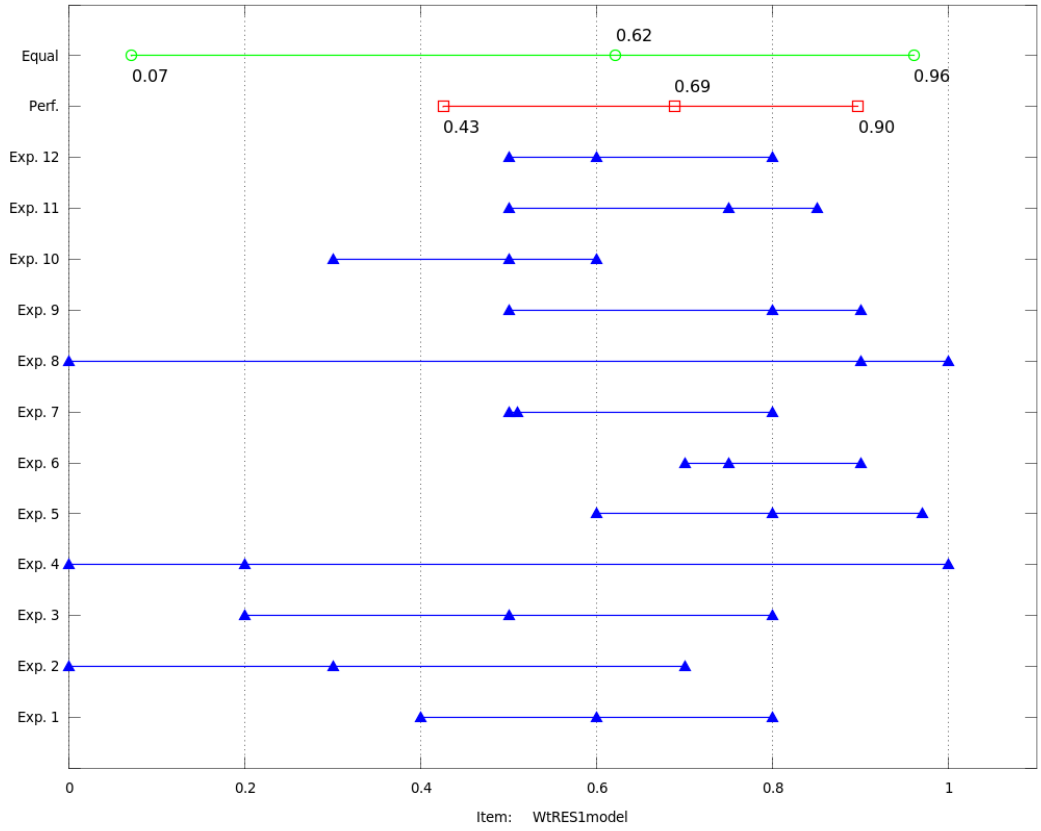

Figure 4.1: For characterizing the likely Regional Evolution over the period 100 kyr to 1 Myr, what relative weight would you give to the RES 1 model option?

Facilitator's comments:

There are wide-ranging uncertainties in individual judgments; credible intervals vary, but mostly overlap across the group.

The Performance Weights solution credible interval is narrower than the Equal Weights solution.

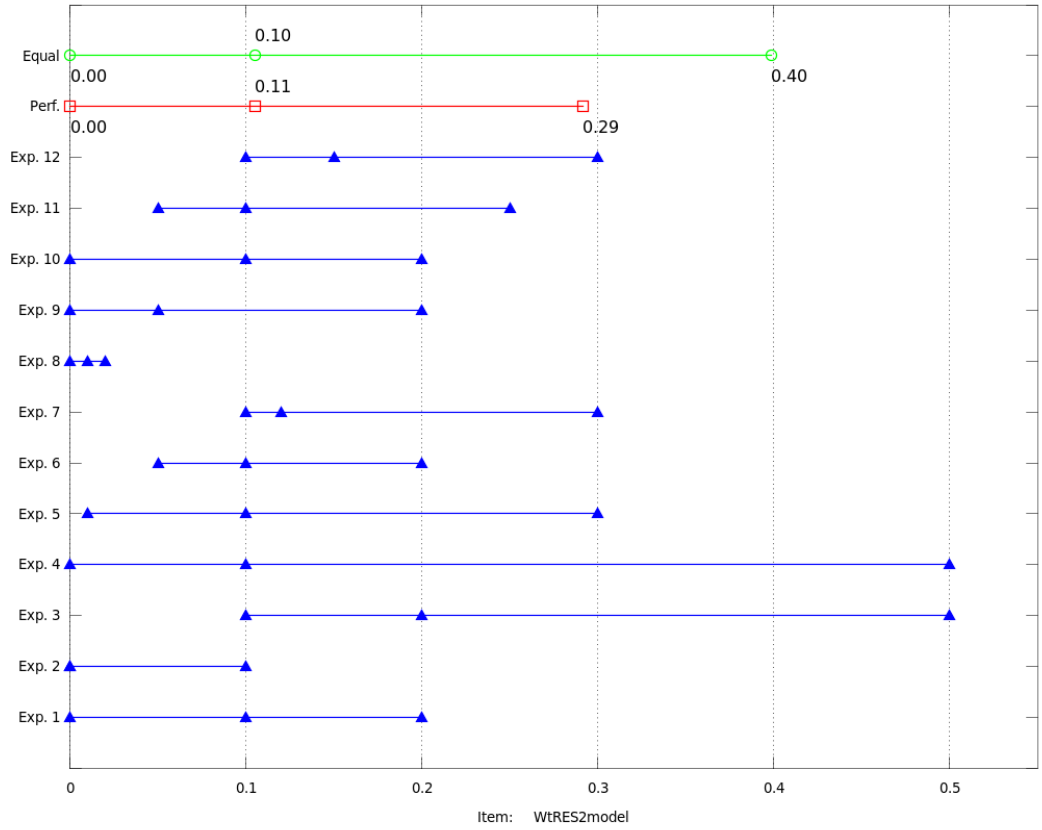

Figure 4.2: For characterizing the likely Regional Evolution over the period 100 kyr to 1 Myr, what relative weight would you give to the RES 2 model option?

Facilitator's comments:

There are wide-ranging uncertainties in individual judgments; credible intervals vary, but mostly overlap across the group.

The Performance Weights solution credible interval is narrower than the Equal Weights solution.

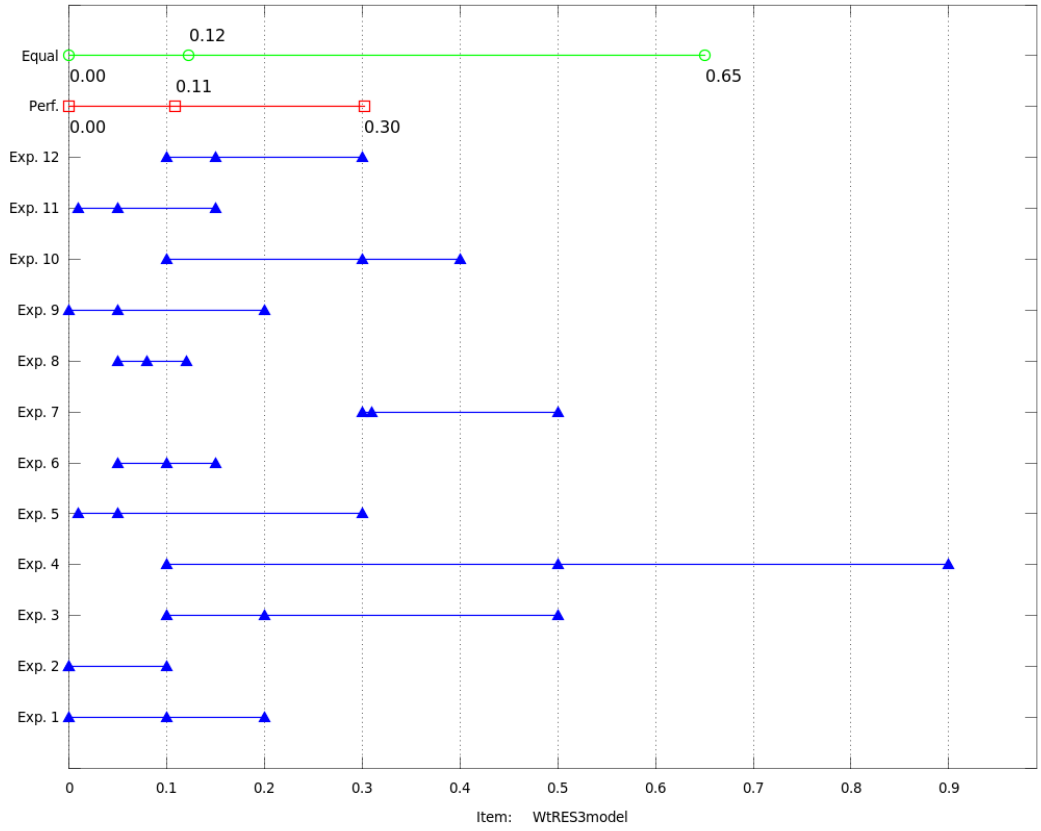

Figure 4.3: For characterizing the likely Regional Evolution over the period 100 kyr to 1 Myr, what relative weight would you give to the RES 3 model option?

Facilitator's comments:

There are wide-ranging uncertainties in individual judgments; credible intervals vary, but mostly overlap across the group.

The Performance Weights solution credible interval is narrower than the Equal Weights solution.

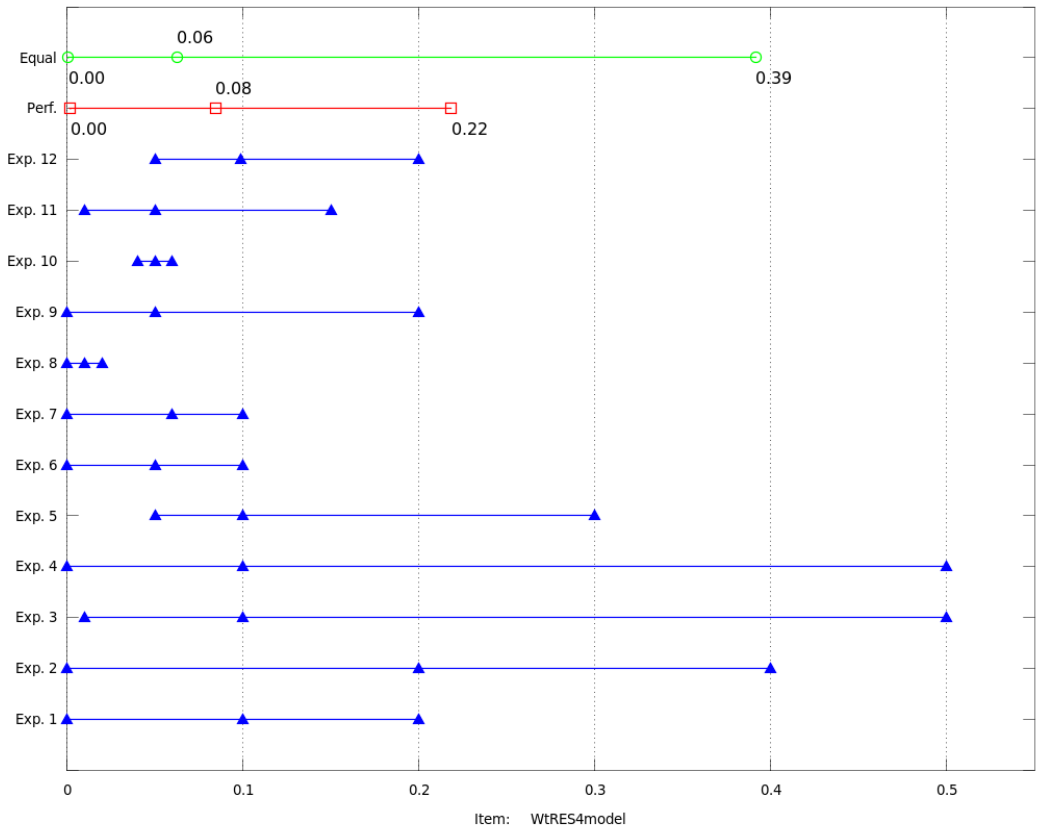

Figure 4.4: For characterizing the likely Regional Evolution over the period 100 kyr to 1 Myr, what relative weight would you give to the RES 4 model option?

Facilitator's comments:

There are wide-ranging uncertainties in individual judgments; credible intervals vary, but mostly overlap across the group.

The Performance Weights solution credible interval is narrower than the Equal Weights solution.

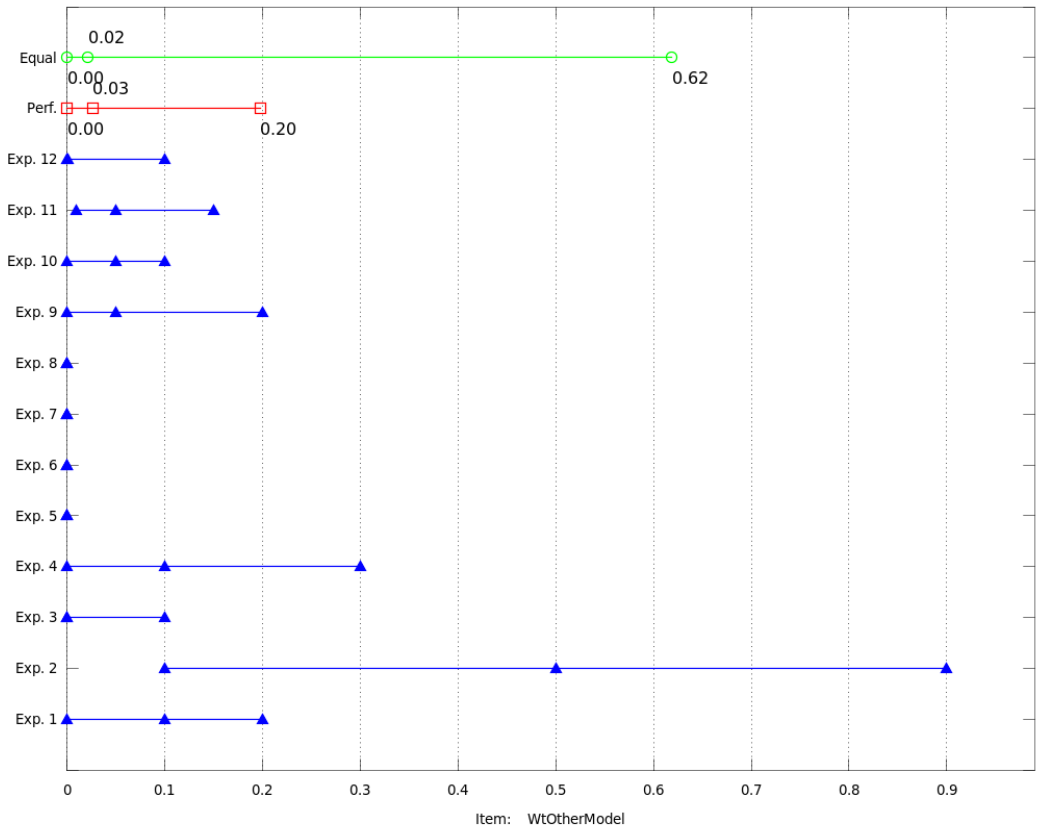

Figure 4.5: If you think an alternative model, distinctly different from models RES1, RES2, RES3 and RES4, is feasible for characterizing the likely Regional Evolution over the period 100 kyr to 1 Myr, what relative weight would you give to this other model?

Facilitator's comments:

The disparities in individual judgment credible intervals are marked for this Target Item, with several of the group providing zero or negligible weights to the possibility of an alternative model; others ascribe real non-zero weights to this possibility.

The Performance Weights solution credible interval is narrower than the Equal Weights solution.

4.4 Weights for the SESs

Figure 4.6 summarises the numerical values for three quantiles (5%ile; 50%ile; 95%ile) on each of the SES questions outlined in Section 4.1, obtained by weighted pooling of the experts' judgments. Three decimal places are displayed below in order to report low values, but limited significance should be ascribed to this level of precision and values should be rounded appropriately.

Item Nr.	Item Id.	5%ile	50%ile	95%ile	Description
T1	WtRES1model	0.425	0.688	0.897	Relative weight to RES 1 model for 100 kyr to 1 Myr future
T2	WtRES2model	0	0.105	0.291	Relative weight to RES 2 model for 100 kyr to 1 Myr future
T3	WtRES3model	0	0.109	0.302	Relative weight to RES 3 model for 100 kyr to 1 Myr future
T4	WtRES4model	0.002	0.084	0.218	Relative weight to RES 4 model for 100 kyr to 1 Myr future
T5	WtOtherModel	0	0.027	0.198	Relative weight to different model for 100 kyr to 1 Myr future
T6	RES1Strain2x	0.009	0.204	0.361	Rel. weight strain rate increases by 2x for RES1 over 1 Myr
T7	RES1Strain=	0.395	0.556	0.884	Rel. weight strain rate remains same for RES1 over 1 Myr
T8	RES1Strain0.5x	0	0.201	0.350	Rel. weight strain rate decreases by 2 x for RES1 over Myr
T9	RES2Strain2x	0.215	0.582	0.992	Rel. weight strain rate increases by 2x for RES2 over 1 Myr
T10	RES2Strain=	0	0.241	0.585	Rel. weight strain rate remians same for RES2 over 1 Myr
T11	RES2Strain0.5x	0	0.025	0.276	Rel. weight strain rate decreases by 2x for RES2 over 1 Myr
T12	WtRES1_GPS	0.068	0.267	0.498	Rel. weight for GPS-based strain rate model under RES1
T13	WtRES1_Seism	0.067	0.261	0.496	Re. weight for seismicity-based strain rate model under RES1
T14	WtRES1_Fault	0.151	0.358	0.644	Rel. weight for active faulting-based strain rate model under RES1
T14b	WtRES1_Other	0	0	0.303	Rel. weight for different strain rate model
T15	WtRES2_GPS	0.051	0.130	0.394	Rel. weight for GPS-based strain rate model under RES2
T16	WtRES2_Seism	0.044	0.129	0.389	Rel. weight for seismicity-based strain rate model under RES2
T17	WtRES2_Fault	0.215	0.669	0.989	Rel. weight for active faulting-base strain rate model under RES2
T17b	WtRES2_Other	0	0	0.303	Rel. weight for different strain rate model
T18	RES1Birth_3x	0.066	0.166	0.340	Rel. weight volcano birth rate increases 3x under RES1
T19	RES1Birth=	0.384	0.525	0.944	Rel. weight volcano birth rate unchanged under RES1
T20	RES1Birth_0.3x	0.066	0.166	0.340	Rel. weight volcano birth rate decreases 3x under RES1
T21	RES2Birth_3x	0.086	0.271	0.498	Rel. weight volcano birth rate increases 3x under RES2
T22	RES2Birth=	0.118	0.444	0.599	Rel. weight volcano birth rate unchanged under RES2
T23	RES2Birth_0.3x	0.077	0.270	0.495	Rel. weight volcano birth rate decreases 3x under RES2
T24	RES1_Tight	0.076	0.512	0.747	Rel. weight tight cluster model under RES1
T25	RES1_Smooth	0.069	0.340	0.500	Rel. weight smooth cluster model under RES1
T26	RES1_Random	0.000	0.058	0.397	Rel. weight random density model under RES1
T26b	RES1_VolcMap	0	0	0.097	Rel. weight for different cluster model
T27	RES2_Tight	0.063	0.278	0.518	Rel. weight tight cluster model unde RES2
T28	RES2_Smooth	0.077	0.446	0.600	Rel. weight smooth cluster model under RES2
T29	RES2_Random	0.077	0.258	0.470	Rel. weight random density model under RES2
T29b	RES2_VolcMap	0	0	0.092	Rel. weight for different cluster model

Figure 4.6: Numerical values for three quantiles (5%ile; 50%ile; 95%ile) on each of the SES questions outlined in Section 4.1, obtained by weighted pooling of the experts' judgments.

4.5 Scenario tree weights leading to SES probabilities

The following series of eight chart panels show the two scenario sub-trees which were the framework for the elicitation exercise, with central value weights for branch nodes added sequentially, as derived from the elicitation exercise.

Where, in the range graph results presented above, elicited results for combinations of weights on companion branches do not sum exactly to unity these have been normalised before being entered on the sub-tree plots that follow.

The purpose of these particular plots is simply to illustrate how the results from a structured elicitation can be used to populate such probability trees. The tree plots also allow ease of comparison across the various Target Items.

In a formal quantitative hazard or risk assessment, the corresponding distributional spreads would be utilised also, in order to express related ranges of scientific uncertainty.

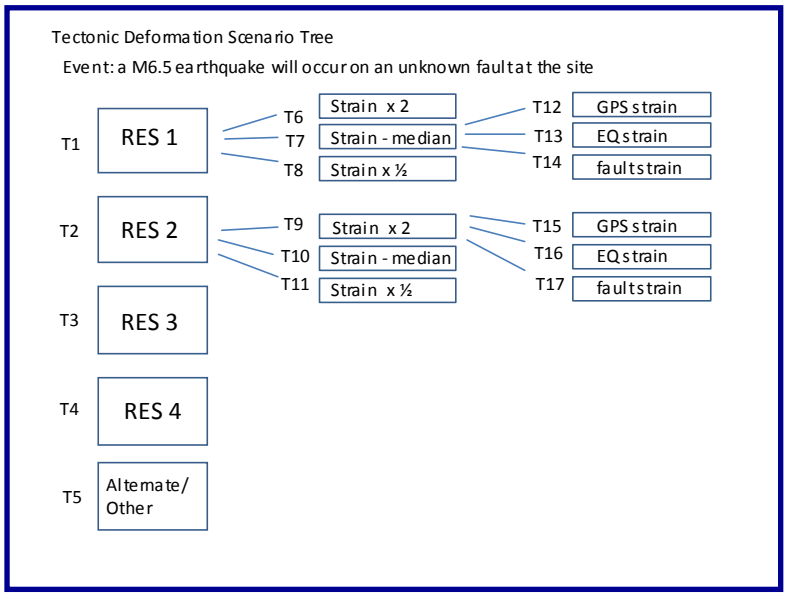

Figure 4.7: The two scenario sub-trees, which were the framework for the elicitation exercise, with central value weights for branch nodes added sequentially, as derived from the elicitation exercise.

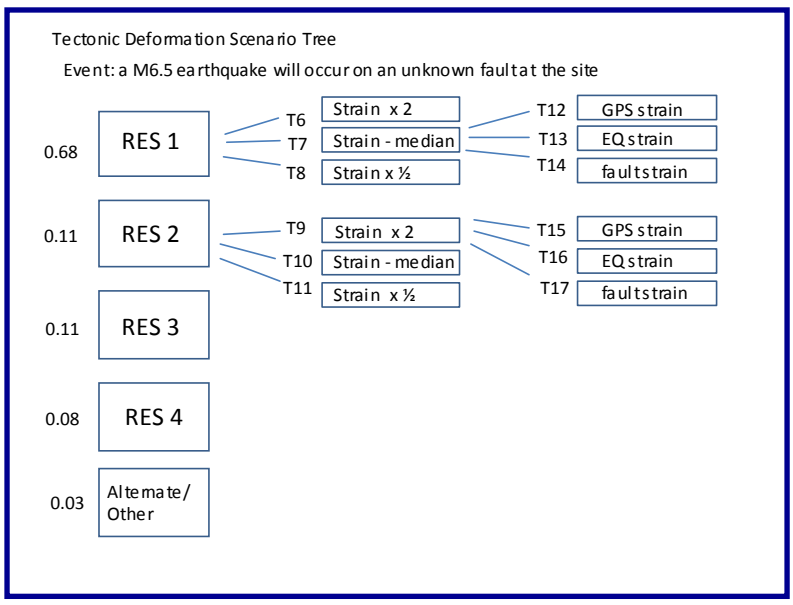

Figure 4.8: (same as above).

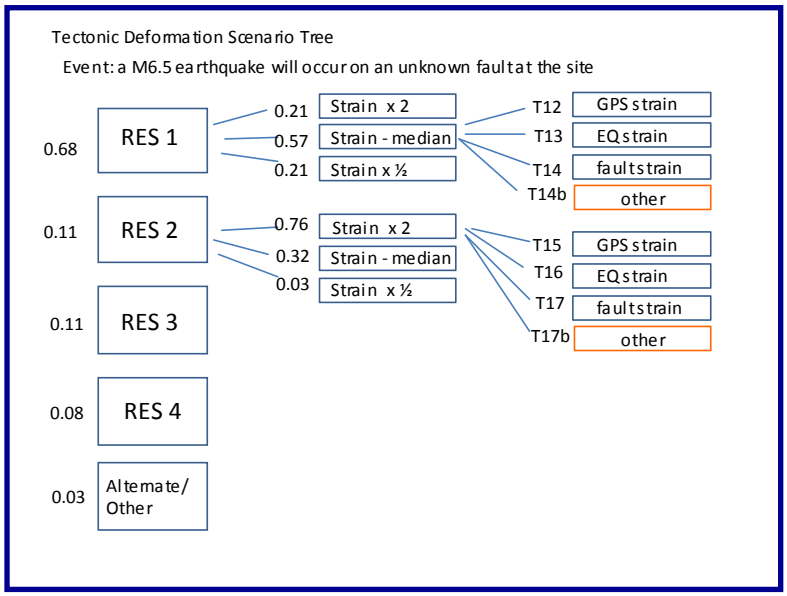

Figure 4.9: (same as above).

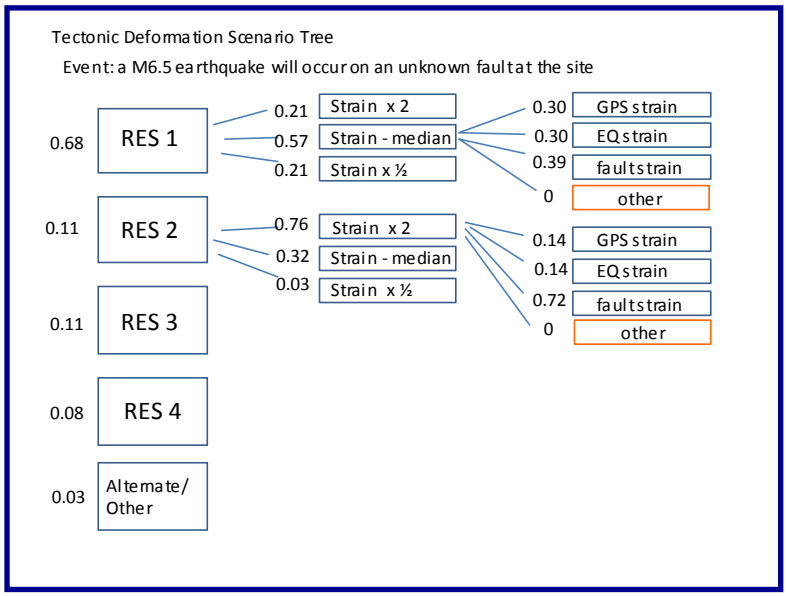

Figure 4.10: (same as above).

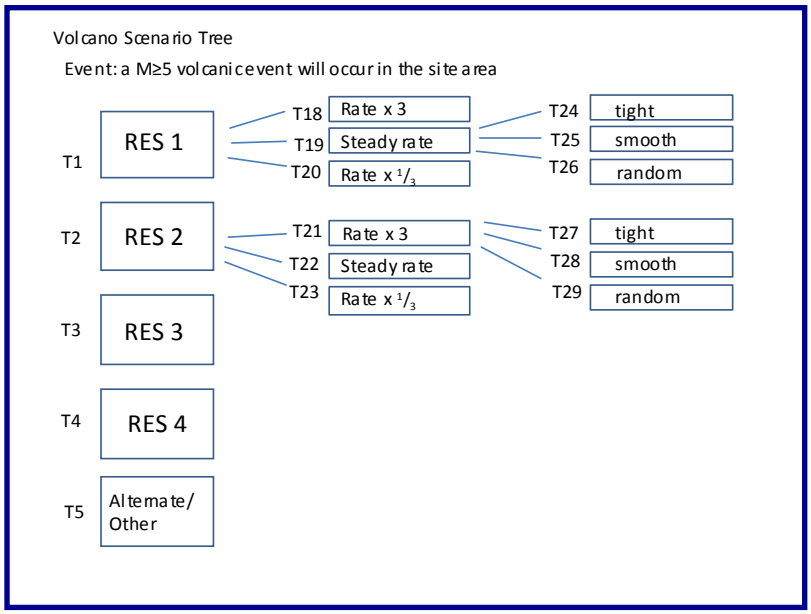

Figure 4.11: (same as above).

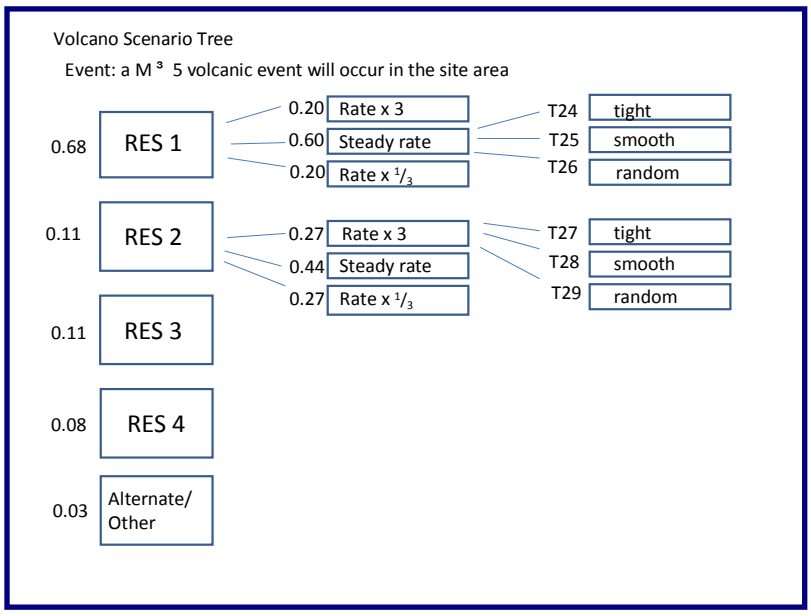

Figure 4.12: (same as above).

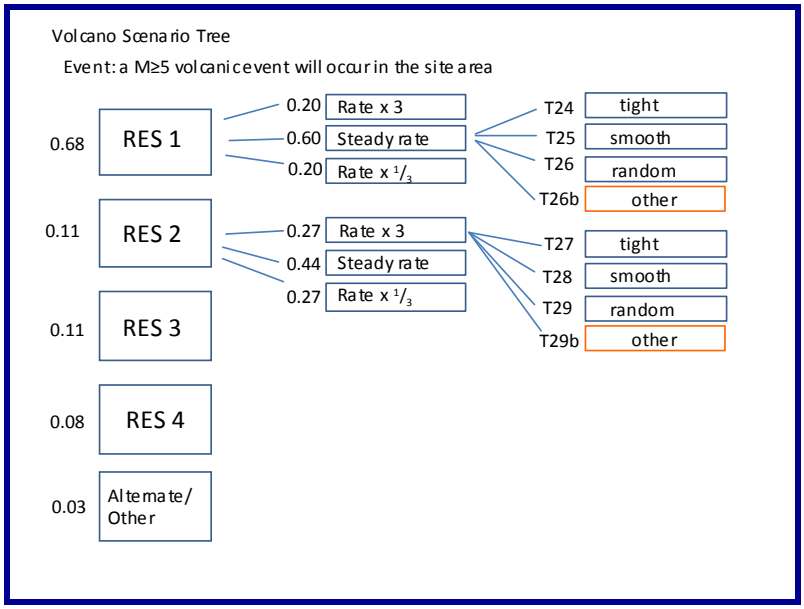

Figure 4.13: (same as above).

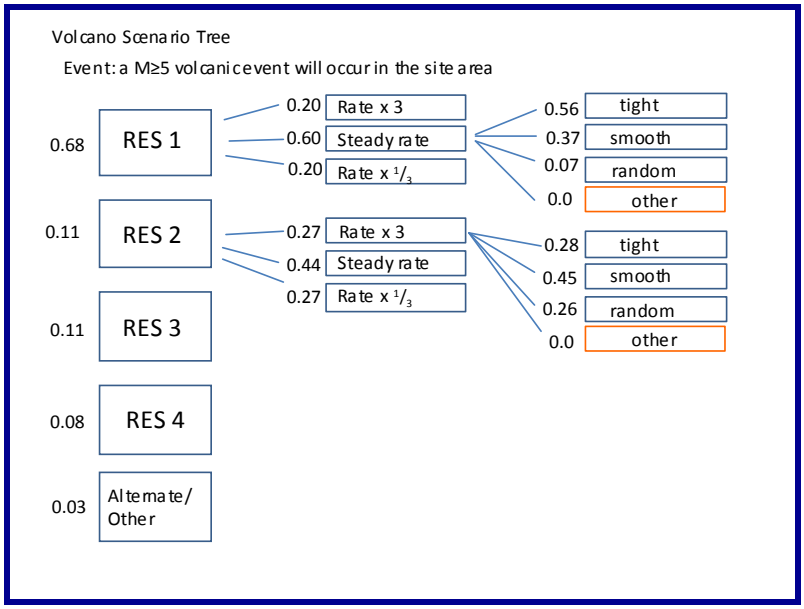

Figure 4.14: (same as above).

4.6 Discussion of the Expert Elicitation

In this demonstration exercise, the usual procedures for a structured elicitation with analysis using the Cooke Classical Model were followed. The exercise – as an expert elicitation – can only be regarded as a very preliminary attempt at teasing out where significant knowledge gaps exist in relation to the problem of forecasting long-term scenarios for hazards and risks for proposed geological repository sites of radioactive wastes in Japan, at quantifying certain factor uncertainties in present models, and at identifying issues and factors that might be amenable to targeted further work.

In terms of experts' responses to the Seed Item questions, the general pattern was one of wide-ranging uncertainties in individual judgments. This said, individual credible intervals

almost invariably overlapped across the group, and there was little indication of systematic dichotomies due to question ambiguity or misunderstanding. The credible intervals derived from the Performance Weights pooling solutions were almost universally narrower than those of the corresponding Equal Weights solutions and, with one exception, realization values fell consistently within the credible ranges of both the Performance Weights and Equal Weights credible ranges, with the Performance Weights solutions doing marginally better, overall.

In similar vein, experts' judgments on nearly all the scenario questions had large credible intervals associated with them, indicating extensive uncertainty in relation to the questions posed. While there are varied uncertainties in the individual judgments for all the scenario questions, collectively the credible intervals usually overlapped across the group. With just a few marginal exceptions, the Performance Weights solution credible intervals were consistently narrower than those of the Equal Weights solutions.

Taking the elicitation scenario questions outcomes overall, the scientific uncertainties on many factors are seen to be large and quite difficult to quantify precisely. This said, the exercise served to show that a formalised expert elicitation can be useful for providing rational constraints on the ranges of parameter or probability variations, and for promoting discussion of key issues at the heart of scientific uncertainties.

4.7 Output of the Expert Elicitation

The end result of the Expert Elicitation is a set of SESs for Location 'C' with probabilities attached to each in the form of relative degrees of belief of the group of experts involved. These SESs are propagated to the next stage of the TOPAZ methodology, in Section 5.

5 Estimation of IS probabilities for Location 'C'

Following the approach outlined in Section 1.3, the SES probability results of the Expert Elicitation exercise were integrated with the results of the ITM hazard mapping to determine probabilities that the two selected Impact Scenarios (ISs) could occur over the next 1 Myr. The first step is to provide a clear, specific 'event definition' of credible tectonic-deformation and volcanism ISs for a given RES-SES branch. Based on such 'event definitions, it is possible to use various geological and geophysical data to set initial probabilities for any specific IS. In the following section two illustrative 'event definitions' for ISs of a M6.5-7.5 earthquake and a M5 volcanic event at Location C are described.

5.1 Demonstration of the Quantitative Estimation of the Probability of a Tectonic Deformation Scenario for a M6.5-7.5 Future Earthquake

We use the results of the expert elicitation demonstration exercise together with the ITM strain rate models (Chapman et al., 2009) to demonstrate how tectonic deformation can be quantified. The purpose is to show how the range of RESs, and choice of ITM deformation model (active fault and surface deformation-based, seismicity-based and GPS-based) can be combined and used to quantify the probability of hazardous tectonic events at a site. Our definition of a hazardous event for the purposes of this demonstration is a range of earthquake sizes from M6.5 to M7.5 occurring in the upper 10 km of the 5 x 5 x 20 km crustal volume defining example Location C. The upper several hundreds of metres is the crustal depth within which a repository would potentially be hosted, and M6.5-7.5 ruptures below 10 km would be less likely to impact the shallower repository depths with permanent deformation (see Appendix 1). The earthquake magnitude range is modelled according to a Gutenberg-Richter distribution: $logN = a - bM$, in which N is the number of events of magnitude M, and a and b are empirical constants. We assume the same maximum magnitude defined for the region surrounding location C in the ITM modelling (M7.5; Chapman et al. 2009) and the minimum is chosen largely for demonstration purposes in this study.

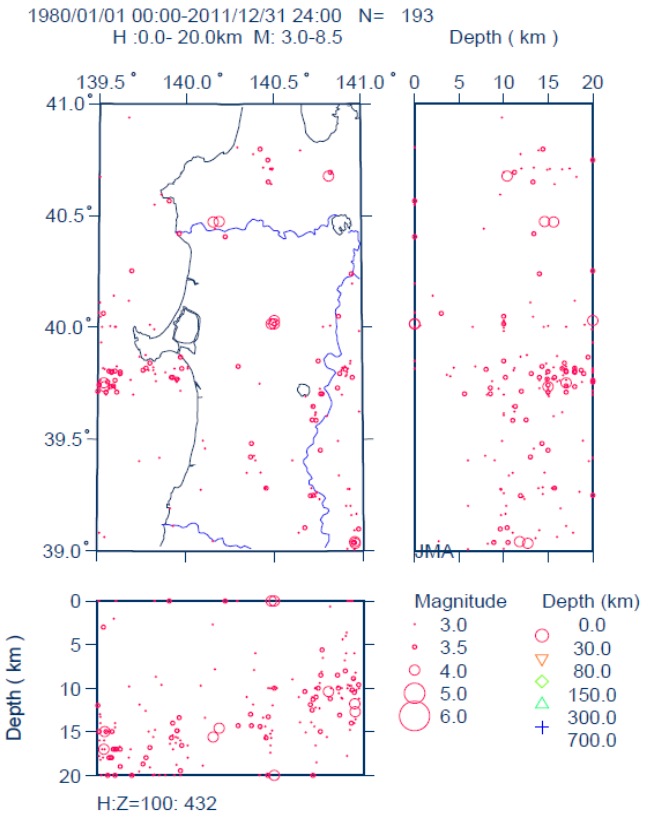

Figure 5.1: Seismicity map with longitudinal and latitudinal depth sections in the vicinity of Location C. The earthquakes are from 1980 to 2011, and M≥3. Clearly, the majority of seismicity lies at depths greater than 10 km. Source http://wwweic.eri.u-tokyo.ac.jp/db/jma/

It is important to note that the epistemic uncertainties have not been fully quantified in this demonstration exercise. The expert elicitation exercise was limited to populating only a few branches of the logic tree. These are: (1) RES1, Deformation constant over 1 Myr, and choice of ITM active fault/surface deformation, seismic, and GPS deformation models, and; (2) RES2, upper plate shortening increasing by a factor of two in 1 Myr, and the same choice of ITM deformation models. The expert elicitation exercise provided performance-based weights for these sections of the logic tree.

Examination of approximately 30 years of seismicity around Location C to a depth of 20 km (Figure 5.1) shows that approximately 25% of earthquakes lie at 0-10 km, and 75% in the lower 10 – 20 km of the 5 x 5 x 20 km crustal volume. This is the basis for modelling the seismicity applied in the tectonic deformation modelling, in that any deformation rate estimates (i.e. seismic moment rates and resulting earthquake rates) originating from the ITM deformation models (based on a 5 x 5 x 20 km crustal volume) are factored down to 25% of the original rate estimates.

5.1.1 Methodology

Our procedure is to use the ITM strain rate-based tectonic deformation models for active fault/surface deformation, seismicity and GPS as input to the expert elicitation logic tree (see logic tree in Section 3). These three deformation models are assigned the weights defined during the expert elicitation procedure, as are the choices of deformation rate increase in the 1 Myr timeframe for RES1 and RES2.

For the purposes of this demonstration we simplify the input from the three ITM deformation models by condensing the earlier histograms of numerous strain rate models (Chapman et al., 2009) down to a single seismic moment rate for each ITM deformation model data type. In this way, we can clearly show the epistemic uncertainties arising directly from the choice of RES, rate increase and ITM deformation model in the demonstration (Figure 5.2).

This involves converting the strain rates into seismic moment rates via the method of Kostrov (1974) and then summing the incremental seismic moment rates. The summed seismic moment rate is then increased by a factor of two for RES2, and maintained at a constant for RES1 according the limited logic tree branches populated by the expert elicitation exercise (see Section 3).

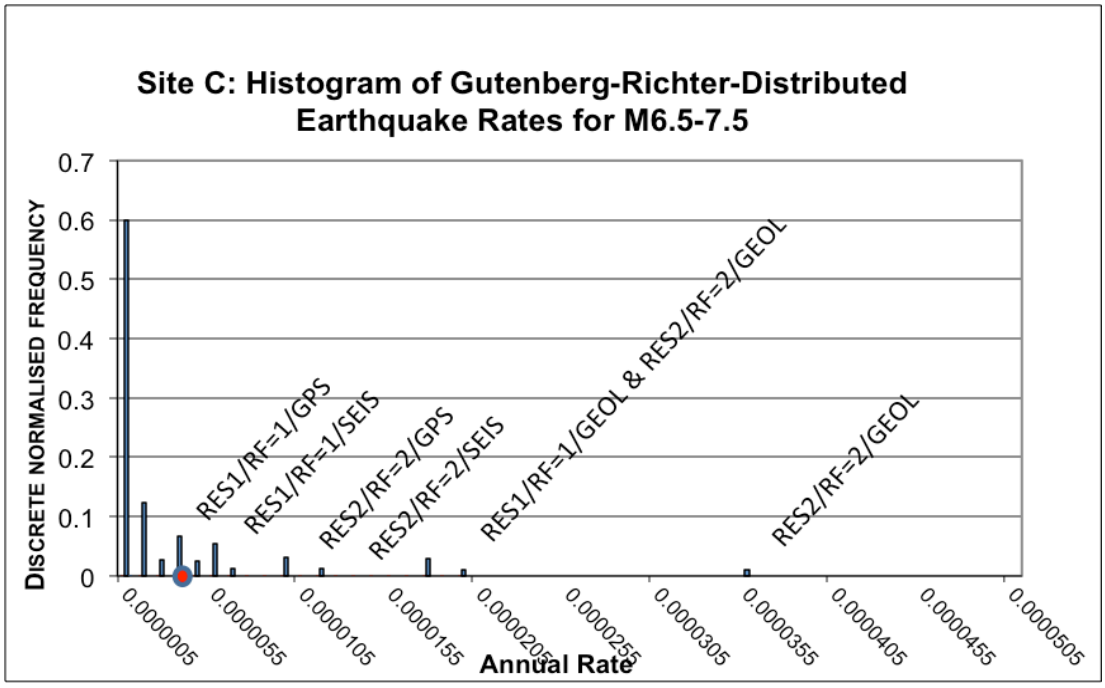

Figure 5.2: The discrete histogram for the 5 x 5 x 20 km location C block, in which the seismic moment rate is factored down to 25% of original moment rate to take account of low seismicity rates in the upper 10 km (Figure 5.1). Particular combinations of RES, rate increase factors for 1 Myr (RF), and tectonic deformation models (GEOL, SEIS, GPS) clearly dominate various parts of the histogram (see labels), despite the Gutenberg-Richter distribution producing a diversity of magnitudes and rates. The red dot shows the position of the arithmetic weighted mean of the entire distribution.

The combinations of RES, deformation rate change and deformation model are then used to distribute the seismic moment rates into Gutenberg-Richter distributions of earthquakes from M6.5 to 7.5. The results of 10,000 Monte Carlo logic tree simulations of M6.5-7.5 Gutenberg-Richter-distributed earthquake rates are shown by the histograms in Figure 5.2 and 5.3.

Figure 5.2 shows the discrete normalised frequency (count per bin/summed count for all bins) of the 10,000 simulations on the y-axis, and the M6.5-7.5 rate bins in the x-axis. Magnitudes within this range are not distinguished in the figures.

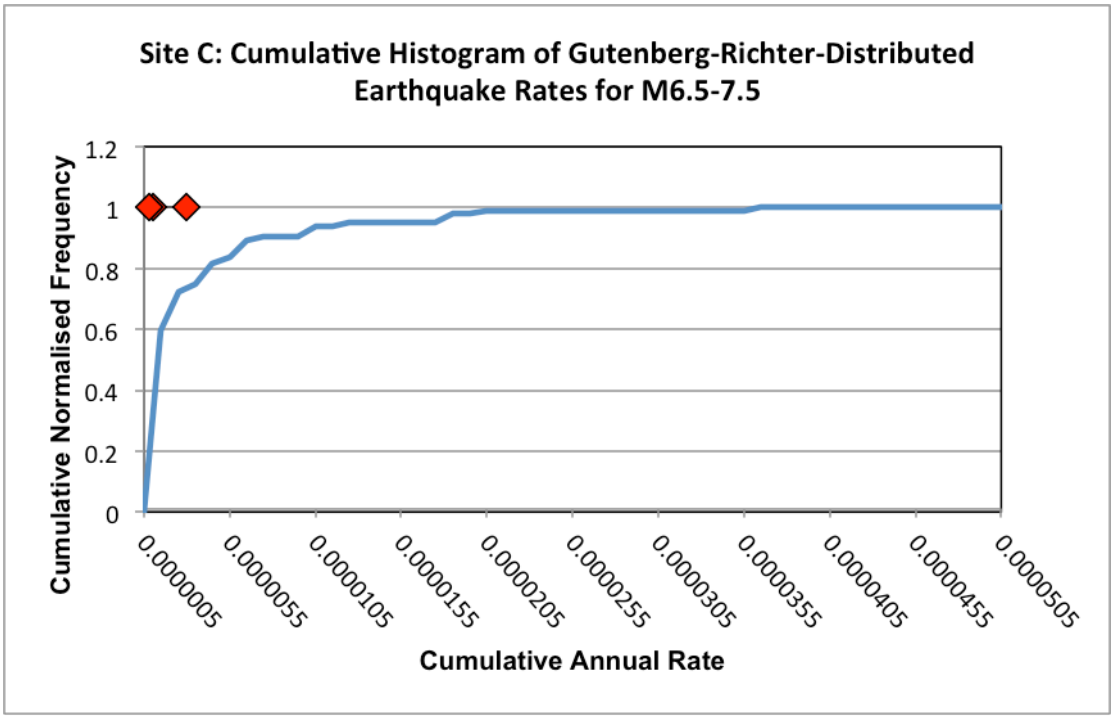

Figure 5.3: The cumulative histogram for the 5 x 5 x 20 km location C block, in which the seismic moment rate is again factored down to 25% of the original moment rate to take account of low seismicity rates in the upper 10km (Figure 5.1). Three "bulk cumulative rates" for M6.5-7.5 earthquakes (i.e. single rate for the sum of all earthquakes from M6.5 to 7.5) derived from the three original ITM deformation models are shown for comparison as red diamonds (seismicity and GPS-derived rates plot on top of one another at the left-most diamond). The rates are calculated for each deformation model by dividing the single condensed seismic moment rate for that dataset (see Section 5.1.1) by the seismic moment integrated over M6.5-7.5. The cumulative histogram shows a broad range of rates to the right of the diamonds, due to the assumption of the Gutenberg-Richter distribution producing a great diversity of rates across the magnitude range.

An alternative, but very simplistic histogram is shown in Figure 5.4. The histogram shows the results of a further 10,000 simulations, but this time assuming that all seismic moment release occurs only by M6.5 scenario earthquakes within the 5 x 5 x 20 km crustal volume. This extreme model is for illustrative purposes and would be relevant in the situation where only one active source is known to exist within the crustal volume. The rates are again scaled down to 25% of original, to take into account the depth distribution of seismicity in the vicinity of the site.

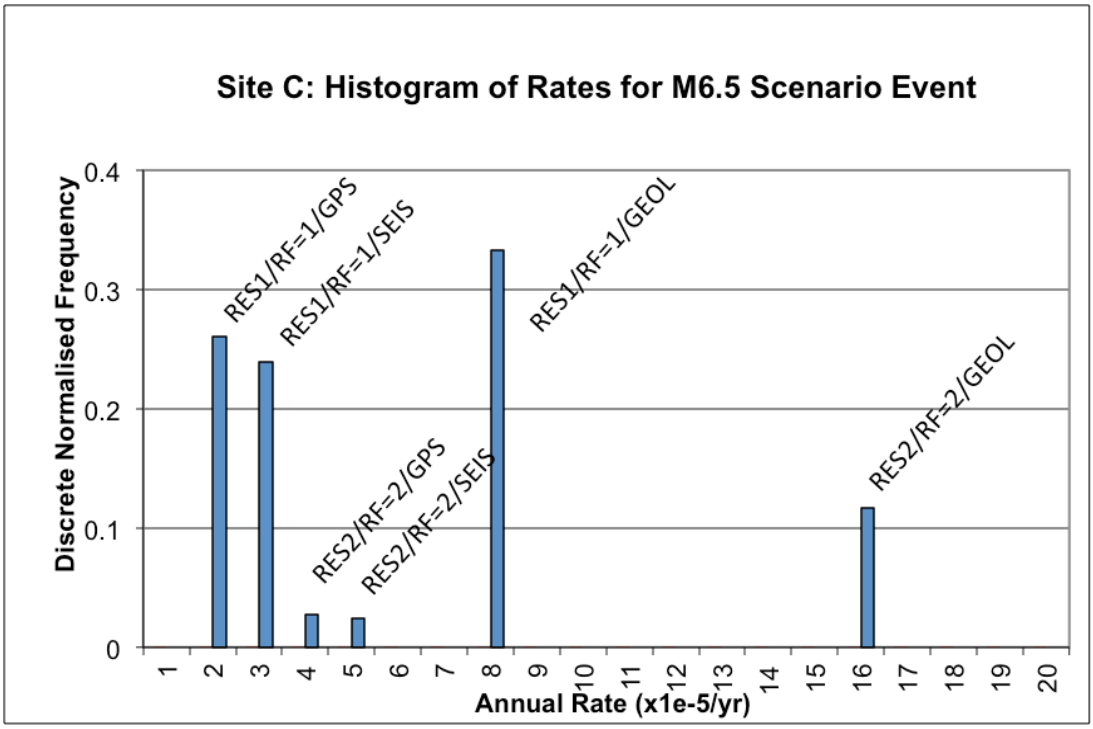

Figure 5.4: Discrete histogram showing the range of rates for a scenario M6.5 earthquake in a 5 x 5 x 20 km crustal volume. The rates are again scaled down to 25% (see above). The particular combinations of RES, rate factor increase and deformation model responsible for the spikes on the histogram are also shown.

5.1.2 Observations

Our methodology of condensing each of the three original ITM strain rate model histograms for sites (Chapman et al. 2009) down to single seismic moment rates allows us to observe the epistemic uncertainty due solely to the choice of RES, rate factor increase, and ITM deformation model in Figures 5.2 to 5.4. We label the discrete histograms accordingly to show the particular combinations of these parameters that produce some of the histogram spikes.

The spikes on this histogram translate to changes in slope on the cumulative plot (Figure 5.3). In general, the frequency of M6.5-7.5 rates fall steeply from about 1e-7/a to about 3e-6/a in Figure 5.2, but with some higher rates encountered in the right of the histogram (3e-5/a). The weighted arithmetic mean of the distribution is 2.8e-6/a. This low rate is a consequence of the very small crustal volume being considered, and the effect of distributing the seismic moment rates across a Gutenberg-Richter distribution from M6.5 to 7.5.

The large earthquakes of the Gutenberg-Richter distribution (M7-7.5) will accommodate eight times the seismic moment release of the moderate earthquakes (M6.5-6.9), so fewer large events are required to accommodate the seismic moment release relative to moderate events. This effect is further illustrated by comparing Figure 5.2 to the simplistic earthquake histogram in Figure 5.4, in which earthquakes are assumed to occur only as M6.5. In this case, the weighted mean is about 8e-5/a, a much higher rate than in the Gutenberg-Richter-based histogram (Figure 5.2). This is because all of the seismic moment rate is assigned to moderate (M6.5) earthquakes in Figure 5.4.

5.2 Demonstration of the Quantitative Estimation of the Probability of a M5 Volcanic Scenario

In the following sections we look first at the probability of any magnitude of new volcanic activity affecting location C (effectively, the SES probability), using the spatial density modelling approaches developed as part of the ITM methodology, weighted according to the results of the expert elicitation exercise reported in Section 4. The Expert Elicitation developed relative degrees of belief in these different evaluation approaches. We then look at the specific probability of occurrence of the defined IS at location C, which is an event of greater than M5 on the VOGRIPA explosive volcanism magnitude scale.

5.2.1 Estimation of SES probability at Location C

The aim of this exercise is to illustrate how expert elicited probabilities are combined with estimated probabilities obtained from probabilistic volcanic hazard assessment models. For the Tohoku region, the ITM methodology was only applied for scenario RES I (Chapman et al., 2009), so only estimated probabilities in relation to that scenario are available for location C.

The data available for the application are given in Table 5.1; the elicited median probabilities correspond to the weighted pooling of the experts judgments on the related target items (see the table in Section 4.4). The estimation of volcanic hazard of any type and magnitude occurring within a 5 x 5 km area at the location C was obtained over a 100 kyr period using the ITM probabilistic methodology (Chapman et al., 2009). Since the period of interest for TOPAZ extends out to a million years, the volcanic hazard values given by the Cluster (Cox) and the smooth Kernel (SAMSE) spatial density models were linearly extrapolated to cover the period of interest. For the Homogeneous Poisson model, simple analytical probabilistic calculations were applied to estimate volcanic hazard at location C over 1 Myr period using the data given in Chapman et al. (2009). In addition, the long-term average rate of formation of new volcanoes in the Tohoku region was assumed to stay the same as the average Quaternary rate.

Therefore, the application is targeted at estimating site evolution scenario (SES) probability in relation to the regional evolution scenario I (RES I) with a recurrence rate model under steady state conditions of volcanic activity (i.e. the recurrence rate model named Model_=). The applied data are displayed in red in Table 5.1.

Table 5.1. Volcanism example: elicited probability and estimated volcanic hazard in relation to RES I.

Volcanism results from expert elicitation (cf. section 4.4)			**ITM methodology (Chapman et al. 2009)**
Scenario [Prob 50%ile]	**Recurrence rate model [Prob 50%ile]**	**Spatial density model [Prob 50%ile]**	**Volcanic hazard at site C**
	Model_3x [0.166]	Cluster (Cox) [**0.512**]	**$3.7 \cdot 10^{-3}$**
RES I [**0.688**]	Model_= [**0.525**]	Kernel (SAMSE) [**0.340**]	**$7.2 \cdot 10^{-3}$**
	Model_1/3 [0.166]	Homogen. Poisson [**0.058**]	**$2.6 \cdot 10^{-2}$**
RES II [0.105]	...	...	
RES III [0.109]	...		
RES IV [0.084]	...		
Other model(s) [0.027]	...		

The specification of a SES scenario is obtained by following a single branch through the logic tree. A given SES scenario is then associated to the following states: i.e. (i) RES scenario, (ii)

recurrence rate model, (iii) spatial density model and (iv) volcanic hazard at location C. Therefore, the probability of igneous activity for a SES scenario is estimated by multiplying the probability values related to his given states (Table 5.2). Using this approach, elicited probability and estimated volcanic hazard are combined in order to estimate values for SES probability of igneous activity at location C, given the occurrence of RES I, specific models and their associated results.

The variability of the SES probability values at location C given in Table 5.2 seems rather low; this effect is likely related to the linear extrapolation performed for the estimation of volcanic hazard over a 1 Myr period. The probabilistic assessment of volcanic hazard for such a longer period requires datasets that extend beyond the Quaternary, possibly up to the Miocene, in order to describe the volcanic patterns likely to occur in space and time.

The key advantage of this approach lies in the capability of assimilating various sources of uncertainty, related to scenarios, models and data, when performing probabilistic hazard assessments.

Table 5.2. Volcanism example: estimation of probability of igneous activity at site C for three SES.

RES I	Model=	Cluster (Cox)	Kernel (SAMSE)	Homogeneous Poisson	Volcanic hazard at location C	SES Probability at location C
0.688	0.525	0.512			$3.7 \cdot 10^{-3}$	**$6.8 \cdot 10^{-4}$**
0.688	0.525		0.340		$7.2 \cdot 10^{-3}$	**$8.8 \cdot 10^{-4}$**
0.688	0.525			0.058	$2.6 \cdot 10^{-2}$	**$5.4 \cdot 10^{-4}$**

5.2.2 Estimation of IS probability of a VOGRIPA M5 event at Location C

Potential for large magnitude volcanic eruptions is particularly relevant for the siting of geological repositories. Such eruptions, should they occur directly through a repository, could result in the release of a large fraction of the inventory into the biosphere. Although the probability of such eruptions is extremely low (Connor et al., 2009) their potential effects are large, so estimation of risk associated with these rare events should be considered as part of the siting process.

Volcanologists have developed at least two methods for characterizing the size of volcanic eruptions. The volcano explosivity index (Newhall and Self, 1982), generally termed VEI, uses an integer scale from 0 to 8 and is based on both the volume of erupted material and the height of the explosive eruption column. For HLW facilities VEI => 5 is of most concern because of the high impact and frequency of events in the VEI 5 range. These eruptions (VEI => 5) have eruptive volumes of tephra greater than 1 km^3 and typically have eruption column heights that reach maximum height of greater than 25 km. Like many indices of natural hazards, the VEI scale is approximately logarithmic. Consequently, the rarest and largest magnitude explosive eruptions have scales of effects on the order of thousands of square kilometers. Indeed, the largest known volcano eruptions have continental scale effects (e. g., the Yellowstone eruption of approximately 600 kyr). The global frequency of VEI => 5 is approximately 0.03 per year, based on the known record of activity in the Holocene (Seibert et al, 2010). Globally, rates of VEI 7 eruptions occur with an annual frequency of 10^{-3} per year; VEI 8 eruptions occur with an annual frequency of approximately 10^{-4} per year.

A second method for classifying eruptions is the magnitude scale proposed by Mason et al. (2004) that is based on the magnitude of the total volume of erupted products. This scale relaxes the assumption of explosivity, including effusive eruptions as potentially large magnitude events. The largest volume effusive eruptions, often referred to as flood basalts because of the large areas inundated by lava flows, are extremely rate, occurring on Earth on time scales of tens of millions of years. Therefore, the largest magnitude eruptions generally

are explosive in nature, producing copious ash fall deposits over vast regions. In the following, we consider the relative frequency of large volume explosive eruptions by tectonic setting using this magnitude scale, acknowledging that large volume effusive events may also occur but are exceedingly rare, even on the time scales of geological repository performance periods.

We have developed an explosive eruptions database of the Japanese islands. This Japan database forms part of the Large Magnitude Explosive Eruptions database of Volcano Global Risk Identification and Analysis (VOGRIPA) project. The database contains information about the age of eruptions, pyroclastic ejecta volume, VEI (Volcanic Explosivity Index), magnitude and data source of volcanic records. The database attempts to include all known explosive eruptions during the Quaternary and VEI magnitude ~4 or greater. We use this database to explore the preservation of products of explosive eruptions and patterns of volcanic activity in Japan and to provide data to help assess the probability of the largest magnitude eruptions occurring at or near a geological repository in Japan during its performance period.

5.2.2.1 The Japan VOGRIPA database

The Large Magnitude Explosive Eruptions database of VOGRIPA has been systematically compiled from primary and secondary sources. Major data sources of explosive events in Japan include:

- The one million year tephra database for the Japanese islands and the Japan 2000 year eruption database. Both of these databases can be found at the website: http://gunma.zamurai.jp/database/ maintained by Professor Hayakawa at the Gunma University, Japan.
- The active volcano database of Geological Survey of Japan (http://riodb02.ibase.aist.go.jp/db099/index-e.html)
- The Quaternary volcano catalogue of the Volcanological Society of Japan (http://www.geo.chs.nihon-u.ac.jp/tchiba/volcano/index.htm)
- The atlas of tephra in and around Japan (Machida and Arai, 1993).

Information from these references was cross-validated and discrepancies addressed where possible.

The database contains a total of 696 explosive eruptions. Half of these eruptions occurred within the last 65 kyr; 77% of the total eruptions occurred since 200 kyr; the oldest eruption in the database is 2.25 Myr. In addition, percentages by eruption magnitude are: VEI 4 (40%), VEI 5 (42%), VEI 6 (13%) and VEI 7 (5%). Given the generally accepted order of magnitude decrease in eruption frequency with order of magnitude increase in eruptive volume (a Gutenberg-Richter style relation for eruption frequency-magnitude), it appears that large magnitude eruptions are over represented in the database. That is, VEI 5 eruptions are nearly as abundant as VEI 4. Similarly, VEI 6 and 7 eruptions are over representative if they truly occur at order of magnitude lower frequencies. Part of this result may be attributable to the preservation potential of volcanic deposits. Because larger volume eruptions are more readily preserved, they may be disproportionately represented in the geologic record. Furthermore, it may be more likely that larger volume explosive eruption deposits will be identified in the geologic record and these deposits described. Thus, there is a clear need to develop a statistical model of the frequency of large magnitude events, given our imperfect knowledge of this frequency based on the geologic record alone. Such models will provide key input parameters to spatial density models (ITM methodology) and will allow improvements of hazard maps linked to specific volcanic events.

5.2.2.2 Development of Statistical Models

Figure 5.5 illustrates empirical survivor functions for eruptions of VEI magnitude 4 and greater as a function of time. This plot is created by normalizing the total number of events in each VEI category, and plotting the complementary cumulative distribution as a function of time. Several features of the plot indicate that eruptions are under-recorded as a function of time. For each VEI category, the number of known eruptions decreases approximately exponentially as a function of eruption age. The half-life of each empirical survivor function (time since the present to 50 percent cumulative number of eruptions) depends on VEI category. VEI 4 eruptions have much shorter “half-life” than VEI 5; VEI 7 eruptions have the

longest “half-life”, as expected given the large magnitude of these events. If eruptions of any age to 2.2 Myr, the total duration of the Quaternary record, were equally likely to be preserved, the expected values of the half-life would be approximately 1.1 Myr. Given that all VEI categories have significantly shorter half-lives than 1.1 Myr, it is clear that many older eruptions are missing from the geologic record. Finally, it is clear that the preservation of relatively small magnitude eruptions (e.g., VEI 4) is much less likely than the preservation of the relatively large magnitude eruptions.

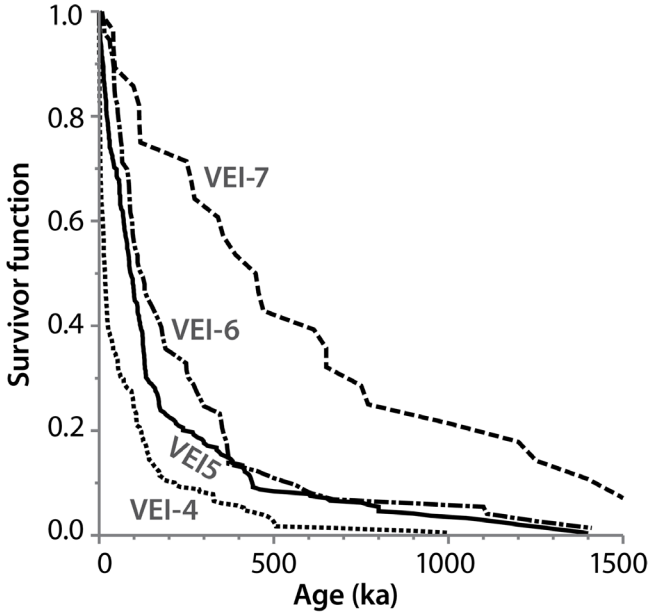

Figure 5.5: Empirical survivor functions for eruptions of VEI magnitude 4 and greater, as a function of time.

Note that the change in half-life as a function of VEI category (Figure 5.5) is a strong indication that eruption frequency has not changed with time. Because VEI 4 eruptions are smaller volume than VEI > 4, they are much more likely to disappear from the geological record in a shorter period of time. Hence the half-life of VEI 4 eruptions is much less than that of the larger eruptions. The most important result of this simple analysis is that estimates of the frequency of explosive eruptions will be underestimated if they are based on average Quaternary rates. That is, we can be certain that the number of Quaternary large-magnitude explosive volcanic eruptions in Japan greatly exceeds 696, the total number identified in the VOGRIPA database.

We developed a double exponential model to describe the change in observed (known) eruptions as a function of time. This model has the form:

$$R(t) = R_1 \exp(-l_1 t) + R_2 \exp(-l_2 t)$$

where R(t) is the rate of preserved (recognised) eruptions as a function of time, t. R and l are estimated from the distribution of explosive eruptions of a given VEI category as a function time in the VOGRIPA database for the Japanese islands. We use a double exponential model because, intuitively, two separate processes may be operating to produce the observed eruption frequency distribution. The first term represents the ability of a deposit to be preserved in the geologic record. The second term represents the ability for geologists to recognise the deposit, given that it is preserved.

The average frequency (recurrence rate) of large magnitude explosive volcanic eruptions in the Japanese islands can be estimated from these fitted distributions, as a function of VEI category. Figure 5.6 illustrates this fit using category VEI 6 eruptions from the VOGRIPA database. Observations from the VOGRIPA database suggest that the current recurrence

rate of VEI 6 eruptions in the Japanese islands is approximately 0.2 events per one thousand years. This value appears to be somewhat low compared to the global estimated rate of VEI 6 eruptions of approximately 1 per one hundred years, based on the global Holocene record. However, detrending this record using the double exponential model yields an average recurrence rate of VEI 6 eruptions of 0.6 per thousand years. Using this average value, the expected number of VEI 6 eruptions in the Japanese islands during a 2.2 Myr period is 1320 eruptions. The record < 100 kyr also gives an indication of the fluctuation in recurrence rate of VEI 6 eruptions, and hence the uncertainty in this estimate. It can be seen (Figure 5.6) that recurrence rate in this period appears to have fluctuated between approximately 0.2 – 0.9 VEI 6 eruptions per thousand years.

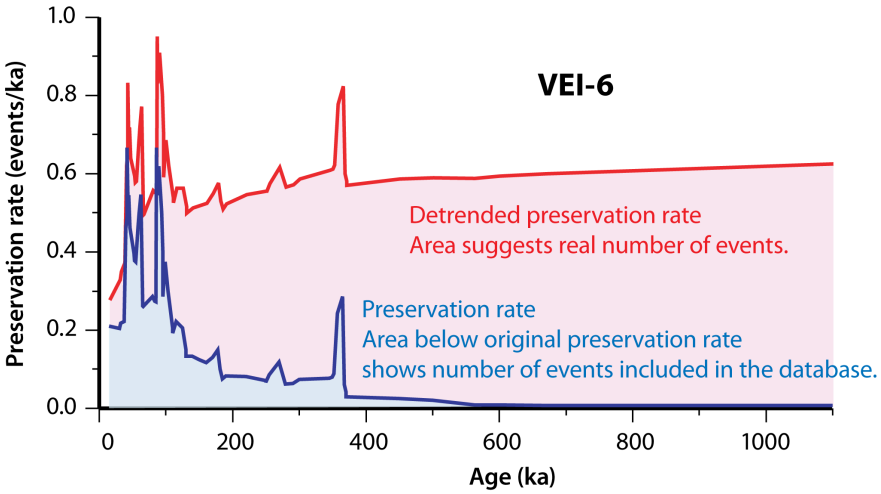

Figure 5.6: Observed (light blue) and modelled (light red) recurrence rate of VEI 6 eruptions from the VOGRIPA database. The integral of the observed recurrence rate, yields 90 VEI 6 eruptions in the Japanese Islands during the Quaternary (last 2.2 Myr). The detrended recurrence rate is much higher, and indicates that on order 1000 VEI 6 eruptions actually occurred in the Japanese islands during this period (average recurrence rate of approximately 0.6 VEI 6 eruptions per 1000 years).

Overall, the results suggest that 97% of VEI 4 events are missing from the record after only 100 kyr, whereas 40% for VEI 5 to 7 are missing after this time period. These results indicate that eruption probabilities based on long term recurrence rate must account for the potential for even large eruptions to be missing from, or unidentified in, the geologic record.

We can also use these data to investigate the frequency-magnitude relationship of large volume explosive eruptions in the Japanese islands as a function of tectonic setting. In order to accomplish this, the Japanese islands were subdivided into tectonic domains. These domains included: Hokkaido, Tohoku, Central Japan, Chugoku, Kyushu, and the Izu-Bonin arc. As with earthquakes, one might expect that the frequency-magnitude relationship, or b-value, of large magnitude explosive volcanic eruptions can vary with tectonic setting. These relationships are shown using detrended recurrence rates for three areas in Figure 5.7.

In Tohoku, the Pacific plate is subducting beneath the North American plate. Results of our analysis suggest that smaller eruptions are much less frequent than expected for a b-value = 1. A b-value of 0.7 is estimated using all of the detrended data. One explanation is that small volume magma batches solidify as intrusions more frequently than expected (compared with Hokkaido and Kyushu), possibly due to thicker or cooler crust. In Hokkaido, the Pacific plate is subducting beneath the North American plate, as in Tohoku. In this region, however, a b-value of approximately one, or slightly less, seems to characterise the frequency magnitude distribution of large-volume explosive volcanism. Similarly, in Kyushu, where the Philippine Sea Plate is subducting below the Eurasia plate, a b-value=1 appears to characterise volcanism. Thus, b-value appears to be different in Tohoku than in these other areas, suggesting that Tohoku is characterised by larger magnitude eruptions than expected using global averages.

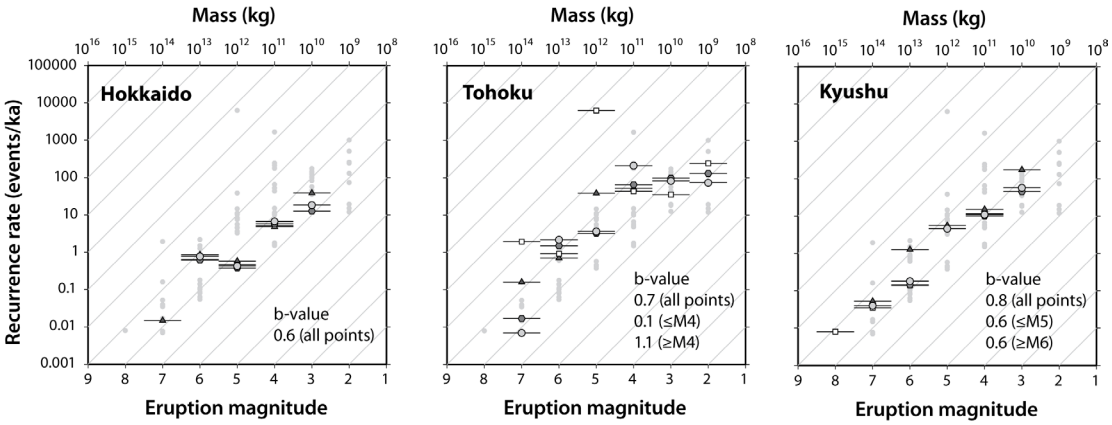

Figure 5.7: Frequency-magnitude relationships for large volume explosive volcanic eruptions in three regions (Tohoku, Hokkiado, and Kyushu) based on analysis of the VOGRIPA database for the Japanese islands.

5.2.3 Implications for potential repository sites

Clearly, estimates of volcanic hazard in active regions cannot simply be based on average numbers of events. Analysis of the VOGRIPA database indicates that such an approach (e.g., using average Quaternary recurrence rates of volcanism) vastly underestimates the potential for large magnitude explosive volcanic eruptions. This is relevant, given typical regulatory requirements to assess repository performance over periods of 100 kyr to 1 Myr (even though the hazard potential of HLW diminishes rapidly over a much shorter timeframe). Assessment periods of the order 100 kyr or 1 Myr require correspondingly long time periods for estimation of recurrence rates. The analysis of the VOGRIPA database indicates that bias invariably occurs in recurrence rate estimates for geologically long periods of time due to the variable preservation potential of deposits.

One approach to estimating the potential for large magnitude explosive eruptions (e.g., VEI => 5) would be to multiple the spatial density of volcanism (derived from Cox process or kernel density models) with the appropriate recurrence rate based on the VOGRIPA-derived frequency-magnitude relationships. Caution is needed in this regard, however, because these frequency-magnitude relationships are derived for existing volcanic systems. For volcanic hazard assessment at a potential geological repository site, no volcanism currently exists at the site, so one needs to consider the potential development of volcanic systems and the type of volcanic system that develops. For example, Mahony et al. (2009) demonstrated that the distribution of dominantly explosive volcanoes in Tohoku is different from the distribution of dominantly-effusive volcanoes. Consequently, the frequency-magnitude relationship cannot be uncoupled from the spatial density estimate, at least for the Tohoku region.

Furthermore, evidence appears to exist that volcanic systems evolve from dominantly effusive to dominantly explosive through time (e.g., Druitt et al., 2002; Connor et al., 2006). Therefore, considering performance periods of 1000 – 10,000 years, the potential for large magnitude explosive volcanism at the site is completely different than would be estimated for a 1 Myr performance period. One thousand years is too short a time period for a volcano to develop and evolve a magma chamber capable of sustaining large volume eruptions. On the other hand, 1 Myr is a perfectly reasonable time period for such developments. Additionally, since the probability of large magnitude events through the repository within the first and critical 1000 years of performance is much less than the average rate (given the evolutionary nature of volcanic systems), radiological consequences and risk associated with large volume explosive eruptions might be overestimated using an average approach.

These factors indicate that considerably more detailed analysis is required to estimate the hazard and risk of large-volume explosive volcanic eruptions at a potential HLW repository site. Nevertheless, the analysis of the VOGRIPA database for the Japanese islands does indicate that recurrence rates of large-magnitude eruptions in the Quaternary must be modelled using statistical methods. Otherwise, hazard rates potentially will be underestimated.

Additional work is required to determine which statistical model is most appropriate, especially for integration into a performance assessment.

6 Repository Relevance of the Selected Impact Scenarios

The TOPAZ methodology described in the previous sections uses expert judgment and statistical analysis to evaluate aggregate probabilities of plausible RES and SES for a given site. Each non-zero branch of the RES-SES logic tree (probability > 0) leads to an 'event definition' in the form of Impact Scenarios (IS) that are relevant to the long-term performance of a deep geological repository. As discussed in Section 1, for a given RES-SES branch, there can be multiple possible ISs that might arise. Eventually, expert judgments must also be used to establish probabilities of individual ISs with such sets of credible ISs. The results of the TOPAZ logic-tree approach, with associated RES, SES and IS probabilities, can then be used by NUMO's performance assessment team to inform, guide and focus their safety analyses based on expert geoscientific judgments.

The preliminary development of ISs by TOPAZ is discussed here. Section 6.1 examines the basic time-dependent evolution and performance of a generic HLW repository. As discussed in Section 1.2, within a relatively short timeframe (of the order of 10,000 years) compared to evolving volcano-tectonic events in Japan, the radiological hazard of HLW diminishes to extremely low levels and the engineered barriers of a HLW reach the end of their design functions. These engineered materials return to a 'natural state' that are relatively inert to thermal-hydrological-mechanical-chemical (T-H-M-C) changes in the deep geological environment. Thereafter the greatest safety concerns are possible ISs leading to the direct transport of radioactive material to the ground surface.

The following sections describe basic attributes of three groups of impact scenarios (IS) for (1) rock deformation, (2) volcanism and (3) repository uplift and exhumation (noting that the latter has not yet been evaluated in the TOPAZ demonstration work, although a preliminary logic tree has been developed to do so when required). Within each IS group there are, of course, a wide number of variants with different impacts, which are briefly reviewed. Recommendations for preliminary aggregation of representative variants for each IS group are made for further consideration by NUMO.

6.1 Evolution of a HLW Repository

Figure 6.1 shows the basic engineered barriers for a generic geological repository for HLW (JNC, 2000). Borosilicate glass is the reference waste form for encapsulation and disposal of reprocessed HLW in Japan. The borosilicate glass is fabricated within a stainless steel vessel that is placed into a massive mild-steel overpack (sometimes called "canister") that is designed to provide initial containment. The HLW plus overpack is called a 'waste package', and the waste package will be emplaced into deposition holes or tunnels within a suitable repository host rock. A bentonite-based buffer barrier containing a large fraction of smectite clay (that swells on contact with water) is placed between the surface of the deposition holes and the waste package. This buffer assures diffusion-only release of any radionuclides from the EBS into the host rock, aided by further retardation of transport by radionuclide-sorption on buffer minerals. Taken together, the buffer, waste package and any other seals or plugs placed into the underground openings of a repository are called the engineered barrier system (EBS).

There are numerous variants to EBS concepts under consideration by NUMO, including different orientations, different dimensions of materials, and different compositions of barrier materials. While it will be important to link and revise the TOPAZ methodology to any specific future repository concept (RC) developed by NUMO, at this preliminary stage the basic generic H12 repository concept shown in Figure 6.1 is selected for this exercise.

After emplacement and sealing of a HLW repository, the initial post-closure phase is often referred to as the "Containment Period" in which the EBS, notably the overpack, acts to prevent contact of the HLW by groundwater. Slow, predictable corrosion of the mild steel overpack prevents any radionuclides releases during the time that radiogenic heating by radioactive decay by short-lived radionuclides elevates both the near-field temperature and temperature gradients from ambient values. Within 300-500 years, the initial thermal pulse has largely dissipated, with ambient thermal conditions returning within several 1000's of years depending on site-specific conditions (JNC, 2000, Volume 3). The 'containment' design

function of the overpack is, therefore, on the order of 1000 to 2000 years (see Figure 3), although somewhat longer containment times may occur due to variable environmental conditions or use of conservative overpack thicknesses.

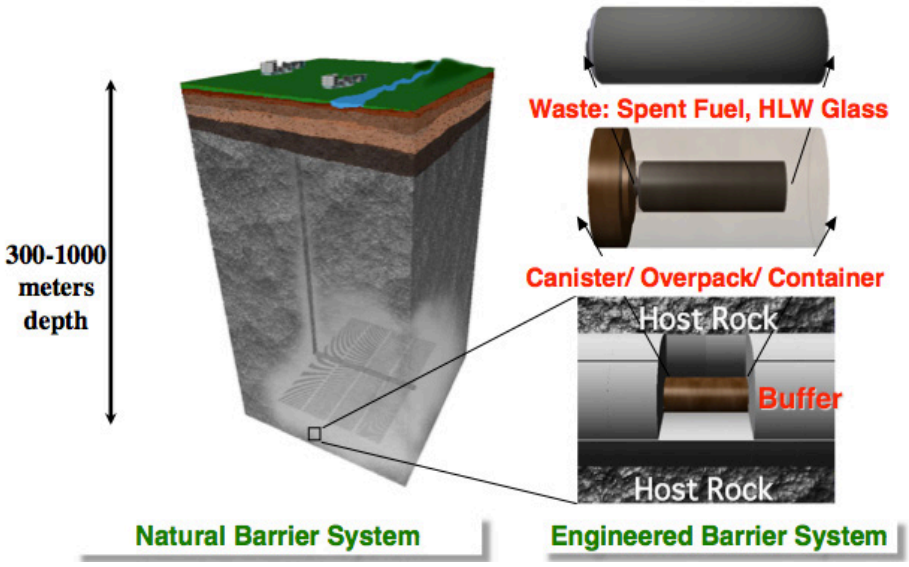

Figure 6.1: Natural and Engineered Barriers for a Generic HLW Repository (from JNC, 2000).

Once the overpack has 'failed', groundwater will contact the HLW borosilicate glass, leading to sustained dissolution and release of radionuclides over a prolonged "Release Period". Under the expected reducing conditions of a deep geological repository, most of the released radionuclides will be incorporated into low-solubility phases that precipitate, thereby limiting the release rate of these radionuclides from the EBS into the host rock. Radionuclides will be transported by groundwater flow to a hypothetical major water-bearing fracture zone that enables advective transport to the surface environment, assumed here to be along a coast as a representative location for a repository (Figure 6.2). A few radionuclides, such as Cs-135, may be extremely soluble under likely repository environmental conditions, so that their release from the EBS will be controlled by the dissolution rate of the borosilicate glass. The time for total dissolution of HLW glass can vary depending on factors, such as the assumed degree of surface cracking, presence and interaction with other engineered barriers and prevailing geochemical conditions, with a range on the order of approximately 10,000 and 70,000 years, and perhaps longer for extremely favorable disposal conditions (e.g., JNC, 2000, H12 report, Table 6.1.2.1-1; US National Academy of Sciences, 2011). The transport time for radionuclides from the repository to the nearest major water-bearing fracture zone is also relatively short because of the assumed relatively short distance (~50-100 metres) to the sub-vertical fracture zone (Figure 6.2).

A key point to understand with respect to assessing impacts from future natural events is that after the combined Containment and Release Period (on order of approximately 50,000-100,000 years after repository closure, see also Figure 6.3), the overpack will likely have been breached by corrosion and mechanical buckling in approximately the first 1000 years (JNC, 2000, Table 6.1.2.1-1), leading to transformation of the initial glass waste form into an assemblage of low solubility alteration phases (JNC, 2000, Table 5.3.1-6; US National Academy of Sciences, 2011).

The original repository has basically converted to a thermodynamically more-stable assemblage of insoluble, slightly radioactive oxides, hydroxides and silicates surrounded by iron hydroxides/ oxides of the corroded overpack, in turn surrounded by a layer of compacted bentonite buffer. At ambient environmental conditions, these residual phases are unreactive over timescales of a million years or more based on numerous geological and natural analogue studies. Soluble radionuclides have been released, retarded, dispersed, diluted in aquifers, and diminished by radioactive decay throughout the rock volume surrounding the

repository, as shown in JNC, 2000 (Chapters 5 and 6, e.g., Figures 5.3.3-2 and 6.1.1-1). Low solubility radionuclides will be isolated and retained in alteration phases of the initial HLW glass (JNC, 2000, Table 5.3.1-6; see also Figure 6.3 of this report). Thus, the engineered barriers of the repository evolve toward a 'natural state', in closer equilibrium to the surrounding host rock environment. The leading concern for any longer term (>50,000 year) combined RES/SES scenario would be if a natural event led to transport of the residual, insoluble radioactive phases to the near-surface oxidizing environment (see Section 6.2.3) or exposure at the ground surface.

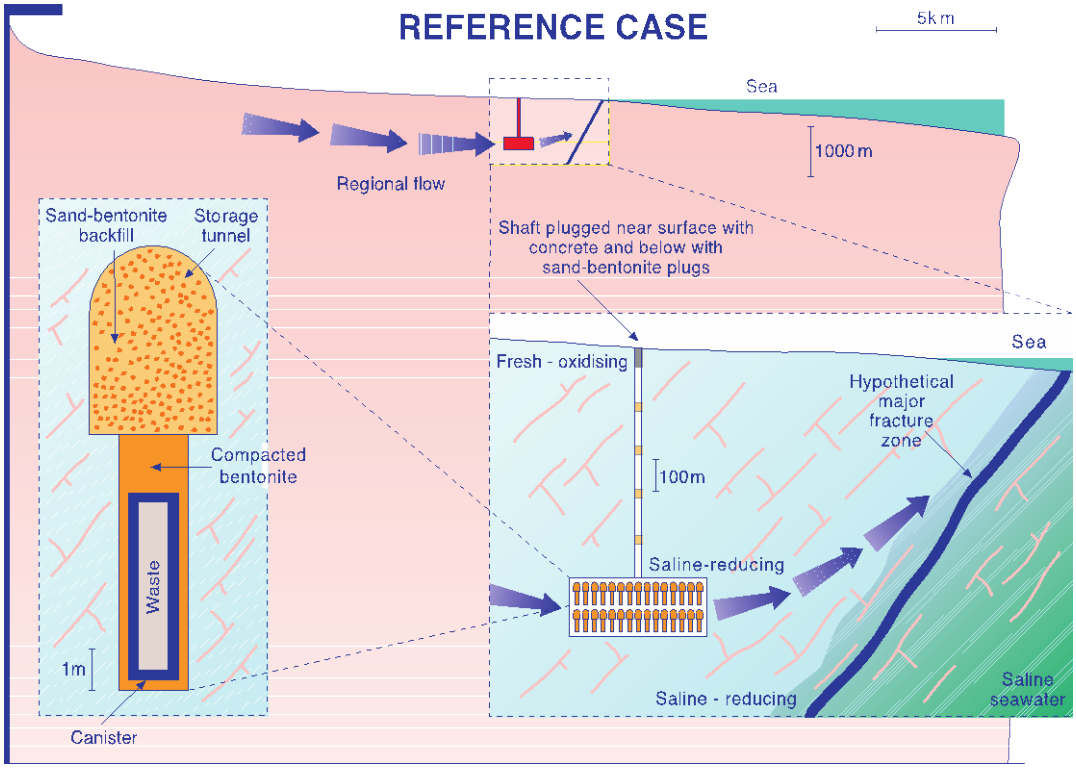

Figure 6.2: Schematic representation of radionuclide release from a deep geological repository for HLW.

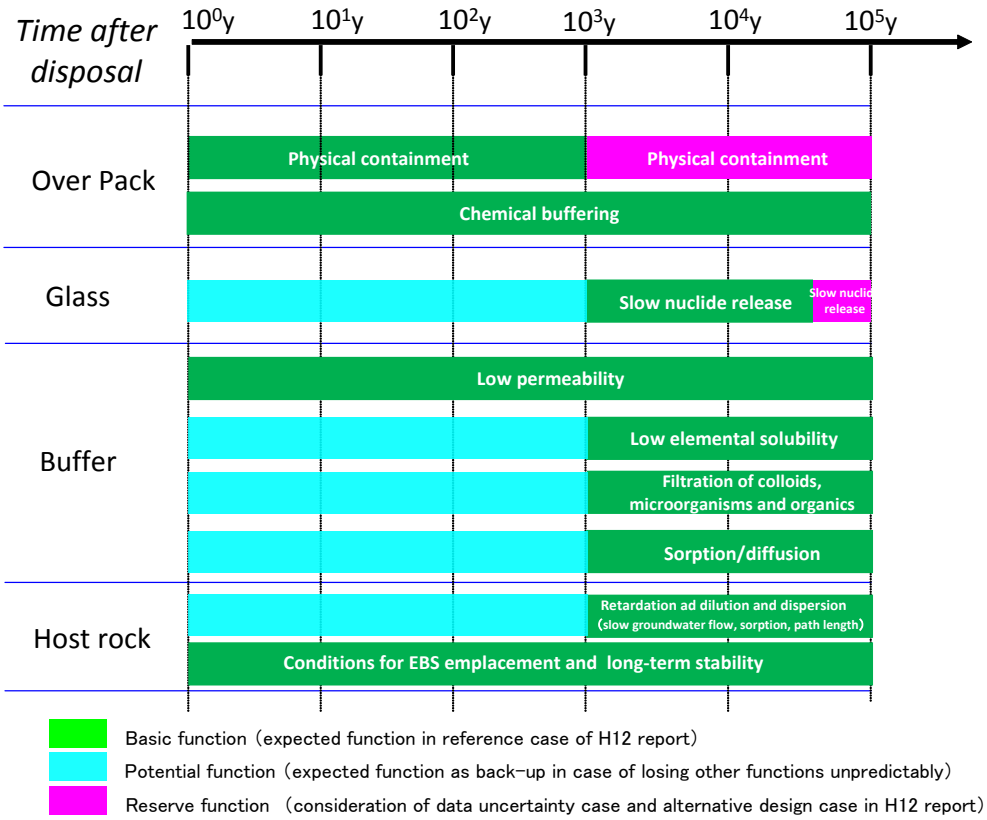

Figure 6.3: Schematic diagram of the assumed safety functions of engineered and natural barriers over time following closure of a generic H12-type repository. Sources for this schematic are JNC (2000) as interpreted by Ebashi et al (2011).

6.2 Illustrative Impact Scenarios

As a preliminary demonstration of the use and utility of the TOPAZ methodology, a representative set of Impact Scenarios that might arise from combined RES/SES scenarios are considered here. These illustrative ISs could serve to provide the necessary link between NUMO's set of geological experts and its performance assessment (PA) team. These representative ISs are based on the following assumptions:

- the generic H12 HLW repository concept (Figure 6.1);
- a generic hard-rock site for the repository;
- a repository depth of 300 metres;
- saline, reducing and near-neutral pH groundwater conditions at the repository depth,
- avoiding placing any waste package across rock discontinuities or fracture zones;
- consideration of the types of volcanic and rock-deformation events that might significantly compromise the expected isolation performance of the engineered and natural barriers of the repository.

The following sub-sections explain the basic variants of volcanism, rock-deformation and uplift and erosion ISs that might arise from future changes in the tectonic setting of Japan.

One illustrative variant for each IS is described and proposed to be used when eventually conducting a full expert elicitation on TOPAZ's RES-SES-IS methodology: that is, extending the expert elicitation exercise presented in this report to include the ISs as well as the RES and SES. It is noted that the October 2011 TOPAZ workshop did not include consideration of ISs and did not explore how to assign expert-judgment probabilities or likelihoods to ISs.

6.2.1 Rock Deformation Impact Scenario

TOPAZ has previously used strain rate as a proxy metric for considering how long-term, sustained tectonic forces might lead to some form of rock deformation at a candidate repository site. Figure 6.4 schematically illustrates a range of possible mechanisms by which sustained strain rate in a repository host rock might manifest rock deformation impacts. At this stage for an unexplored, generic hard-rock site, there is no possibility to sensibly judge the likelihood of one mechanism over another.

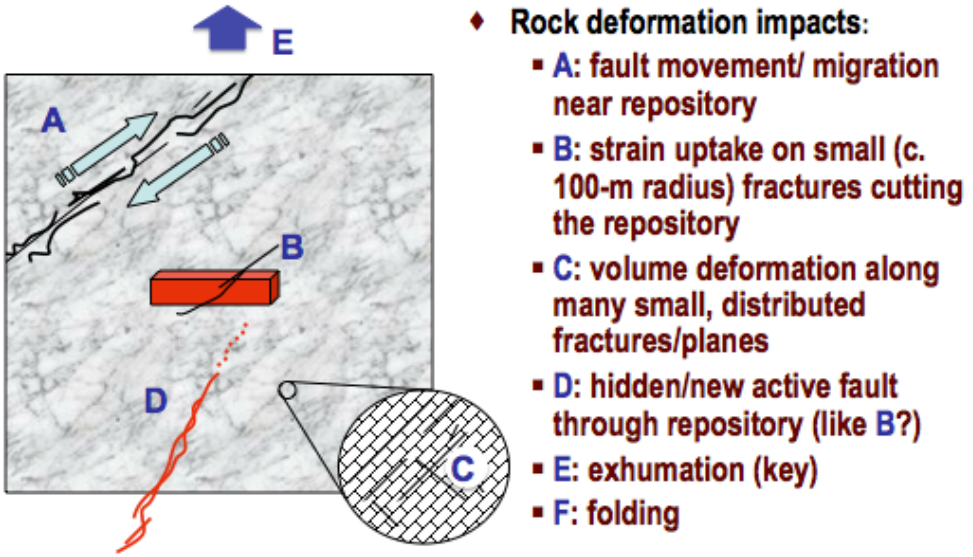

Figure 6.4: Schematic representation of different types of rock deformation that may arise from sustained elevated strain rate.

A leading rock-deformation IS considered for hard rock sites, being considered in Sweden and Finland for example, is a future earthquake causing the “Fault Shear” of one or more waste packages (see Figure 6.5). The physical displacement of the surrounding rock may cause failure of the containment function of the overpack, or failure of the diffusion and sorptive functions of the clay-based buffer. The threshold for fault displacement leading to significant impairment of the functions of engineered barriers is on the order of 5-10 cm, depending on the overall thickness of the buffer and material properties of the overpack/ canister. Of course, the orientation and displacement of the fault, the number of sympathetic rock displacements that may occur surrounding the main fault, and the timing of the faulting event are all important aspects to consider in evaluating the actual impact on repository safety.

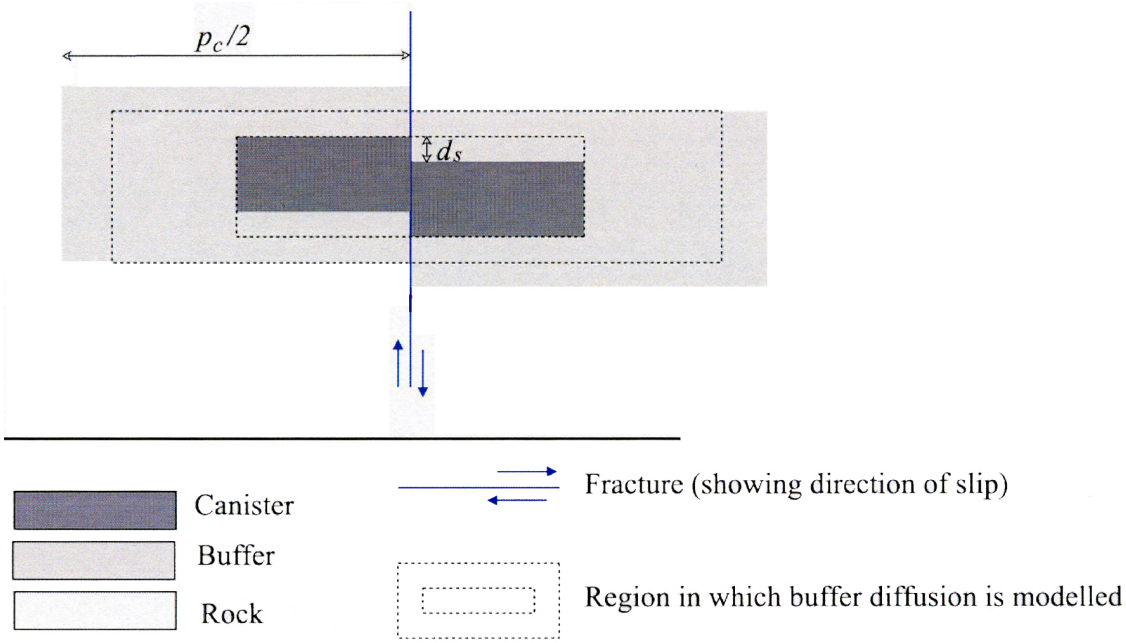

Figure 6.5: Illustrative cross section of the rock-deformation variant case of fault shear of a waste package. "p_c" is the length of the waste package, "d_s" is the length of the fault displacement assumed to occur normal to the axis of the waste package.

As noted in the previous section, however, the containment function for the overpack is a few 1000's years, and the diffusion-sorptive function of the buffer becomes unimportant to limiting peak release rates from the repository system after the HLW has fully dissolved, a period on the order of approximately 10,000 to 50,000 years (Apted and Ahn 2010, also see 'Glass' in Figure 6.3, which shows glass dissolution complete at approximately 50,000 years). This is because the remaining key dose-contributing radionuclides still present within the EBS (e.g., Se-79, Cs-135, Np-237, see JNC, 2000, Figure 6.1.3.2-1, for example) are so long-lived that their sorption-retarded diffusive-transport time across the buffer would be less than one half-life. Hence, no significant decay would occur during diffusive transport, even if the buffer remained intact (Apted and Ahn. 2010). Therefore, the rock shear IS for the buffer is of significant concern only for earthquake events occurring in the about 50,000 years (Apted and Ahn 2010) within the rock block containing the repository.

6.2.2 Volcanism Impact Scenario

The major factors to consider in possible volcanism ISs (Figure 6.6) are:

- the type and magnitude of the volcanic event (e.g., monogenetic, polygenetic, or caldera eruption);
- the location of the event with respect to the repository: whether the volcanic event directly or indirectly intersects the repository itself.

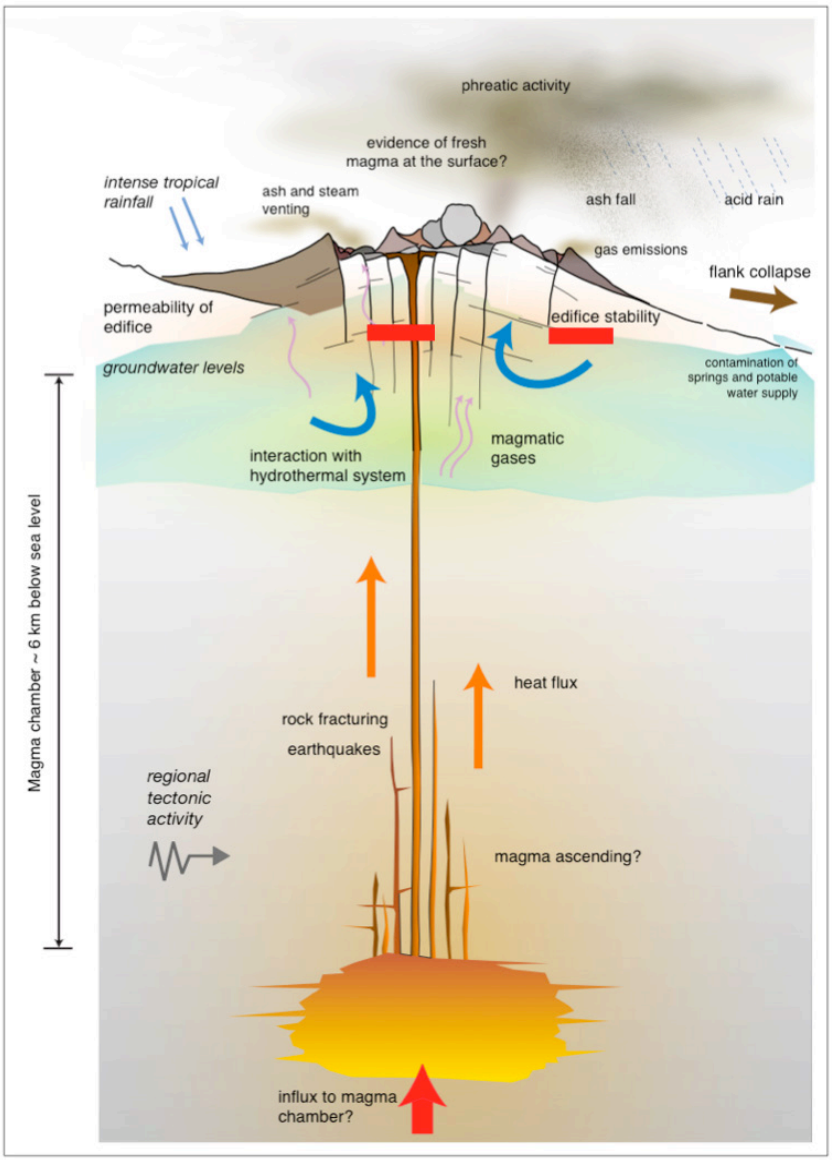

Figure 6.6: Schematic of a volcano either directly or indirectly intruding through a HLW repository (shown as red rectangles) (image from Steve Sparks and Thea Hinks).

The type of volcanic event defines important characteristics such as duration of the volcanism, the lateral extent of the conduits of the volcanic system at repository depth, type and volume of erupted material, magmatic temperature and volatile contents, and the evolution in these characteristics over time.

TOPAZ has not yet made a systematic analysis of either direct or indirect impacts of a volcanic event on repository performance, although recognizing the clear need to do so eventually to aid and guide NUMO's PA efforts.

As a prelude to conducting formal IS analyses, TOPAZ has considered, the following categories or groupings for volcanic ISs:

- direct intrusion of a repository by a polygenetic or caldera event,
- direct intrusion of a repository by a monogenetic event or single dike, or
- nearby intrusion of a repository by a volcanic event, with indirect perturbation of conditions of the repository.

Of course, there can be a wide number of possible variant cases within each IS category. At this time, with no specific site under consideration and no defined set of RES-SES constraints, it would premature to attempt to document the wide range of possible types and

characteristics of variants to volcanic ISs. Aspects and difficulties regarding future, detailed analyses of the three IS categories are outlined below.

The IS category of a large-scale volcanic directly intruding a repository has the potential to transport a significant fraction of the radioactive and non-radioactive materials of the repository to the surface, with significant impacts on repository performance and safety. There are several challenges to devising ISs for large-scale eruptions, however. First, it will be necessary to consider how (and how much of) the radioactive portion of this transported material would be intimately mixed and diluted with both the non-radioactive portion of the repository and the pristine volcanic material erupted. Further aspects of this process are discussed in the following paragraph. Second, radiological exposure analysis of any erupted radioactive material would be complicated by consideration of partitioning of the radioactive-contaminated material among erupted lava, volcanic bombs, and tephra. Third, while geotechnical models for evaluating air-borne dispersal of tephra exist, it is not evident if and how such evaluations would be compared to Japanese radiological safety regulations for a HLW repository, which are based on an assumed groundwater pathway (see Figure 6.2). Fourth, the non-radiological safety impacts from such large-scale volcanic events could conceivable dwarf radiological impacts, especially when the large volume-dilution of radioactive waste by volcanic ejecta is considered. Therefore, this category of volcanic ISs will eventually require considerable assessment to credibly demonstrate the application and linkage of the TOPAZ methodology to NUMO's PA efforts.

The IS category of a monogenetic or single dike directly intersecting a repository presents similar challenges to building competence in defining volcanic ISs. First, it will be necessary to evaluate how ascending magma could directly interact with repository materials, and whether these repository materials (including radionuclide-bearing phases) would be in their initial state or degraded to an evolved 'natural state'. Magmas generally are close to their solidus temperature, meaning the heat necessary for incorporation of repository materials by melting would require a corresponding degree of crystallization of the magma itself. Hydrodynamic incorporation of repository materials in ascending magma as solid "xenoliths" would be an additional mechanism for bringing any radiological material to the surface. The generic HLW repository, whether in an initial or evolved state, is expected to be fully sealed and backfilled, so no lateral re-direction of ascending magma along open-pathways would be expected. Second, and different than consideration of a large-scale eruptive event, it will be necessary to evaluate for a monogenetic event how portions of the repository adjacent to the vertical magmatic conduits might undergo indirect impacts on T-H-M-C conditions. The spatial extent and duration of such indirect T-H-M-C changes will be much shorter for a monogenetic event or single dike intrusion, and there are available models and field evidence to support bounding estimates of such impacts. Third, the possible transport of radionuclide-bearing material to the surface of a monogenetic event also presents the same difficulties as a large-scale vent to NUMO's PA team of how to consider and model such a consequence with respect to Japanese radiological safety standards. Therefore, this category of volcanic ISs also will require further resources to demonstrate the application and linkage of the TOPAZ methodology to NUMO's PA efforts.

The third basic IS category involves intrusion of a volcano nearby the repository, perhaps within a distance of 15 km, the current NUMO exclusion value for siting a repository away from present-day volcanic centres (see discussion in Section 1.3). Analysis of such a volcanic IS is far more tractable (although not necessarily more likely) than the first two, direct-intrusion IS categories. First, such an event would have only indirect T-H-M-C impacts on a repository, with no transport of radiological material to the surface. While there are challenges to this analysis as well, the modelling of indirect T-H-M-C impacts can be accomplished with existing multi-phase T-H and T-H-C models, as well as T-M models. Second, this category of indirect volcanic ISs results only in impacts on the release performance of a repository via groundwater pathways. This is an analysis for which the NUMO PA team has existing models, and even supporting data because of similar thermal-impact modelling needed to evaluate initial radiogenic heating of a HLW repository. Of course, the consequences of a nearby intrusion of a volcano will be significantly less severe than consequences on repository performance compared to either of the direct intrusion category ISs.

As a way forward, it is recognised that a step-wise approach to building up competence on volcanic ISs can be based on the fact that the three IS categories are, in effect, nested sub-sets. That is to say, analyses of T-H-M-C impacts for the indirect volcanic ISs are the most basic (and currently tractable) analyses. Such indirect impacts are a sub-set of the analyses necessary to evaluate the monogenetic/ single-dike ISs, which eventually requires consideration of how a relatively limited portion of radioactive and non-radioactive repository materials might interact with ascending magma. And in turn, analyses of the issues for the monogenetic/ single-dike ISs are a sub-set of range of analyses needed for the large-scale volcanic ISs, in which there would be long-term and spatially extensive disruption to the repository system

6.2.3 Uplift, Erosion and Exhumation Impact Scenarios

While the radiological hazard of HLW does significantly decrease over time, the expected reducing conditions of a repository at depth leads to localised retention of most radionuclides within the EBS, either by precipitation or strong sorption. This spatial retention of insoluble radionuclides within a deep repository is a favourable safety feature. This same feature, however, represents a vulnerability, if sustained uplift and erosion were to bring this concentrated mass toward the near-surface environment (Figure 6.7).

If a repository, even in a degraded 'natural state', nears the surface, enhanced radionuclide release to the accessible environment can occur. This occurs because (1) many radioelements become more soluble and less sorptive under oxidizing conditions, and (2) the transport pathways for radionuclides to reach the surface environment become shorter (Figure 6.8). If taken uplift and erosion is taken to an endpoint, a repository may be exhumed at the ground surface, leading to significant radiological exposure through multiple water and air-borne pathways as well as direct exposure to future humans.

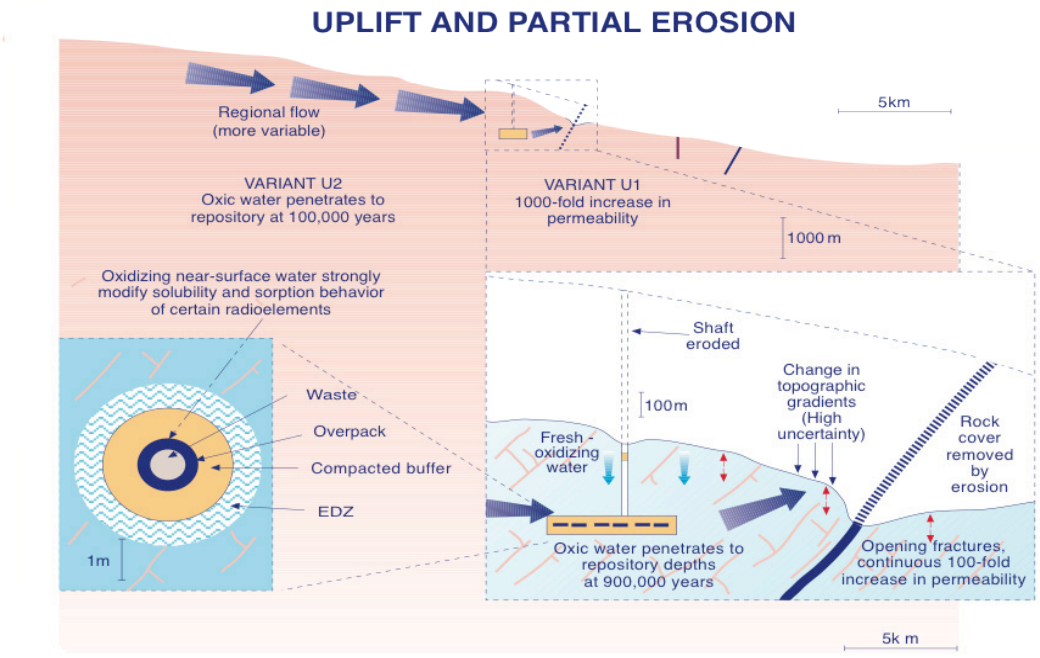

Figure 6.7: Schematic illustration of uplift and erosion impact scenario.

There are numerous possible variant cases for the uplift and erosion IS, some of which are illustrated in Figure 6.7. One variant is the erosion of the overburden above a repository, leading to depressurization and an increase in bulk permeability of the rock. An increase in permeability, as well as influences of surface topography on hydraulic head and formation of new or extended fractures in the rock surrounding a repository (Figure 6.8), could lead to

faster groundwater flow and shorter transport pathways, hence faster radionuclide transport to the surface. Another variant is based in a boundary layer of oxic surface water penetrating down into a repository that is being uplifted (Figure 6.8). In this variant, the intruding boundary layer of oxic conditions would first lead to enhanced mobilization of previously released redox-sensitive radionuclides sorbed on mineral surface of the rock. Eventually, as the oxic boundary layer intruded into the EBS portion of the repository, the solubility of many redox-sensitive radioelements would greatly increase, further enhancing radionuclide mobilization. This 'shrinking core' variant case, based on gradual intrusion of oxygenated water into a disposal site. A third variant, with the most extreme radiological consequences, would be the endpoint of uplift and erosion in which the repository is exhumed at the surface.

There are existing, verified models that could be used to address the impacts on radionuclide release via groundwater for both the 'increased permeability' and 'shrinking core' IS variants. It will be important to carefully describe the evolution in hydrological, mechanical and chemical conditions over discrete time and spatial intervals, to avoid overly conservative estimates of impacts on radionuclide release (as, for example, in JNC, 2000). At the same time, caution will need to be used to avoid overly optimistic assumptions regarding the approach-rate, orientation and characteristics of a repository as it reaches the near-surface environment in the far future. As for the 'exhumation' variant IS, NUMO's PA team would need to consider in what way to model and evaluate radiological consequences for not only groundwater pathways, but also air-borne pathways and direct external exposure.

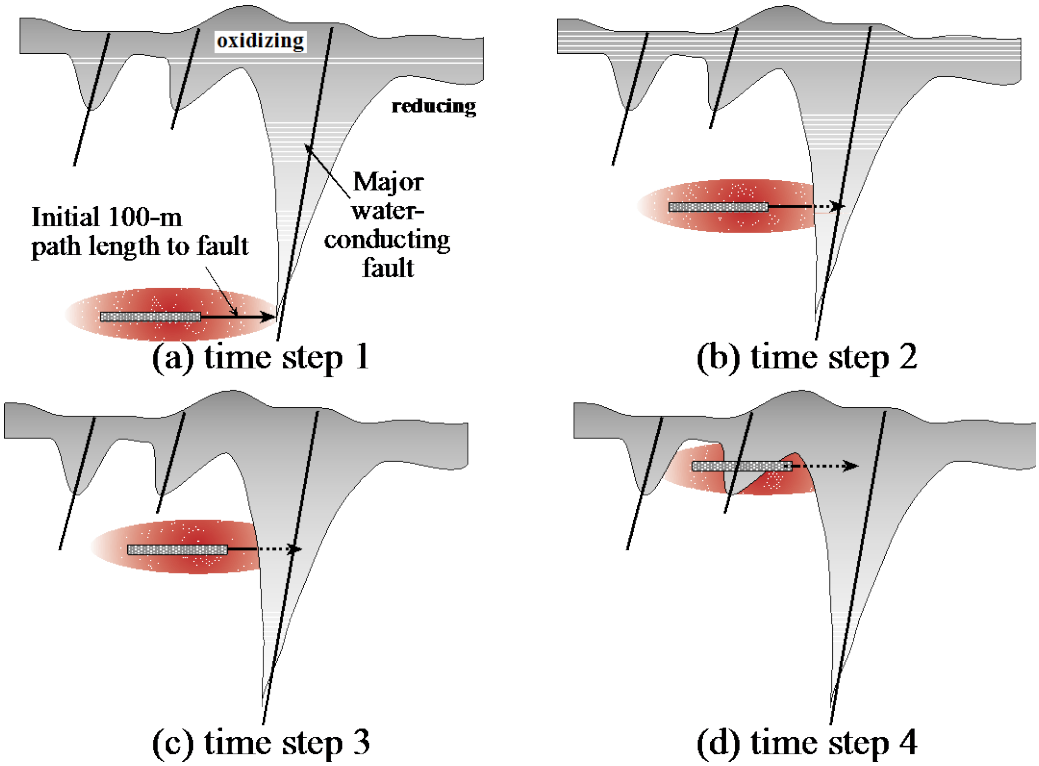

Figure 6.8: Schematic illustration of sequential impacts from uplift and erosion. Path lengths for radionuclide transport to major water-conducting faults decrease, while ascent of repository and developed release plume (shaded red) into oxidizing zone leads to increase in radioelement solubilities and decrease in radioelement sorption.

6.3 Aggregation of Impact Scenarios

A potential issue in applying the TOPAZ methodology is that geoscience experts may identify a large number of possible variants for each of volcanism, rock-deformation and uplift-erosion impacts scenarios (ISs). The conceptual basis of the TOPAZ methodology can accommodate any number of ISs, however, the computational burden can become acute for expert elicitations. This is because a large set of ISs would need to be defined, discussed

with respect to site-specific and region-specific data, applied, and probabilities evaluated for each of the previous RES-SES branches for a given site. In order to allow a more accessible demonstration and testing of the full TOPAZ methodology, therefore, an effort was made in the current project to consider the aggregation of volcanism, rock-deformation and uplift-erosion ISs in a limited set that could be broadly applied to any hypothetical candidate repository site (Table 6.1). It is recognised, of course, that when real candidate repository site were to be evaluated in the future, a much fuller range of ISs would need to be needed in order to confidently assure that all credible variants had been considered.

Table 6.1 shows one possible formulation of volcanism, rock-deformation and uplift ISs. Three combined rock-deformation and uplift-erosion ISs are listed down the side of Table 6.1.

- no new faulting within the repository block and no significant uplift;
- formation or re-activation of faults intersecting part of the repository but no significant uplift;
- re-activation of faults intersecting part of the repository and significant uplift.

Volcanism ISs are listed across the top of Table 6.1:

- no volcanic event occurring within 15-km of the repository;
- volcanic event occurring 15-km of repository, but no direct intrusion of the repository;
- volcanic event directly intruding the repository.

It is proposed that these nine ISs would capture all credible impacts that might arise from future tectonic and volcanic events at a site, while implicitly aggregating the large number of possible variant cases within each of the ISs. Another advantage is that these nine ISs can be used to highlight for NUMO's PA team what issues and capabilities they may need to be considering for safety assessment of natural event scenarios. While careful and prudent site selection and characterization may reduce or eliminate the possibility of one or more IS (for example, future volcanism may have a vanishingly small probability at certain locations in Japan), it is unlikely that past safety assessment models applied to the static Reference Case will be fully capable of safety assessment for other ISs shown in Table 6.1.

6.4 Summary

The TOPAZ effort on Impacts Scenario (IS) analysis to date has focused on identification of categories for volcanism, rock-deformation and uplift-erosion ISs, as well as specific variants within each IS. The October 2011 TOPAZ workshop did not have the opportunity to elicit specific views from Japanese geoscience experts as to possible impacts. A key result of the workshop, however, was recognition that the large number of potential variant cases for each IS category could quickly overwhelm the ability to initially demonstrate and test the TOPAZ methodology.

The TOPAZ methodology can conceptually accommodate any number of ISs. The difficulty is the computational burden arising from multiplying the large number of possible ISs by a large number of RES-SES branches for a given site. In order to allow a more straightforward future demonstration of the TOPAZ methodology, therefore, an initial suggestion is made to aggregate volcanism, rock-deformation and uplift-erosion ISs. A preliminary set of nine ISs is proposed that can be broadly applied to any hypothetical candidate repository site and associated RES-SES assessments. In the future, when real candidate repository site are to be evaluated, a much fuller range of ISs variants could be considered within the same TOPAZ methodology in order to assure decision makers and other stakeholders that all credible ISs have been considered.

Table 6.1: Possible aggregation of impacts scenarios, with associated issues regarding performance assessment analyses.

	No future volcanic event	Volcanic event; no intrusion into repository	Volcanic event; intrusion into repository
No new faulting **No uplift to near-surface**	**IS-1** • Reference Case • current PA models applicable	**IS-2** • groundwater pathway only • current T-H-M-C codes probably suitable • need for careful IS description	**IS-3** • IS-2 analysis • need to consider radiological exposure pathways at surface • need to evaluate magma impacts
Fault reactivation intersecting repository **No uplift to near-surface**	**IS-4** • need to evaluate number of waste packages damaged • need model for loss of buffer safety functions	**IS-5** • combined IS-2 and IS-4 analyses	**IS-6** • combined IS-3 and IS-4 analyses
Fault reactivation intersecting repository **Uplift to near-surface**	**IS-7** • IS-4 analysis • groundwater pathway analysis for 'shrinking core' from oxic water • groundwater pathway analysis for reduced path length/ higher flow • radiological assessment of exhumed repository?	**IS-8** • combined IS-2 and IS-7 analyses	**IS-9** • combined IS-3 and IS-7 analyses

7 Conclusions

The TOPAZ project is a continuation and development of the ITM project that extends the probabilistic methodology of ITM to provide information on the likelihood and nature of tectonic impacts for timescales up to 1 Myr in the future. As with the ITM project, TOPAZ has developed, but only partially tested, the methodologies that will be needed as potential repository sites emerge and require evaluation. Refinements and some further development will undoubtedly be needed as the methodology is applied.

The TOPAZ project team considers that probabilistic approaches are fundamental to any evaluation of tectonic hazards to long-term repository safety in Japan. The Fukushima disaster has highlighted graphically how, even on a much shorter-term basis, the use of multiple geoscientific data sets and probabilistic techniques is necessary to characterise hazards to facilities for quantitative risk assessments. Although the regulatory approach to geological disposal is still under consideration in Japan, the TOPAZ project team considers that it will be vital to be able to present estimates of event likelihood when discussing hazards and potential health impacts of a repository. These may be in the form of actual risk estimates (as used in the regulatory guidelines and requirements for geological disposal in several countries), or in the form of disaggregated estimates of radiation doses and their likelihoods. Whichever direction regulatory development takes, it will be necessary to present hazard potential and uncertainty estimates clearly to various audiences in a probabilistic as well as a deterministic sense. The ITM-TOPAZ methodology will be an effective tool for doing this. In particular, the approach presented in this report addresses the key issue of uncertainty over long future time periods.

Increasing uncertainty with time in the tectonic evolution of any region in Japan is captured in the ITM-TOPAZ approach by applying elicitation techniques to incorporate the range of expert opinion on alternative tectonic evolutionary models. This range of uncertainty is weighted and converted to quantitative estimates of likelihood (probabilities) of different evolutionary paths. As different paths will have different outcomes in terms of tectonic events that may impact a geological repository, and the time at which they might occur, these quantitative forecasts can be transferred to probabilities of occurrence of certain safety relevant impacts. This provides safety assessors with quantitative information both to compare alternative sites with respect to relative tectonic hazard and to provide regulatory authorities with either risk-based hazard forecast or deterministic estimates of health impacts accompanied by relative likelihoods of occurrence of specified exposure scenarios.

In the TOPAZ project reported here, only a sample of all the requisite steps in the application of expert elicitation has been tested. Using the results of the previous ITM Tohoku Cases Study and focussing on one of the example locations from that study, the TOPAZ project has demonstrated the application of expert elicitation, principally to the RES stage, and then provided a condensed demonstration of how it could be used at the SES and IS stage, by simplifying the 'SES set' considerably and by modelling only two example ISs. Nevertheless these two ISs will be critical components when developing a safety case. The TOPAZ project has not yet illustrated the full range of information that can be derived from the elicited credible intervals on each probability, as we have only used the median values in the demonstration.

When the methodology is applied to a 'real' prospective siting location, then elicitation will have to be applied to scenario definition in more detail at both the SES and IS level. The TOPAZ project has shown how this can be done and prepared the ground for a real site evaluation.

An important outcome of TOPAZ is that it shows how the wide range of geosciences data and expert opinion that exists in Japan can be incorporated into a safety analysis. NUMO considers it important to be able to explain a logical approach to the complex problem and uncertainties of tectonic impact forecasting and to take account of differing views in the geosciences community. TOPAZ not only provides a method for involving and informing the community, but also for sampling these opinions and actively including them in its assessment and site suitability work.

References

Apted, M. J., and Ahn, J, (2010), Multiple-barrier Geological Repository Design and Operational Strategies for Safe Disposal of Radioactive Materials in *Geological Repository Systems for Safe Disposal of Spent Nuclear Fuels and Radioactive Waste*, J. Ahn and M. Apted (eds.). Woodhead Energy Series No. 9, London, U.K., 3-28

Aspinall, W. P., G. Woo, B. Voight, and P. J. Baxter, (2003), Evidence-based volcanology: Application to eruption crises. Journal of Volcanology and Geothermal Research 128: 273-285.

Chapman, N. A. and Hooper, A, (2012), The Disposal of Radioactive Wastes Underground. *Proceedings of the Geologists' Association,* 123, 46–63.

Chapman, N., M. Apted, J. Beavan, K. Berryman, M. Cloos, C. Connor, L. Connor, O. Jaquet, N. Litchfield, S. Mahony, W. Smith, S. Sparks, M. Stirling, P. Villamor and L. Wallace, (2008), Development of Methodologies for the Identification of Volcanic and Tectonic Hazards to Potential HLW Repository Sites in Japan: The Tohoku Case Study. Nuclear Waste Management Organisation of Japan, Tokyo. Technical Report: NUMO-TR-08-03. 135 pps.

Chapman, N., M. Apted, J. Beavan, K. Berryman, M. Cloos, C. Connor, L. Connor, T. Hasenaka, O. Jaquet, K. Kiyosugi, N. Litchfield, S. Mahony, M. Miyoshi, W. Smith, S. Sparks, M. Stirling, P. Villamor, L. Wallace, J. Goto, T. Miwa, H. Tsuchi and K. Kitayama, (2009), Development of Methodologies for the Identification of Volcanic and Tectonic Hazards to Potential HLW Repository Sites in Japan: The Kyushu Case Study. Nuclear Waste Management Organisation of Japan, Tokyo. Technical Report: NUMO-TR-09-02. 186 pps.

Connor, C.B., R.S.J. Sparks, M. Diez, A.C.M. Volentik, and S.C.P. Pearson, (2009), The nature of volcanism. In: Volcanic and Tectonic Hazard Assessment for Nuclear Facilities. Edited by C.B. Connor, N.A. Chapman, and L.J., Connor. Cambridge University Press, 74-115.

Connor, C.B., McBirney, A.R., and Furlan, C., (2006), What is the probability of explosive eruption at a long-dormant volcano? In: Mader, H.M., Coles, S.G., Connor, C.B., and Connor, L.J. (eds.) Statistics in Volcanology. Special Publications of IAVCEI 1. Geological Society, London, 39-48.

Cooke, R. M, (1991), Experts in Uncertainty - opinion and subjective probability in science. New York, Oxford University Press; 321.

Cooke, R. M. and L. L. H. J. Goossens, (2008), TU Delft expert judgment data base. Reliability Engineering & System Safety - Expert Judgement. Vol. 93: 657-674.

Coppersmith, K. J., K. E. Jenni, R. C. Perman and R. R. Youngs, (2009), Formal expert assessment in probabilistic seismic and volcanic hazard assessment, In: Volcanic and Tectonic Hazard Assessment for Nuclear Facilities. C.B. Connor, N.A. Chapman, and L.J., Connor (eds.), Cambridge University Press, Cambridge.

Cox, A., and Engebretson, D., (1985), Change in motion of Pacific plate at 5 Myr BP: Nature, v. 313, p. 472-474.

Davidson, J., and De Silva, S., (2000), Composite volcanoes: in Sigurdsson, H., ed., Encyclopedia of Volcanoes: Academic Press, San Diego, p. 663-681.

Druitt, T. H., L. Edwards, R. M. Mellors, et al. (editors), (2002), Santorini Volcano, Geological Society of London, Memoirs, 19.

Ebashi, T., Kaku, K., and Ishiguro, K, (2011), NUMO's Approach for Long-Term Safety Assessment, Proceedings of the ASME 2011 14th International Conference on Environmental Remediation and Radioactive Waste Management, ICEM 2011-59.

Engebretson, D. C., Cox, A., and Gordon, R. G., (1985), Relative motions between oceanic and continental plates in the Pacific basin: Geological Society of America Special Paper 206, 55 pp.

Finn, C., (1994), Aeromagnetic evidence for a buried early Cretaceous magmatic arc, northeast Japan: Journal of Geophysical Research, v. 99, p. 22,165-22,185.

Finn, C., Kimura, G., Suyehiro, K, (1994), Introduction to the special section Northeast Japan: A case history of subduction: Journal of Geophysical Research, 99, 22,137-22,145.

Hasegawa, A., A. Yamamoto, N. Umino, S. Miura, S. Horiuchi, D. Zhao, and H. Sato, (2000), Seismic activity and the deformation process of the overriding plate in the northeastern Japan subduction zone, Tectonophysics, 319, 225-239

Hasegawa, A., S. Horiuchi, N. Umino, (1994), Seismic structure of the northeast Japan convergent margin: A synthesis, J. Geophys. Res., 99(B11), 22295-22311.

Heki, K, (2004), Space geodetic observation of deep basal subduction erosion in northeastern Japan, Earth Planet. Sci. Lett., 219, 13-20.

Heki, K., Miyazaki, S., Takahashi, H., Kasahara, M., Kimata, F., Miura, S., Vasilenko, N., F., Ivashchenko, and Ki-Dok, A., (1999), The Amurian plate motion and current plate kinematics in eastern Asia: Journal of Geophysical Research, v. 104, p. 29,147-29,155.

Honda, S., (1985), Thermal structure beneath Tohoku, northeast Japan -- A case study for understanding the detailed thermal structure of the subduction zone: Tectonophysics, v. 112, p. 69-102.

Jolivet, L, K., Tamaki, K., Fournier, M., (1994), Japan Sea, opening history and mechanism: A synthesis: Journal of Geophysical Research, v. 99, p. 22,237-22,259.

JNC, (2000), *H12: Project to Establish the Scientific and Technical Basis for HLW Disposal in Japan: Volume 2 Repository Design and Engineering Technology; Volume 3 Safety Assessment of the Geological Disposal System*. Japan Nuclear Cycle Development Institute (JNC), Tokai-mura, Japan.

Kondo, H., Tanaka, K., Mizuochi, Y., and Ninomiya, A., (2004), Long-term changes in distribution and chemistry of middle Miocene to Quaternary volcanism in the Chokai-Kurikoma area across the Northeast Japan Arc: Island Arc, v. 13, p. 18-46.

Kostrov, B.V, (1974)., Seismic moment and energy of earthquakes and seismic flow of rock. Izv. Acad. Sci. USSR Physics. Solid Earth 1, 23040.

McCaffrey, R, (1992), Oblique plate convergence, slip vectors, and forearc deformation, *Journal of Geophysical Research, 97(B6),* 8905-8915.

McCaffrey, R., P.C. Zwick, Y. Bock, L. Prawirodirdjo, J.F. Genrich, C.W. Stevens, S.S.O. Puntodewo, and C. Subaraya, (2000b), Strain partitioning during oblique plate convergence in northern Sumatra: Geodetic and seismologic constraints and numerical modeling, *Journal of Geophysical Research, 105(B12),* 28,363-28,376.

Machida and Arai, (1993), The Atlas of Tephra in and Around Japan, Tokyo University Press, Tokyo

Mahony, S.H., R.S.J. Sparks, L.J. Connor, and C.B. Connor, (2009), Exploring long-term hazards using a Quaternary volcano database. In: Volcanic and Tectonic Hazard Assessment for Nuclear Facilities. Edited by C.B. Connor, N.A. Chapman, and L.J., Connor. Cambridge University Press, 326-345.

Marzocchi, W., L. Sandri, P. Gasparini, C Newhall and E. Boschi, (2004), Quantifying probabilities of volcanic events: an example from volcanic hazard at Mt. Vesuvius, Journal of Geophysical Research 109: B11201, doi: 10.1029/2004JB003155.

Marzocchi, W., L. Sandri, and C. Furlan, (2006), A quantitative model for volcanic hazard assessment. In: Mader, H. M., S. Coles, C. Connor, and L. Connor (editors). Statistics in Volcanology, Special Publications of IAVCEI 1: 31-37, Geological Society, London.

Mason, B. G.; Pyle, D. M.; Oppenheimer, C., (2004), The size and frequency of the largest explosive eruptions on Earth. Bulletin of Volcanology 66 (8): 735–748.

Minoura, K., Imamura, F., Sugawara, D., Kono, Y., and Iwashita, T., (2001), The 869 Jogan tsunami deposit and recurrence interval of large-scale tsunami on the Pacific coast of northeast Japan: Journal of Natural Disaster Science, v. 23, p. 83-88.

Miura, S., Sato, T., Tachibana, K., Satake, Y., and Hasegawa, A., (2002), Earth, Planets, Space, v. 54, p. 1071-1076.

Miura, S., T. Sato, A. Hasegawa, Y. Suwa, K. Tachibana and S. Yui, (2004), Strain concentration zone along the volcanic front derived by GPS observations in the NE Japan arc, Earth Planets Space, **56**, 1347-1355.

Nakajima, T., Danhara, T., Iwano, H., and Chinzei, K., (1996), Uplift of the Ou Backbone Range in northeast Japan at around 10 Myr and its implication for the tectonic evolution of the eastern margin of Asia: Palaeogeography, Palaeoclimatology, Palaeoecology, v. 241, p. 28-48.

Newhall, C. G.; Self, S., (1982), The volcanic explosivity index (VEI): An estimate of explosive magnitude for historical volcanism". Journal of Geophysical Research 87 (C2): 1231–1238. doi:10.1029/JC087iC02p01231.

Newhall, C. G., and R. P. Hoblitt, (2002), Constructing event trees for volcanic crises. Bulletin of Volcanology, 64: 3-20.

NUMO, (2004), Evaluating Site Suitability for a HLW Repository. Technical Report of the Nuclear Waste Management Organisation of Japan, NUMO-TR-04-04, 74 pps.

Okamura, Y., Watanabe, M., Morijiri, R., Satoh, M., (1995), Rifting and basin inversion in the eastern margin of the Japan Sea: Island Arc, v. 4, p. 166-181.

Okamura, Y., Ishiyama, T., and Yanagisawa, Y., (2007), Fault-related folds above the source fault of the 2004 mid-Niigata Prefecture earthquake, in a fold-and-thrust belt caused by basin inversion along the eastern margin of the Japan Sea: Journal of Geophysical Research, v. 112, B03S08, 14 pp.

Okubo, Y., and Matsunaga, T., (1994), Curie-point depth in northeast Japan and its correlation with regional thermal structure and seismicity: Journal of Geophysical Research, v. 99, p. 22,363-22,371.

Otsuki K, (1992), Oblique subduction, collision of microcontinents and subduction of oceanic ridges: their implications on the Cretaceous tectonics of Japan, Island Arc 1, 51-63.

Pollitz, F. F., (1986), Pliocene change in Pacific-plate motion: Nature, v. 320, p. 738-741.

Sagiya, T., Miyazaki, S., Tada, T., (2000), Continuous GPS array and present-day crustal deformation of Japan: Pure and Applied Geophysics, v. 157, p. 2303-2322.

Sato, H., (1994), The relationship between Late Cenozoic tectonic events and stress field and basin development in northeast Japan: Journal of Geophysical Research, v. 99, p. 22,261-22,274.

Sato, H., and Amano, K., (1991), Relationship between tectonics, volcanism, sedimentation and basin development, late Cenozoic, central part of northern Honshu, Japan: Sedimentary Geology, v. 74, p. 323-343.

Siebert, L., T. Simkin, and P. Kimberly, (2010), Volcanoes of the World, 3rd edition. Smithsonian Institution and the University of California Press, Berkeley.

Simons, M., Minson, S. E., Sladen, A., Ortega, F., Jiang, J., Owen, S. E., Meng, L., Ampuero, J.-P., Wei, S., Chu, R., Helmberger, D. V., Kanamori, H., Hetland, E., Moore, A. W., Webb, F. H., (2011), The 2011 Magnitude 9.0 Tohoku-Oki earthquake: Mosaicking the megathrust from seconds to centuries: Science, v. 332, p. 1421-1425.

Sugimura, A., and Uyeda, S., (1973), Island Arc -- Japan and its Environs: Elsevier, Amsterdam, 247 pp.

Taira, A., (2001), Tectonic evolution of the Japanese island arc system: Annual Reviews of Earth and Planetary Sciences, v. 29, p. 109-134.

Takeuchi, H., Uyeda, S., and Kanamori, H., (1970), Debate about the Earth: Approach to Geophysics through Analysis of Continental Drift: Freeman, Cooper and Company, San Francisco, 281 pp.

Tamaki, K., and E. Honza, (1985), Incipient subduction and obduction along the eastern margin of the Japan Sea, Tectonophysics, 119, 381-406.

Tamura Y., Y. Tatsumi, D. Zhao, Y. Kido, H. Shukuno, (2002), Hot fingers in the mantle wedge: new insights into magma genesis in subduction zones, *Earth and Planetary Sciences Letters*, 197, pp. 105-116.

US National Academy of Science, (2011), Waste Form Technology and Performance: Final Report. The National Academies Press, Washington DC.

Von Huene, R., and Lallemand, S., (1990), Tectonic erosion along the Japan and Peru convergent margins: Geological Society of America Bulletin, v. 85, p. 1159-1170.

Walcott, R. I, (1987), Geodetic strain and the deformational history of the North Island of New Zealand during the late Cainozoic, Philos. Trans. R. Soc. London, Ser. A, 321, 163–181.

Wallace, L.M.; Beavan, R.J.; McCaffrey, R.; Berryman, K.R.; Denys, P., (2007), Balancing the plate motion budget in the South Island, New Zealand using GPS, geological and seismological data. *Geophysical Journal International, 168(1):* doi:10.1111/j.1365-246X.2006.03183.x

Wallace, L.M., J. Beavan, S. Miura, R. McCaffrey, (2009), Using Global Positioning System data to assess tectonic hazards, in, *Volcanism, Tectonism and Siting of Nuclear Facilities*, eds. Charles Connor, Laura Connor, and Neil Chapman, Cambridge University Press, pp. 156-175.

Wei, D., and Seno, T., (1998), Determination of the Amurian plate motion: American Geophysical Union, Geodynamics series, v. 27, p. 337-346.

Wessel, P., and L. W. Kroenke, (2000), Ontong Java plateau and late Neogene changes in Pacific plate motion, J. Geophys. Res., 105(B12), 28,255–28,278.

Wessel, P., and L.W. Kroenke, (2007), Reconciling late Neogene Pacific absolute and relative plate motion changes, Geochemistry, Geophysics, Geosystems, 8(8).

Zhao, D. Ochi, F., Hasegawa, A., Yamamoto, A., (2000), Evidence for the location and cause of large crustal earthquakes in Japan: Journal of Geophysical Research, v. 105, p. 13,579-13,594.

Appendix: Concealed Active Faults Workshop

Notes on the Concluding Discussions

A three-day workshop was held in Christchurch, New Zealand from 31st January to 2nd February 2012, hosted by GNS Science staff and involving NUMO staff and consultants, plus some of the other members of the TOPAZ team. The aim was to discuss the characteristics of concealed active faults, particularly in the light of the ongoing series of earthquakes in the Canterbury Plains area, which had resulted in devastating damage and loss of life in the city of Christchurch in 2011. The workshop participants were able to discuss the nature of the basement faults in the area and see evidence for deformation at the surface. This enabled a lively discussion on the concerns being addressed by NUMO with respect to identifying environments where active faults may be concealed and means of tackling this issue in their siting programme. This note provides a short summary of the concluding discussions.

1 Context

Concealed active faults (CAFs) have been considered a potential problem in NUMO's siting programme as (a) they are legally required to reject sites that lie on active faults and (b), if they failed to locate a deep active fault beneath a repository during site investigations (SI) there is a risk to the safety case. Therefore, the interest in discussing them is to find out whether:

- There is some possibility that their potential presence can be indicated in advance of committing to a site (to avoid problem (a) above);
- There is good prospect that a detailed SI will identify all deep, blind faults (those that have no surface expression and whose activity cannot be inferred with confidence) that have the potential for reactivation as AFs in the future, allowing repository location to be closely linked to the deep structural geometry and thus avoid problem (b) above.

2 What do we mean by CAF?

There are certainly many AFs that are not on the AF Map of Japan – they have simply not been recognised and mapped, as they may be in inaccessible terrain or simply not have been examined in sufficient detail to determine whether they are active (i.e. have evidence of movement in the last c.200 kyr) or not. Provided that these faults have a surface expression, then detailed mapping and sampling/trenching carried out in an area of interest, should locate these 'missing' AFs.

AFs should be assumed to be present anywhere, unless exhaustive geological investigations have eliminated the possibility of their presence.

A CAF is 'concealed' because there is no surface expression of displacement by a fault that is not exposed at the surface. The range of tectonic and geomorphic conditions that could lead to concealment of AFs are:

1. Rapid sedimentation rates relative to tectonic rates (e.g., away from a plate boundary in areas of rapid glacial sedimentation, such as the Greendale Fault beneath the Canterbury Plains). If the sediments covering the basement rocks that host the AF are thick (hundreds of metres) weak, generally homogeneous and have little internal structure, then even high resolution reflection seismic techniques may be unable to indicate whether an observed basement fault has been active during the period over which the sediments were deposited.
2. Rapid denudation rates in soft rock, relative to tectonic rates leading to erosion of surficial displacement evidence for the presence of a deep AF (e.g. mountainous soft Tertiary sediments in humid terrains such as central NZ North Island environments).
3. A contractile tectonic environment is most likely to produce blind thrust CAFs that have no/subtle geomorphic expression.

3 When is a CAF a threat to a repository?

Even under the circumstances of (1) above, an old, mature AF is likely to have evolved to a sufficiently large average annual displacement that it could host earthquakes large enough to have broken the surface (M6.5; rule of thumb). Even if this has not yet occurred, repeated events of lower magnitude should produce surface geomorphological deformation indicative of the presence of a fault at depth. However, it is also rather unlikely that such a geological environment would ever be considered suitable for a repository as the sediments would be a poor host formation and the basement may be too deep to be a host (e.g. >1000 m).

A repository could be threatened with direct shear if a deep basement fault is activated or reactivated and displacement penetrates upwards to repository depth (typically about 500 m). In this context, whilst the 2010 Darfield M7.1 EQ broke surface, the February 2011 Christchurch M6.1 EQ probably did not rupture to within 1000 m of the surface.

The EQ magnitude threshold for surface rupture varies greatly according to tectonic environment. This parameter, and the associated uncertainties, should be established in a hazard modelling effort, and priority given to identifying CAFs with potential magnitudes greater than the magnitude of surface rupture. There is no sense in searching for CAFs on the ground surface for a magnitude range less than that associated with surface rupture.

A real issue is that faults capable of hosting a M6.5 event are on the verge of being 'repository significant' whilst, at the same time, being on the border of being discoverable.

A volume of basement rocks that contains immature AFs and is 'blinded' by sediments present perhaps the largest problem of identification, although again the complex fault pattern may make the basement an unattractive host for a repository. With an immature fault pattern and evidence of stress accumulation that points to potential activity in the future, the complexity of the system may make it very difficult to forecast which fault will move, in what sense, or by how much. A Bayesian, evidence weighting, approach (related to the expert elicitation approach being developed in TOPAZ) may be a valuable tool in this respect. In particular, it is unlikely that all the stress accumulation will be relieved by movement along a single fault, so complex displacements may occur in a network of capable fractures. This situation can be seen in the current series of Christchurch EQs across the Canterbury Plains.

4 How can we identify CAFs?

The ITM methodology that develops strain maps and budgets at a regional and local scale provides a first indication of areas where CAFs might be suspected: essentially, the presence of an obvious anomalous stress accumulation in a region where no fault activity has been recorded indicates that stress relief is likely to occur on features that have not been observed, or on reactivated 'inactive' faults (that have not been active since before stress accumulation began and might thus have been regarded as inactive). Comparison of different datasets in a multidisciplinary ITM analysis can reveal areas of significant activity not otherwise evident from active fault datasets. The probabilistic approach allows frequency information to be part of the overall assessment.

The ITM methodology will be informed by geomorphic evidence: is the region of interest characterised by any of the three tectonic and geomorphic conditions listed in Section 1? If these conditions exist and if the strain mapping from other approaches (e.g., GPS, seismicity) indicates accumulated strain potential with no clear features that would allow stress relief, then there is a high likelihood that CAFs may be present.

Moving to the site scale, a standard sequence of investigations focussed on seismic surveying linked to borehole data will identify AFs if they break the surface (trenching will be a major tool to help confirm their activity) and potentially active faults at depth in the basement (CAFs). A prerequisite is high quality geological mapping. As noted above, faults that are capable of hosting less than a M6.5 EQ are likely to be difficult to isolate from all other fractures with similar dimensions and geometries. Consequently, a safety case is likely to need to treat a network of such features as potentially capable and will then need to forecast how displacement magnitudes might evolve (and perhaps focus onto one feature alone) over the next 10,000 and 100,000 years. The Christchurch earthquake sequence provides a valuable example of how low-activity faults can be virtually impossible to detect in areas of high sedimentation and considerable geomorphic modification.

The CHCH earthquake sequence has further demonstrated the value of developing a background or distributed seismicity model for tectonic hazard analysis. The background models provide no information on the geometry of CAFs, but do provide first-order information on the magnitude-frequency of future hazardous events. Efforts to develop realistic, defensible background models should be supported, particularly using multiple approaches (seismicity and GPS) and constraining them into a systems approach to modelling (e.g. with all source models consistent and matching plate motion constraints). Ideally, candidate faults identified from seismic reflection, inference from offshore areas etc, could be used to reassign an otherwise grid-based background seismicity model.

Moreover, GPS data suggested ~15 nanostrain/yr of strain accumulation across the Canterbury Plains prior to the sequence of earthquakes in Christchurch (Wallace et al., 2007). The GPS data clearly highlighted the strong likelihood of CAFs in the Christchurch region, and emphasises the need for inclusion of datasets such as GPS when assessing CAF hazard.

Once identified, CAFs often prove to have long recurrence intervals so, for hazard analyses, they would best be characterised in time-dependent models (i.e. taking account of the elapsed time since the last earthquake as well as the long-term recurrence interval). This is difficult information to obtain for the vast majority of fault sources, but such information should be sought wherever possible.

5 Conclusions

Concealed active faults do not need to be regarded as an intractable siting problem, for two main reasons:

1. They tend to occur in geological and tectonic environments that, for a number of reasons, would probably not, in any case, be considered suitable for a geological repository (weak sediments down to repository depth; high erosion rates; immature and complex tectonic setting;).
2. We have ITM and SI techniques to identify regions where CAFs might be expected to be present and we have a toolbox of techniques that can then be deployed to assist in identifying potentially capable faults (capable of M6.5 or greater EQs) at depth.

Through ITM, NUMO has developed strain budget mapping techniques for identifying regions that may have a higher potential for concealing AFs, which, if combined with basic geomorphic analyses of environments that could hold CAFs, allow initial decisions to be taken about potential site suitability. Existing SI programmes have the capacity to identify CAFs and to classify them in terms of their capability to host repository-relevant displacement in the 10 kyr to 100 kyr timeframe.